63-2-5

AFCRL-62-1091

297 368

05016-1-S

THE UNIVERSITY OF MICHIGAN

COLLEGE OF ENGINEERING

DEPARTMENT OF ENGINEERING MECHANICS

METEOROLOGICAL LABORATORIES

Scientific Report No. 1

A Study of Raindrop-size Distributions and their Variation with Height

KENNETH R. HARDY

Project Director, A. NELSON DINGLE

Project 8620
Task 862002
Contract No. AF 19(628)-281

Under contract with:

Geophysics Research Directorate
Air Force Cambridge Research Laboratories
Office of Aerospace Research
United States Air Force
Bedford, Massachusetts

Administered through:

December 1962

OFFICE OF RESEARCH ADMINISTRATION · ANN ARBOR

Requests for additional copies by Agencies of the Department of Defense, their contractors, and other Government agencies should be directed to the:

ARMED SERVICES TECHNICAL INFORMATION AGENCY
ARLINGTON HALL STATION
ARLINGTON 12, VIRGINIA

Department of Defense contractors must be established for ASTIA services or have their "need-to-know" certified by the cognizant military agency of their project or contract.

All other persons and organization should apply to the:

U. S. DEPARTMENT OF COMMERCE
OFFICE OF TECHNICAL SERVICES
WASHINGTON 25, D. C.

ERRATA

Page	
5	Line 17: for $\Sigma\sigma^6$ read ΣD^6
9	Line 18: for calibers read calipers
12	Line 14: for coalescense read coalescence
47	Line 13: for intefvals read intervals
50	Line 1: for adequate read adequately
66	Line 8 from bottom: for imitial read initial
79	Delete last word of line 16.
82	Line 12 from bottom: for exponenets read exponents

AFCRL-62-1091

THE UNIVERSITY OF MICHIGAN

COLLEGE OF ENGINEERING
Department of Engineering Mechanics
Meteorological Laboratories

Scientific Report No. 1

A STUDY OF RAINDROP-SIZE DISTRIBUTIONS AND THEIR VARIATION WITH HEIGHT

Kenneth R. Hardy

ORA Project 5016

Project 8620
Task 862002
Contract No. AF 19(628)-281

under contract with:

GEOPHYSICS RESEARCH DIRECTORATE
AIR FORCE CAMBRIDGE RESEARCH LABORATORIES
OFFICE OF AEROSPACE RESEARCH
UNITED STATES AIR FORCE
BEDFORD, MASSACHUSETTS

administered through:

OFFICE OF RESEARCH ADMINISTRATION ANN ARBOR

December 1962

Project Director,
A. Nelson Dingle

ACKNOWLEDGMENTS

The author wishes to thank all who assisted him during the progress of this study. The advice and guidance of Professor A. Nelson Dingle, Chairman of the Doctoral Committee, is particularly appreciated. The author is also indebted to Professors Ernest F. Brater, Edward S. Epstein, E. Wendell Hewson, and Richard D. Remington for serving as members of the Committee and for their willingness to be of help when requested.

The constant interest and encouragement of my colleagues, particularly Messrs. James B. Harrington, Jr., Charles Young, and Frank D. Haurwitz are greatly appreciated. Mr. Floyd C. Elder was responsible for collecting most of the radar data used in this study, and the author is deeply grateful for his help in the interpretation of this data and for his valuable criticism.

Without the cooperation of many individuals this work would not have been possible. Mr. Daniel J. Provine helped with the technical operation of the spectrometer. Mr. Morton Glass supplied measurements of the cloud systems near the spectrometer site. Raw data were provided by the Department of the Geophysical Sciences, University of Chicago, by Meteorology Research, Inc., and by the Geophysics Research Directorate. Mr. Larry M. McMillin, Miss A. Lucia Torres, and Mrs. Helen Stewart rendered valuable assistance in the reduction of data, and Mr. Peter C. Werner prepared some of the diagrams.

The author wishes to thank Mr. Walter Kent for his cooperation and generosity in the use of his ranch as a field site for the spectrometer. The author is also thankful for

the painstaking and careful typing of the manuscript by Mrs. Bonnie Axtell.

The support provided by the Geophysics Research Directorate, Air Force Cambridge Research Laboratories for the analysis of the Flagstaff data is gratefully acknowledged. The support provided by a University of Michigan Research Fellowship from February to June 1961 is also appreciated. Finally the author wishes to acknowledge the support of the University of Michigan Computing Center, Professor R.C.F. Bartels, Director for the use of the IBM 709 and 7090.

ABSTRACT

The purpose of this study is to describe rain in terms of raindrop-size distributions and to relate these distributions to the physical processes which affect the growth or evaporation of the raindrops. The immediate significance of the present work is that (1) it contributes to our understanding of the final stage of precipitation growth, and (2) it provides information which is useful in the interpretation of weather radar observations.

Computations of the changes of the raindrop-size distributions with distance fallen are made using an electronic digital computer. Assuming a steady mass flux of raindrops just below the melting level, changes brought about in the distribution through coalescence among raindrops, by accretion of cloud droplets, and by evaporation are considered. It is shown that the numerical procedures which are used introduce negligible errors in the computations. In addition, these procedures remove all restraints on the form of the initial raindrop-size distribution, and on the properties of the cloud and the atmosphere through which the drops are falling.

Raindrop-size distributions may frequently be expressed satisfactorily by a function of the form:

$$\ln\left(\frac{N_D}{N_o}\right) = -\Lambda D ,$$

where D is the drop diameter, $N_D dD$ the number of drops of diameter between D and D+dD in unit volume of space, N_o the value of N_D for D = 0, and Λ is the magnitude of the slope of the distribution. It is found that an initial raindrop-size distribution having a relatively large slope at the melting level is considerably modified as the rain falls

by the processes of coalescence, accretion, and evaporation. Whereas the number of smaller drops is markedly depleted by each process, the number of larger drops is increased by coalescence and accretion but is decreased by evaporation. On the other hand, a distribution with a relatively small slope at the melting level is only slightly modified by the above three processes. By considering raindrop-size distributions with various slopes but equal rainfall intensity, it is found that the depletion of cloud liquid water content and the amount of evaporation increase as the slope of the distribution becomes larger.

A photoelectric raindrop-size spectrometer developed by Dingle and Schulte is used to measure the raindrop sizes which are reported in the study. The calibration of the instrument is described; and a correction, based on a combination of geometric considerations and experimental evidence, is applied to the observed distributions. It is shown that these corrected distributions have rainfall intensities which are in good agreement with intensities measured with a special weighing bucket rain-gage. It is concluded that the spectrometer provides raindrop-size spectra which adequately represent the natural distributions.

The problem of relating the rainfall intensity to the radar echo power is discussed. For the rains observed with the spectrometer, the least squares regression equation of the radar reflectivity factor, Z, on the rainfall rate, R, is

$$Z = 312R^{1.36}$$

provided that R is greater than 5 mm hr^{-1}. The scatter about this regression line is large.

A procedure is presented whereby the raindrop-size distribution at the melting level can be deduced. This is possible by combining the information obtained from the computations of the change in the distribution below the melting level with the observed distribution at the ground. One study of this type for the light rain on 31 July 1961 at Flagstaff, Arizona shows that at the melting level (1) more large drops must be present than is indicated by the Marshall and Palmer distribution, and (2) the concentration of the larger drops must not be substantially different from their concentration observed at the ground.

TABLE OF CONTENTS

TABLE OF CONTENTS (CONCLUDED)

LIST OF TABLES

LIST OF FIGURES

LIST OF FIGURES (CONTINUED)

LIST OF FIGURES (CONTINUED)

LIST OF FIGURES (CONCLUDED)

1. INTRODUCTION

1.1 AIM OF THE STUDY

> Water is one of the basic commodities on which our civilization depends and it is no accident that the highly developed regions of the world are those which are endowed with good supplies of water. Practically the whole of our usable water comes in the form of precipitation from the atmosphere, and few studies could be more important than those which lead to a complete understanding of how it is stored in the atmosphere and how it precipitates out.
>
> E. G. Bowen, in Foreword to "The Physics of Rainclouds" by N. H. Fletcher.

Although rain is one of the most important products of atmospheric processes, only a few of its properties can be derived from the observations which are now generally available. For example, some rain gages provide a continuous record of the rain intensity but most are used to provide a measure of the total rainfall over a period of six hours or even a day. If the gages are not too widely separated the records provide information on the duration, frequency of occurrence, seasonal variation, and the areal distribution of the rainfall. Such information is certainly useful, but it does not shed any light on the basic mechanism of rain formation. On the other hand, the raindrop-size distribution is a fundamental property of the rain, and its measurement can be used to increase our knowledge of the precipitation process. The research reported herein is primarily an attempt to describe rain by means of its drop-size distributions and to relate these distributions to the physical processes which affect the growth and evaporation of the raindrops.

1.2 DESCRIPTION OF RAINDROPS

A raindrop is a drop of water of diameter greater than 0.2 mm[1] falling through the atmosphere.[2] The limiting diameter of 0.2 mm is rather arbitrary, but has been chosen because drops of this size fall rapidly enough relative to the air (about 70 cm sec^{-1}) to survive the evaporation over several hundred meters which may occur below the cloud base. Raindrops greater than 6 mm are rarely observed in natural rain, and it may be assumed that drops larger than this usually break up during their fall towards the ground.

The terminal velocity of raindrops has been measured by several investigators (Lenard, 1904; Laws, 1941), but the most extensive, and probably the most accurate, measurements have been made by Gunn and Kinzer (1949). Their results are shown in Fig. 1. At small drop diameters the drop velocity increases rapidly with drop size, whereas the velocity approaches an asymptotic value of about 920 cm sec^{-1} for drops greater than 5 mm.

The predominant force in the case of drops smaller than about 1 mm is surface tension, with the result that the drops take on an essentially spherical shape. However, other forces become important for larger drops, and the shape is considerably deformed from the spherical (Lenard, 1904; Spilhaus, 1948; McDonald 1954). Magano (1954) and Jones (1959) have taken high speed photographs which show that a large water drop falling at terminal velocity exhibits a marked flattening on its lower surface and smoothly

---

[1] In this study all drop sizes will refer to the diameter unless noted.

[2] Falling drops with diameter lying in the interval 0.2 to 0.5 mm are usually called drizzle drops, but this is an unnecessary refinement for the purpose of this study.

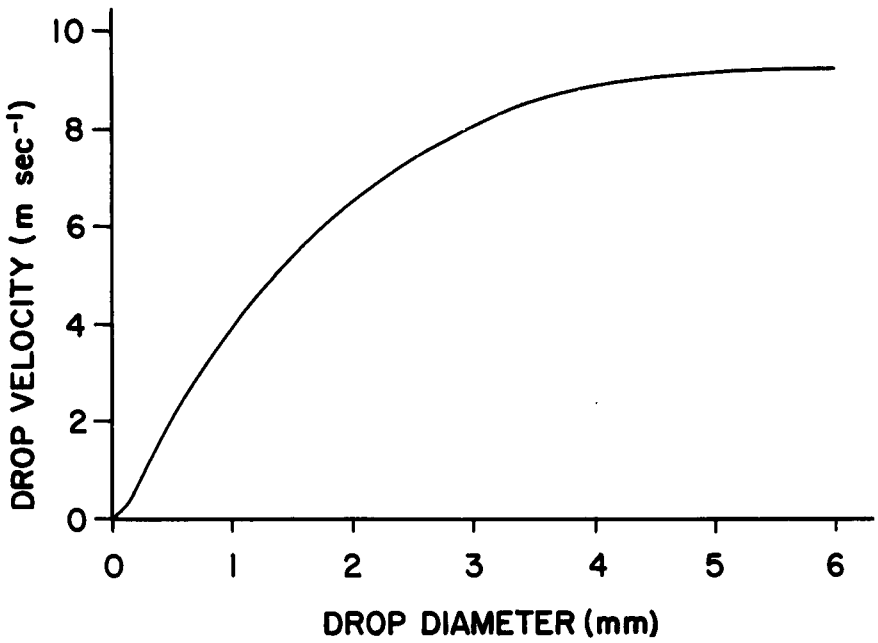

Fig. 1. The terminal velocity of water drops in still air, pressure 760 mm, temperature 20C (Gunn and Kinzer, 1949).

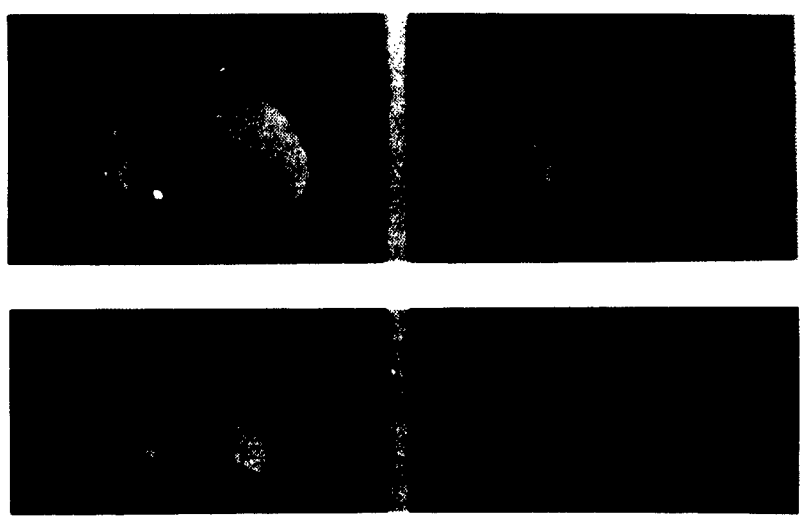

Fig. 2. Large water drops falling at terminal velocity. Equivalent spherical diameters and measured fall velocities as follows: upper left, 6.5 mm and 890 cm sec^{-1}; upper right, 6.0 mm and 880 cm sec^{-1}; lower left, 4.8 mm and 830 cm sec^{-1}; lower right, 2.8 mm and 680 cm sec^{-1} (Magono, 1954).

rounded curvature on its upper surface (Fig. 2). This flattening increases the drag force on the drops which consequently limits the terminal velocity of the largest raindrops.

The maximum size of raindrops appears to depend greatly on the turbulence regime of the air through which the drops fall. In still air, drops as large as 10 mm diameter can be produced, but in the free atmosphere drops of 6 mm are quite rare. The exact manner in which the raindrops break up is of considerable interest because this process affects the drop-size distribution. However, at present there is no adequate information on the mechanism or character of the break-up of large drops.

Compared to raindrops, cloud droplets are extremely small, typical drop diameters being in the order of 0.01 - 0.02 mm. Therefore, in terms of volume it takes about 10^6 cloud droplets to form a typical raindrop of 1 - 2 mm. The mechanism whereby cloud droplets grow to raindrop size is a fundamental problem in cloud physics.

Throughout this study the quantity "W" will refer to the liquid water content per unit volume in the form of raindrops within the atmosphere, and "M" will denote the liquid water content per unit volume in the form of cloud droplets (i.e. from about 0.001 - 0.2 mm).

1.3 THE USES OF RAINDROP-SIZE DISTRIBUTIONS

1.3.1 Quantitative precipitation measurements using radar

The average power received by radar from a meteorological target is given by

$$\bar{P}_r = \frac{P_t A_e h k}{8 \pi r^2} \Sigma\sigma \quad , \qquad (1)$$

where $\sum_1$ designates summation over a unit volume, P_t is the transmitted power, A_e is the effective area of the radar antenna, h is the linear distance occupied by a pulse of the transmitted energy in space, r is the range of the target, k is the attenuation factor, and $\sum_1 \sigma$ is the total backscatter cross section of the particles in a unit volume of the contributing region. The derivation of Eq. (1) (Battan, 1959) involves the consideration of a large number of factors and need not be of concern here. The quantities P_t, A_e, and h are properties of the radar, and the choice of their values has an important bearing on the radar performance. The attenuation factor k is very close to unity for normal rain intensities and for radar wave lengths greater than about 3 cm. If the precipitation particles are composed of raindrops (maximum diameter about 5.5 mm), then for radar wavelengths of 3 cm or greater, $\sum_1 \sigma$ is essentially proportional to $\sum_1 \sigma^6$ (usually denoted by Z and called the radar reflectivity factor), the sum of the sixth powers of the diameters of the raindrops contained in a unit volume (Ryde, 1946; Gunn and East, 1954). Since the characteristics of the radar can be kept constant, Eq. (1) reduces to

$$\bar{P}_r = \frac{C}{r^2} \sum_1 D^6 \quad , \tag{2}$$

where C is a constant. Eq. (2) points to the strong dependence of the returned power on the drop-size distribution of the particles which make up the target.

Unfortunately, the rainfall intensity provides little information on the raindrop-size distribution. A volumetric distribution may be composed of many small drops, but because of their smaller fall velocities, the rain intensity may be identical to that resulting from a distribution composed of a few large drops. However, the power of the

returned radar signal will be quite different for these two distributions even though the distributions produce equal rain intensities. Therefore, information on the raindrop-size distribution must be available if radar is to be used for quantitative rainfall measurements.

1.3.2 Precipitation growth processes

The drop-size distribution and intensity are the two essential features which describe rain. Cursory observations are sufficient to reveal that the raindrops from a summer shower have a different character than the drops from the light rains common to the cooler seasons. Even on this basis, it is apparent that a study of the drop-size distributions will aid in our understanding of the basic formation and growth of raindrops, particularly if other meteorological variables are included and related to the drop-size data.

The prospect of modifying clouds to produce additional rainfall provides an important need for research in precipitation physics. In the past, very little research has been carried out on the effect of cloud seeding on the drop-size distribution of the resulting rain. However, it is probable that a study of raindrop spectra will yield valuable information not only on the effect of seeding on the raindrop sizes but also on the effectiveness of the cloud modification methods which are used.

1.3.3 Soil erosion studies

Some of the first quantitative work on the effect of rain on soil erosion was reported about 20 years ago. Laws and Parsons (1943), Ellison (1944), Chapman (1948), Ellison (1949), and Ekern (1950) carried out fairly comprehensive

studies of soil erosion, and in some cases they considered the effect of the drop-size distribution. However, greater use of drop-size data will allow the development of indices which are related to the erosive character of the rain and which have application to soil conservation studies.

1.4 THE APPROACH TO THE PROBLEM

This study does not deal exclusively with a single problem. It is intended more as a critical analysis of some characteristics of raindrop sizes, and the research is directed toward the significance and use of drop-size distributions in the field of precipitation physics.

The following section is a review of the research which has given some consideration to the measurement and use of raindrop sizes. A comprehensive treatment of the processes affecting the size of raindrops as they move from the melting level to the ground is given in Section 3. The information thus obtained is used to deduce some important aspects of cloud and precipitation physics. In addition, information is provided on raindrop-size distributions in regions above the ground which are usually observed by radar. The raindrop-size distributions which were observed in Flagstaff during the summer of 1961 are presented in Appendix D, and an attempt is made to explain these observations in terms of the meteorological conditions which are most significant in shaping the surface raindrop-size spectra.

2. REVIEW OF RESEARCH ON RAINDROP-SIZE DISTRIBUTIONS

2.1 THE MEASUREMENT OF RAINDROP SIZES

The sampling of a representative volume of raindrop sizes within the atmosphere is a difficult problem and one which has still not been ideally solved. The simplest and most common method is to expose a piece of filter paper treated with a water soluble dye (rhodamine, eosin, or methylene blue) to the rain. The drops moisten the paper, and on drying, leave circular stains whose diameters can be related to those of the raindrops by suitably calibrating the paper beforehand. This method has been used successfully by Lenard (1904), Defant (1905), Niederdorfer (1932), Blanchard (1953), Sivaramakrishnan (1961) and many others. A slight variation of this method was devised by Engelmann (1962) who exposed a sheet of blueprint paper to the rain and then developed it using ammonia fumes. When properly handled the yellow-orange stains are outlined with a black ring on a yellowish-gray background. The difficulty with this general procedure is that (1) the sampling area and time of exposure must be adjusted on the basis of the rainfall intensity, and usually the method is not workable for high rates of rainfall, (2) the reduction of the data is usually messy and rather time consuming, and (3) in general the sample is rather small for representative distributions. A further modification of this basic method involves the use of very fine mesh screens which are dusted with either soot or powdered sugar. The drops pass through the screens and remove a circular area of the dusting material. This has produced some excellent raindrop samples but the reduction problem is not improved over that of the filter paper method.

Bentley (1904) measured the size of raindrops by allowing them to fall into an inch deep layer of fine flour which was contained in a shallow pan about four inches in diameter. The raindrops were left in the flour until the dough pellets were hard and dry. Through prior calibration the dough pellets were found to correspond roughly in size with the raindrops that made them.

A photographic technique has been developed and used successfully by Jones and Dean (1953). A series of pictures of a volume of the atmosphere is taken, and the drops thus photographed are counted and sized. The equivalent sampling volume is greater than one cubic meter per minute. The reliability of the measurements for raindrops one millimeter and larger is high. However, the drops of diameter between 0.5 and 1.0 mm are subject to error. The reduction of the data is likewise tedious, although recently it has become possible to measure the drops from the photographs with a pair of electric calibers and have the measurement punched directly onto cards.

Other methods which have been tried but have not attracted wide acceptance include a raindrop spectrograph by Bowen and Davidson (1951) and a device employing a microphone diaphragm by Cooper (1951). The device by Bowen and Davidson is a type of mass spectrograph in which falling raindrops are deflected by a horizontal air-current within a wind tunnel. The drops enter through a funnel and the distance through which the drops are deflected is proportional to their mass so that drops are spread out along the bottom of the tunnel according to size. The disadvantages of this instrument are that (1) the observations are limited to those rains in which the drops are falling vertically, and

(2) the data reduction is tedious since the samples are usually collected on filter paper. Cooper's instrument measures the amplitude of the pulses produced by raindrops impinging upon a microphone diaphragm. This device has the tremendous advantage of being able to transmit the pulses, and thus is suited to being carried aloft to measure the vertical variations of the raindrop spectrum. Unfortunately, the only results which have appeared using this instrument seem somewhat questionable, and apparently further development is required before reliable results are obtained.

Mason and Ramanadham (1953) developed an optical method for measuring raindrop sizes. The drops fall through a narrow beam of light, and the light scattered by them is focused onto the slit of a photomultiplier tube. The instrument has the advantage of being able to record drops which are not falling vertically. However, the sampling volume is necessarily small since only one drop is to be in the light field at a given instant. Illumination problems have prevented its use during daytime showers, and other problems may also be present since relatively little data collected with it have been reported.

A photoelectric raindrop-size spectrometer, described by Dingle and Schulte (1962), overcomes most of the disadvantages which are present in other raindrop measuring instruments. Since observations of raindrop sizes obtained with the spectrometer are used throughout this study, a brief description and the calibration of the instrument are given in Appendix A.

2.2 EARLY RESEARCH WITH RAINDROP-SIZE DISTRIBUTIONS

One of the earliest accounts of the measurements of raindrops is that given by Lowe (1892). He observed the

diameter of the spots which were produced by drops falling on sheets of slate. He did not attempt to relate these "slate" diameters to the actual drop diameters. The discussion following the presentation of Lowe's paper was also published, and it was mentioned that a plan to measure drops falling on chemically prepared paper had been put forth previously. However, this method was not adopted until Wiesner (1895) used it to measure the size of raindrops in tropical rain. Lenard (1904) allowed the drops to fall on a dye-impregnated filter paper. He was interested in measuring raindrop velocity, but he also obtained samples of raindrop sizes in natural rains from 1898 to 1899 at Kiel, Germany and near Luzern and Lugano, Switzerland.

Bentley (1904), using the flour-pellet method, obtained raindrop-size distributions in 51 storms between 1899 and 1904. His observations included samples from different portions of thunderstorms, rain showers, and general rainstorms. His data indicated too many large sized drops as compared with later measurements, and it is probable that this was because he did not account for the non-sphericity of the larger drops. Nevertheless, Bentley emphasized the synoptic features during his observations and had an insight into the significance of his work when he states:

> The mechanism of rain formation and the phenomena connected therewith is of great interest and import, and should receive from scientists a larger measure of attention than hitherto. It seems certain that systematic study of this and allied phenomena would, through the increase of our exact knowledge regarding it, richly repay patient and thoroughgoing investigation.

Except for contributions by Defant (1905), Becker (1907), and Schmidt (1908), all of whom aroused interest by finding that drops appeared to show a preference for certain drop

volumes, Bentley's words were not heeded for more than 20 years.

Efforts to show that preferred drop sizes exist whose volumes bore the relationship 1:2:4:8:16 were initiated by Defant, and this phenomenon appears to have dominated the research on drop-size distributions in rain for the period from 1925 to 1938 (Kohler, 1925; Niederdorfer, 1932; Landsberg and Neuberger, 1938). The effect has been explained on the assumption that the rain consists of drops, initially of approximately the same size, which coalesce with each other probably by some sort of transverse motion when falling at their common terminal velocity. The drops which do coalesce have twice the original mass, and these are now capable of coalescense by a similar mechanism. The result is a distribution with masses of the required ratios. More recent measurements and work on this problem (Horton, 1948; Blanchard, 1953; Jones, 1955; Dingle and Hardy, 1962) failed to show these preferred peaks. Landsberg and Neuberger (1938) remark on the Defant phenomenon as it applies to their data:

> If liberally interpreted, this can be taken as representing the proportions: 1:2:4:8:16. Other values are, nevertheless, frequently enough represented to show that these proportions may be a predominant feature of drop-size distribution but are by no means a lawfully required order.

This statement is still applicable, and further work is required to show whether these mass ratios are a significant property of drop-size distributions.

Research during the early 1940's on drop-size distributions was climaxed by the work of two soil conservationists, Laws and Parsons (1943). They refined the Bentley

flour-pellet method and obtained results which are still considered to be among the best. Their data show that the median-volume diameter, D_o, (defined as the drop diameter such that the distribution of liquid water with raindrop size is divided exactly in half) is related to the rainfall intensity, R, by,

$$D_o = 1.24R^{0.182} \qquad (3)$$

The basic result that the median drop diameter increases with increasing rain intensity is not surprising because increased flux of rainwater should accompany large raindrops. Of greater significance is the fact that this represents one of the first attempts to describe a property of the drop-size distribution quantitatively. Later it was found that quite different relationships may hold for different types of rain (Best, 1950; Blanchard, 1953). However, Laws and Parsons' work was the first of a long series of attempts to describe drop-size distributions by means of a single quantity (i.e. D_o in this case).

2.3 RESEARCH AFTER 1943

During the same years that Laws and Parsons were carrying out their measurements on raindrop sizes, cloud and precipitation physics acquired an added significance. The two factors responsible for a renewed interest in this subject were (1) the development of radar as an instrument for weather observation, and (2) the gradual emergence of a scientific basis for weather modification or control (reviewed by Langmuir, 1948 a). A great number and variety of experiments associated with cloud physics have been conducted since that time. A few of the important advances, particularly as they relate to the measurement or use of

raindrop-size distributions, are described below.

2.3.1 Drop-size distribution and radar meteorology

The detailed characteristics of radar echoes from meteorological targets have been extensively studied. Battan (1959) emphasizes the application of radar to various phases of meteorological research and hydrology, whereas more general reviews of radiometeorology have been given by Ligda (1951), Wexler (1951), and Marshall and Gordon (1957). Problems which primarily relate to the use of radar in the estimation of such cloud parameters as median volume diameter, D_o, the liquid water content, M, and the radar reflectivity factor, $Z = \Sigma D^6$, are discussed in a series of papers by Bartnoff and Atlas (1951), Atlas and Bartnoff (1953), and Atlas (1954). These latter papers indicate the importance of the cloud droplet distribution in arriving at reliable values for the quantities desired, and in many respects the problems discussed are also applicable to the study of raindrop-size distributions.

One of the most useful and obvious applications of radar to meteorology is in the determination of precipitation intensities. Shortly after World War II, the finding of a relationship between the radar reflectivity factor, Z, and rainfall rate, R, immediately suggested that a single radar could be used for measuring rainfall over an area of several thousand square miles. However, the magnitude of the task was quickly revealed as the accumulation of data on raindrop-size distributions showed an increasing number of Z-R relationships (Wexler, 1948; Twomey, 1953; Battan, 1959, p 56). Observations of drop-size spectra have been made at different latitudes, in many types of rains, and during storms in various stages of their development. Some of

the Z-R relationships obtained from these observations and other pertinent data are given in Table 1. All of the values of Z and R which were used to determine the regression equations given in Table 1 were computed from raindrop-size data. The precipitation intensities were calculated using the terminal velocities of raindrops as given by Gunn and Kinzer (1949), whereas no assumptions or other data were required for the calculation of Z from the drop-size distribution.

A logical step in selecting the Z-R relationship from Table 1, which is applicable for a particular situation, is to catagorize the regression equations according either to the synoptic situation or to the stage of development of the storm. A notable attempt along these lines is made by Atlas and Chmela (1957). They show that the Z-R function is related in a physically consistent manner to the rainfall type. However, quite large variations are still observed to fall within each type. Some causes of these variations are also investigated by Atlas and Chmela and these will be discussed further in Section 3.9.2. One other attempt to link Z-R relations with the synoptic pattern is reported by Jones and Mueller (1960). These investigators compare the data collected at Champaign, Illinois and Miami, Florida. The greatest differences in Z-R relationships between the two locations is found to occur with thunderstorms. The Miami thundershowers generally show a smaller Z for a given R than the thundershowers in Illinois. The difference is most significant at very high rainfall rates. It appears that further investigation along the lines suggested in the above two papers would aid in choosing the proper Z-R relation for a particular situation.

Table 1. Empirical relations between radar reflectivity factor, Z ($mm^6\ m^{-3}$), and precipitation intensity, R ($mm\ hr^{-1}$).

Equation	Reference	Source of Data	Location	Remarks
$320R^{1.44}$	Battan(1959)	Laws & Parsons(1943)	Washington,D.C.	8 rain intensities, each a mean of about 10 storms of same intensity
$214R^{1.58}$	Battan(1959)	Laws & Parsons(1943)	Washington,D.C.	98 storms - original data
$180R^{1.55}$	Battan(1959)	Boucher (1951)	Cambridge, Mass.	63 rain samples, widespread rain both uniform and variable; showers and thunderstorms
$16.6R^{1.55}$	Battan(1959)	Blanchard (1953)	Hawaii	Orographic rain within cloud
$31R^{1.71}$				Orographic rain at cloud base
$290R^{1.41}$				Non-orographic rain - thunderstorms
$396R^{1.35}$	Battan(1959)	Jones(1955)	Central Ill.	1,270 one-minute observations - all rains
$220R^{1.60}$	Battan(1959)	Marshall & Palmer(1948)	Various locations	Various types of rain
$188R^{1.48}$	Hardy & Dingle(1960)	Hardy & Dingle(1960)	Ann Arbor,Mich.	28 one-minute samples, complete thundershower, R = 0.2 - 54 $mm\ hr^{-1}$

Table 1 (continued)

Equation	Reference	Source of Data	Location	Remarks
$430R^{1.29}$	Appendix D		Flagstaff, Arizona	35 five-minute samples, light rain, R = 0.1 - 3 mm hr^{-1}
$109R^{1.64}$	Ramana Murty & Gupta(1958)		Khandala, India	About 80 samples from monsoon showers
$242R^{1.42}$	Ramana Murty & Gupta(1958)		Delhi, India	About 80 samples from monsoon showers
$66.5R^{1.92}$	Sivarama-krishnan(1961)		Poona, India	Data from three rains in July, 1959.

Thus far only the variation in the Z-R function obtained from drop-size data has been mentioned. This in itself may introduce large variations since the drop sizes are generally measured over a volume that is less than a cubic meter. Any statistical fluctuations in the drop-size distribution on this scale may then be reflected in the observations. In contrast, the resolution of radar is such that normally the sampled volume is in the order of 10^4-$10^6 m^3$, and offhand it would appear that radar is capable of giving a good estimate of the average rainfall over rather large areas. However, radar is plagued with many problems of its own when it comes to quantitative measurements of returned power from meteorological targets (Austin and Geotis, 1960; Marshall and Gordon, 1957). The primary problems are the accurate measurement of the intensity of the radar signal received and the deduction of the rainfall rate from the measured radar signal intensity. The obvious approach to these problems is to measure simultaneously the rainfall rate, the drop-size distribution, and the intensity of the radar signal from the precipitation just above the rain gage. The general conclusion from studies of this type (Marshall, Langille and Palmer, 1947; Austin and Williams, 1951; Gerhardt and Tolbert, 1957) is that the relative increase in the signal intensity with precipitation rate is in agreement with the Z-R relationship, but the absolute value of the measured radar signal is a factor of between two and five below that computed from the drop-size data. This problem has not yet been resolved, but recent work by Probert-Jones (1962) has considerably reduced the possible sources of the discrepancy. At present, quantitative measurements of rainfall rate can best be obtained by coordinating rain gage and radar data;

the rain gages serving as a calibration to prevent large errors in the absolute values deduced from radar. However, much work still remains in establishing appropriate Z-R relationships for the many types of rain. This problem is further examined in Section 3.9.

2.3.2 Empirical relationships of raindrop-size distributions

The raindrop-size distributions ordinarily observed at the surface of the earth have the common feature that the number of drops in a given size-range decreases rapidly with increasing size. Often a similar decrease is also observed in the number of very small drops, but most measuring techniques are limited to drops too large for this effect to be seen.

Probably the first, and undoubtedly the most widely used, empirical relationship of drop-size distributions is that found by Marshall and Palmer (1948). They fitted their own observations and those of Laws and Parsons (1943) to the relation,

$$N_D = N_o \exp(-\Lambda D) , \qquad (4)$$

where D is the diameter of the raindrop, $N_D dD$ the number of drops of diameter between D and D+dD in unit volume of space, N_o the value of N_D for D = 0 and found to be 8000 $m^{-3}mm^{-1}$ for any intensity of rainfall, and

$$\Lambda = 41R^{-0.21} \ cm^{-1} , \qquad (5)$$

where R is the rate of rainfall in mm hr^{-1}. Eq. (5) was obtained by comparing the rain gage observations of R with Λ as found from logarithmic plots of observed distributions. Throughout the remainder of this study the distribution given by (4) is referred to as the M-P distribution. The

empirical relation represented by this equation and some of the data upon which it is based are shown in Fig. 3.

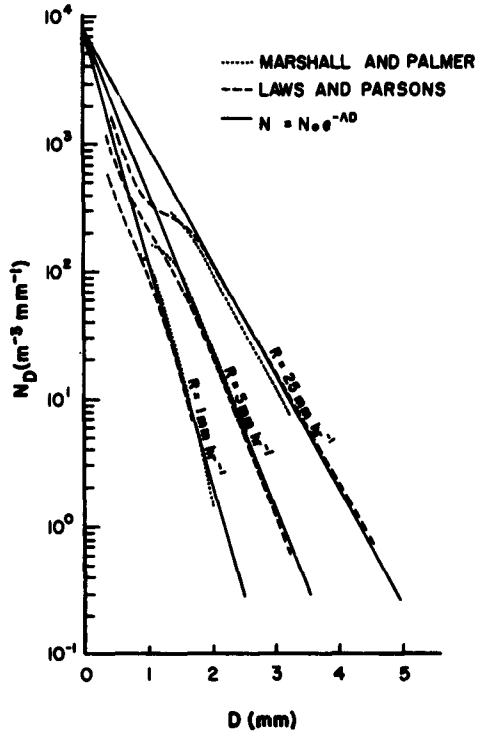

Fig. 3. Observed raindrop-size distributions (Marshall and Palmer, 1948).

The observed curves are averages of data obtained on several different occasions with different types of weather. The fit is excellent for drops greater than about 1.5 mm in diameter. However, for drops less than about 1.0 mm the M-P distribution considerably overestimates the number of drops. Eq. (4) has had wide acceptance in theoretical work because it leads to expressions which can be readily integrated. However, care must be exercised in integral expressions at low rainfall rates where the difference between the observed distribution and the M-P distribution introduces rather large errors in the values of such quantities as W, D_o, and R.

Best (1950) has examined the observations of a considerable number of earlier workers and has shown that their data can be fitted by an empirical relation of the form

$$1-F = \exp[-(x/a)^n] , \qquad (6)$$

where F is the fraction of liquid water comprised by drops of diameter less than x, and "n" is a constant with an average value of 2.25. The value of "a" depends on the precipitation rate, R, and has the value

$$a = 1.30R^{0.232} , \qquad (7)$$

where x and a are measured in centimeters and R is in mm hr^{-1}. Expressing (7) in terms of drop numbers so that N_D has the same meaning as in (4), the average spectrum is given by

$$N_D = BD^{-2} \exp(-CD^2) , \qquad (8)$$

where B and C are constants. Eq. (8) describes the observed distributions quite well except at their extremes, but in view of its greater complexity as compared to (4) it has not received wide acceptance.

A somewhat different approach has been adopted by Levin (1954) who remarks that all observed drop-size distributions are very close to the log-normal distribution. The log-normal distribution is one for which a plot of frequency of occurrence or concentration against the logarithm of the drop diameter produces a symetrically normal distribution. This implies that drops of say twice the median diameter should occur with the same frequency as drops of half the median diameter. He further points out that the M-P distribution is a close approximation to the log-normal

distribution at values of D rather greater than the median value. The log-normal distribution has the added advantage of limiting the number of very small drops in the distribution, which is a definite improvement over Eq. (4).

2.3.3 Drop-size distributions and precipitation processes

Before discussing precipitation processes it is necessary to have a clear understanding of the basic problem in the formation of raindrops. The density of water vapor at saturation is about 10 g m^{-3} at 10°C, a temperature which may be considered representative of the lower portion of a rain cloud during the summer. For rain from stratiform clouds typical cloud liquid water contents range from 0.1 to 1.0 g m^{-3}. Similarly the total amount of water which is present in the form of raindrops is in the range of 0.1 to 1.0 g m^{-3} depending of course on the precipitation intensity and the drop size distribution. The condensation process involves the transition of a small fraction of the water vapor in the air to cloud droplets, whereas other processes must be postulated for the formation of the raindrops (Johnson, 1954, p 214-221). Fig. 4 shows a plot of a plausible distribution of water content over the entire range of drop size. Such a distribution is probably most applicable near the base of a precipitating stratiform cloud. The criteria by which this figure was drawn are that (1) the liquid water content contained in drops less than 0.2 mm is equal to that contained in drops greater than 0.2 mm (i.e. the areas beneath the two regions of Fig. 4 are equal, but this is not evident because of the logarithmic scale of the ordinate), (2) the distribution of cloud droplets is that

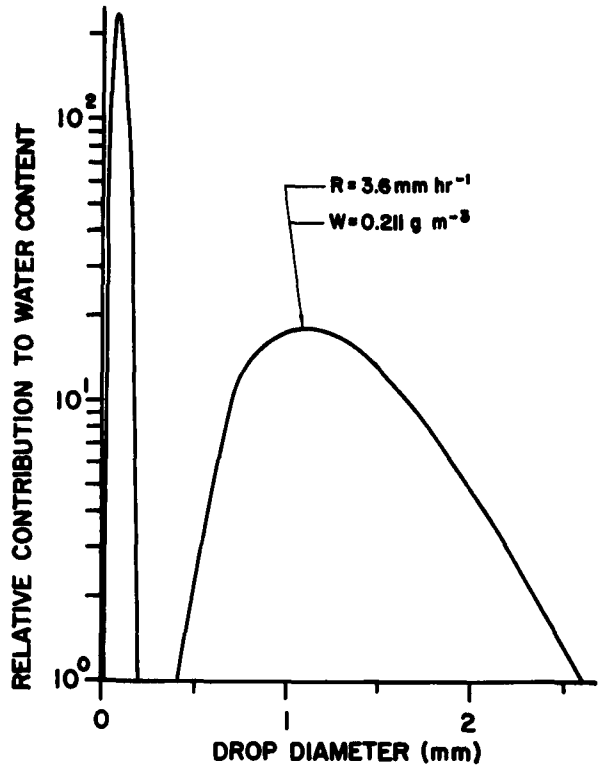

Fig. 4. Distribution of liquid water content with drop diameter.

given by aufm Kampe and Weickmann (1957) for an altocumulus cloud, and (3) the distribution of raindrops chosen was considered typical for a rainfall intensity of 3.6 mm hr^{-1}. The distribution of cloud droplets used for constructing Fig. 4 is probably not representative of an actual raincloud, but this is of little concern here. The main point is that near the lower section of the cloud there is approximately the same amount of liquid water in the cloud droplets and the raindrops (Fig. 4), and it is the task of the cloud physicist to explain the mechanism whereby such a distribution is established. The other point is that the distribution of liquid water throughout a precipitating cloud is by no means constant. For example, the top of a precipitating

cloud presumably has a uni-modal distribution of liquid water content which occurs at some intermediate drop diameter between the two modes shown in Fig. 4.

Currently there are two prevalent and mutually consistent theories which have application to the formation of precipitation. One of these considers the situation in which supercooled water droplets and ice crystals exist simultaneously within a cloud. The other considers the mechanism whereby a cloud produces raindrop-size particles at temperatures above 0C. The latter mechanism is referred to as the condensation-coalescence process and has been studied quantitatively by Bowen (1950). The success of Bowen's theory depends on the existence of an initial distribution of cloud droplets that includes at least a moderate number of very large cloud droplets. These larger cloud droplets have fall velocities which differ sufficiently from those of their neighbors that they begin the process of sweeping out smaller droplets. Such large initial droplets may occur through occasional collisions of small cloud droplets or through condensation on large sea salt nuclei which, at least in the tropics, are apparently present in approximately the required concentration (Woodcock, 1952). Numerous studies (Best, 1952; Mason, 1952; East, 1957) on the further growth of these large droplets show that they are capable of growing to precipitation size particles in reasonable lengths of times merely through the collision and capture of some of the smaller drops in their path. Favorable conditions for growth to raindrops include moderately strong updraft velocities, large liquid water contents, and cloud dimensions and wind fields such that the larger drops will not be carried

out of the top or the sides of the clouds.

The other theory of precipitation formation hinges on the observation that at temperatures below 0C clouds commonly consist of both ice crystals and liquid water drops. Such a mixture is unstable because the equilibrium vapor pressure with respect to water is greater than with respect to ice at the same temperature. The actual difference is zero at 0C, reaches a maximum at -12C, and then gradually decreases. Thus, provided that the total water content is sufficiently high, the ice crystals gain mass by sublimation at the expense of the liquid droplets which lose mass by evaporation. The tendency is to create a single ice phase of large particles which have a fall velocity downward relative to their neighbors. This theory was proposed by Bergeron (1935) and was further developed by Findeisen (1938). It is called the Bergeron-Findeisen theory (sometimes referred to as the ice-crystal process). The theory received definite quantitative support through the work of Houghton (1950) who showed that the growth rates are fast enough to produce sufficiently large ice crystals in times of the order of 10-30 minutes. As the ice crystals become larger, the diffusion process becomes less important compared with the growth which can now occur through coalescence as described by the Bowen theory. Thus, although clouds which everywhere have temperatures above 0C can only grow through the condensation-coalescence process, the frozen particles of a mixed cloud of ice crystals and supercooled cloud droplets are able to grow through the Bergeron-Findeisen process and in addition through the coalescence process during the latter part of their growth.

Drop-size distributions are such an intimate characteristic of the rain that it would be surprising if they did not reveal something of the processes which led to their formation. Unfortunately, many of the data collected on raindrop sizes have not taken account of the process by which the rain originated, and often even the synoptic features are inadequately described or lacking. Numerous drop-size spectra have been observed in temperate latitudes where the tops of the rain producing clouds invariably build to heights greater than the melting level. The data of Laws and Parsons and Marshall and Palmer shown in Fig. 3 are perhaps representative of the average drop-size distributions from widespread rain falling from clouds whose tops have a temperature of less than 0C. The Bergeron-Findeisen process of raindrop formation would undoubtedly have played a part in the development of these distributions.

Raindrop-size distributions from non-freezing clouds have been observed rather infrequently, and the most reliable values available are those of Blanchard (1953) for rain from orographic clouds over the island of Hawaii. Blanchard was able to sample the raindrop sizes at various heights up the side of a mountain which was often engulfed within the rainclouds. His results are shown in the curves of Fig. 5. Curves 1-3 were taken a few thousand feet above the cloud base. They show a relatively large number of small drops and a scarcity of the larger drops. Curves 4-7 were obtained near the cloud base and the trend toward fewer small drops and more large drops at this lower level is striking (i.e. compare curves 2 and 4 which have approximately the same intensity but quite different distributions). A second

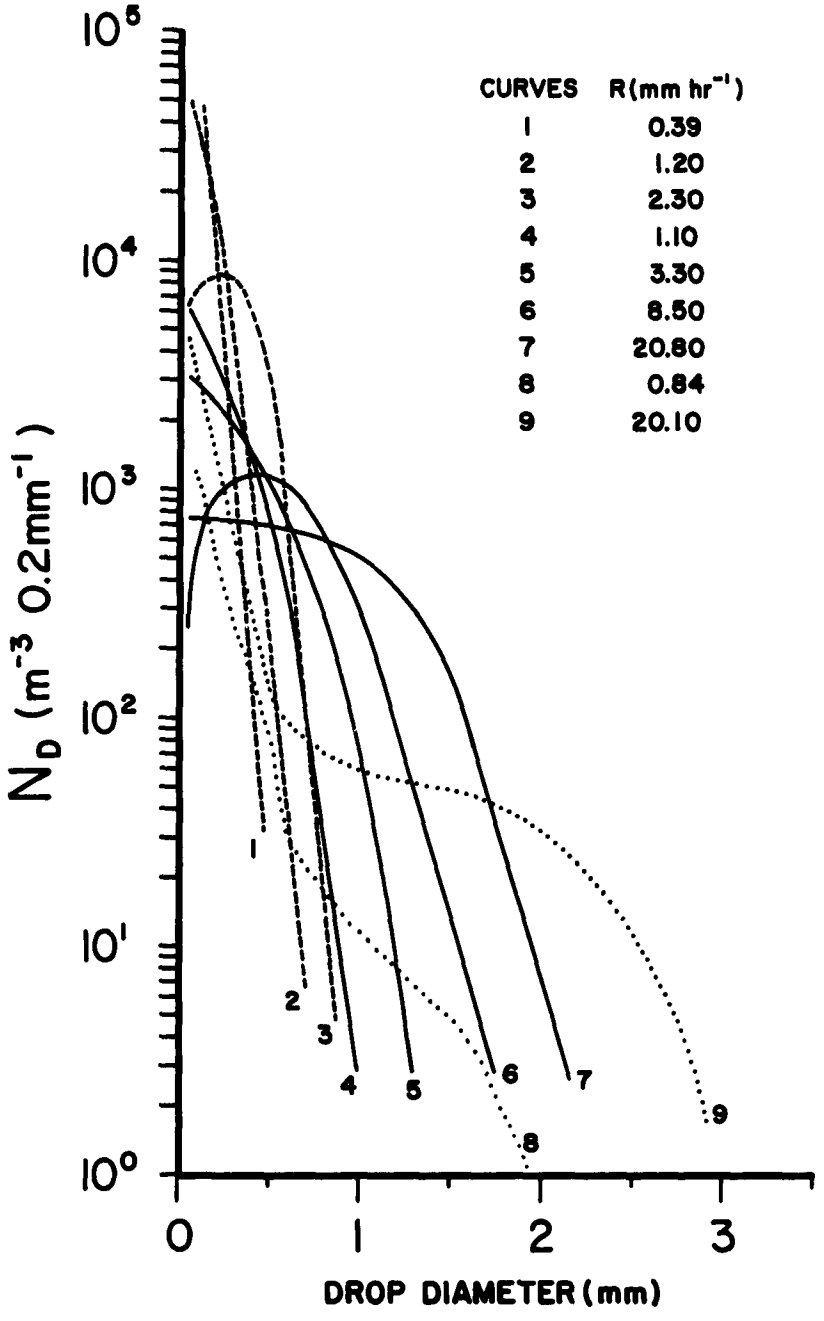

Fig. 5. Average raindrop-size distribution for Hawaiian orographic rain. Curves 1-3 are for measurements made at or near the dissipating edge of the cloud, about 1 - 3000 ft above the cloud base, while curves 4-7 represent samples taken at cloud base. Curves 8 and 9 are for non-orographic rain distributions (Blanchard, 1953).

feature of these curves is that, in general, the number of drops at the small end of the spectrum is an inverse function of the intensity. Blanchard thought that the scarcity of small drops at high intensities was caused by the large drops which tended to capture some of the drops in their path. It is shown in Section 3 that this is undoubtedly the primary cause for the change in the distribution with height.

Blanchard also observed distributions from rains of non-orographic origin. These rains fell from several different storms, but in all cases the clouds extended higher than the melting level. Therefore, it is probable that the Bergeron-Findeisen process was effective in precipitation formation. Curves 8 and 9 of Fig. 5 are averages of some of the non-orographic rain distributions. These curves have high concentrations of small drops, and a considerably flatter distribution for the middle and large sized drops (i.e. the slope became less negative at these larger drop sizes). At least at the larger drop sizes the general slope of distributions 8 and 9 can be approximated by the empirical relationship given by either Eq. (4) or (6) in contrast to curves 1-7 of Fig. 5 which, in general, have considerably steeper slopes. This can be taken as evidence that Eqs. (4) and (6) are most useful in describing the average shape of the drop-size distribution for rain which was initiated through the Bergeron-Findeisen process.

One other pertinent piece of work on this problem has been presented by Todd (1960, p 402). In conjunction with the Santa Barbara Cooperative Seeding Project, Todd studied the physics of storms which occurred along the coast of

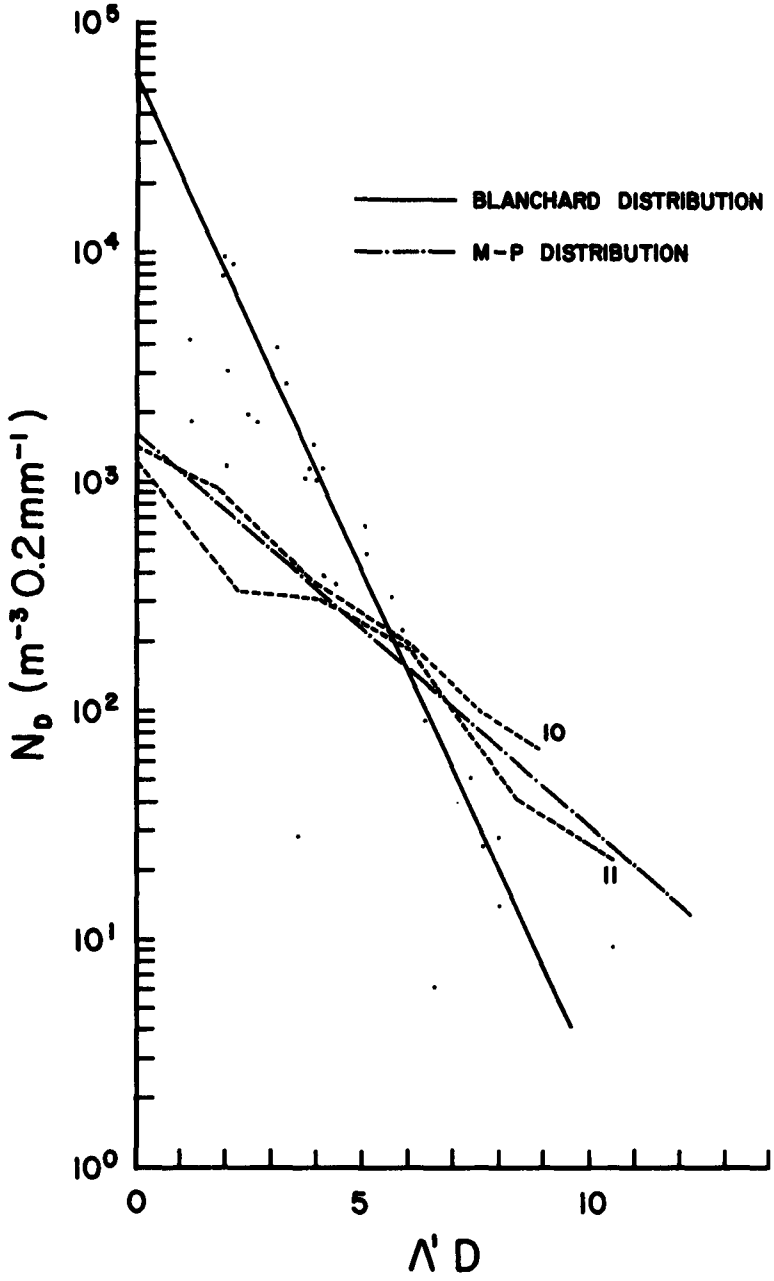

Fig. 6. Raindrop-size distributions from warm clouds (dots) and from clouds with tops above the melting level (Sample 10 and 11). Blanchard and M-P distributions are indicated by the solid line and the dash-dot line respectively (Todd, 1960).

California. Using radar he was able to determine whether the rain came from warm clouds (i.e. temperatures above 0C throughout the cloud depth) or whether part of the cloud was at heights above the melting level. The distributions that were observed under these two conditions are revealing. Fig. 6 is a summary of the results. The abscissa is $\Lambda'D$ which is proportional to ΛD of Eq. (4), and its use permits the distributions of all intensities to be readily compared. Nine samples from warm clouds were collected and these data are given as dots. The straight solid line which is drawn represents an idealized distribution derived from Blanchard's data. The distributions marked 10 and 11 are samples taken after the ice-crystal process was initiated, and these agree very well with the M-P distribution. Todd also remarks that sometimes the drop-size distribution indicates that both processes occur together. However, the almost inescapable conclusion is that the distributions of rain initiated by the ice crystal process have a flatter slope than the distributions which are observed if rain develops entirely by the coalescense process. Offhand this may suggest that the ice crystal process is more effective for precipitation growth. However, it must be remembered that many other factors are important in shaping the distribution of raindrops. It is possible that the clouds which have tops whose temperatures are below freezing are also considerably deeper than warm clouds. Thus, drops in the deeper cloud have a longer period of growth during their traverse through the cloud. In addition, the vertical velocity profile has an important bearing on the length of time a drop remains within a cloud. All of these factors must be taken into account

before the many aspects of drop-size distributions can be adequately explained.

Since 1958 numerous raindrop-size measurements have been made in India under various meteorological conditions. Sivaramakrishnan (1961) has studied the raindrop spectra from thunderstorms, from warm-process rains, and from rain resulting from the ice-crystal process. The data which he presents do not suggest any firm conclusions as to the basic differences between these three types of rain, except that the samples from the thunderstorms have relatively greater numbers of large drops as compared with the two other types of rain. Sivaramakrishnan was primarily interested in the relationship between the rainfall intensity and (1) the median volume diameter, D_o, (2) the rain water content, W, and (3) the radar reflectivity factor, Z. His conclusions that (1) any two of the four raindrop-size quantities (R, D_o, W, Z) fix the other two, and that (2) the rain intensity corresponding to most size spectra can be represented by a uniform collection of drops with size equal to D_o are similar to those given by Atlas and Chmela (1957). However, it is interesting that these same conclusions were deduced from observations of rain from different climatic regions of the world. In a somewhat similar fashion Srivastava and Kapoor (1961) collected data at New Delhi, India. They studied the drop-size distributions of rain from thunderstorms and from layer type clouds whose tops were above the melting level. They found that the distributions from the thunderstorms were considerably more variable than the distributions from the stratiform clouds, although their results are not basically different from earlier investigators.

A detailed analysis of raindrop-size data from monsoon rain at Delhi, India, a station situated about 700 miles inland, and at Khandala, a high level station near the west coast of India has been made by Ramana Murty and Gupta (1959). At low intensities these authors found the distributions to be roughly similar to that given by the M-P distribution. As the rainfall intensity increased the distribution exhibited a rather flattened section at the intermediate drop sizes. Such a feature has been observed by several investigators, particularly in the temperate latitudes (Atlas and Chmela, 1957; Imai, 1960; Mason and Andrews, 1960; Dingle and Hardy, 1962). Dingle and Hardy (1962) suggested that the factors which would contribute to the formation of such a distribution are (1) splash and/or aerodynamic break-up of the largest drops which gave the observed increase in the number of the smaller drops, and (2) an effective sorting of drops by the wind field and by gravity during the early stages of rain which tends to give a relative increase in the number of the larger drops. An entirely different explanation has been given by Ramana Murty and Gupta for the monsoon rains. They postulate that the distribution results from a combination of the ice-crystal and coalescence processes acting together. The explanation depends on the rather surprising statement that a raindrop formed through the coalescence process on a cloud droplet of relatively large size is smaller than the raindrop grown on a droplet which is smaller initially. Since there are initially many more small cloud droplets than large ones, on the above basis this pattern must be reversed when the drops grow to raindrop size. By superposing this coalescence produced distribution

onto an exponential distribution, which is characteristic of rain from an ice-crystal process, the authors show that a distribution with a rather flat section over a certain intermediate size range will develop. The validity of their hypothesis depends on their conception of the development of a drop-size distribution through the coalescence process. In fact, Bowen (1950) does show that under certain conditions of cloud depth and updraft velocities the smaller cloud droplets have a longer residence time in the cloud and, therefore, it is possible for them to grow into some of the larger raindrops. However, observations of a raindrop-size distribution in which more large drops are present than small drops for a rain which formed through the coalescence process are indeed very rare. It would appear that the actual processes responsible for the distribution with a flattened central section must await further observations and research.

Sivaramakrishnan (1960, 1961), in addition to observing the drop-size distribution, made measurements of the electrical charge carried by rain at Poona, India. He observed that for raindrops to have appreciable charge they must have started as ice or at least have been in the form of ice for some part of their history. On the other hand, non-freezing rain was found to have less or no electrical charge. On this basis, Sivaramakrishnan claims that the measurement of the amount of electrical charge carried by the rain affords a method of identifying the process which initiated the rain. Further studies along these lines should help in explaining some of the observed characteristics of raindrop-size spectra.

It appears firmly established that the precipitation growth process affects the raindrop-size distribution, but

as yet it has not been possible to describe these effects quantitatively. Two factors capable of affecting the drop-size distribution observed at the ground are (1) the wind shear which sorts out the drops in a manner similar to a mass spectrograph (Appendix D), and (2) evaporation between the cloud base and the ground. The evaporation of raindrops and the effect of collisions between raindrops and (1) cloud droplets and (2) other raindrops are investigated in Section 3.

In general, the large scale cloud dynamics are not considered in this study. Unfortunately, it is the details of the air motion which often dictate whether precipitation will form, but a concise description of the laws governing such motion are not firmly established. Atlas (1962) states: "The field of vertical motion is a direct key to our understanding of storm dynamics, and storm dynamics is the missing link in all our theories of precipitation physics". Although it has not been possible to account for the possible atmospheric motion, it is hoped that the research reported here will contribute to our knowledge of the processes governing the formation of precipitation.

3. THE DEVELOPMENT OF RAINDROP-SIZE DISTRIBUTIONS AND IMPLICATIONS RELATED TO THE PHYSICS OF PRECIPITATION

3.1 PRELIMINARY REMARKS

The photoelectric raindrop-size spectrometer (Appendices A and D) provides data on the absolute end product of the precipitation process: namely, raindrop-size distributions at one point on the earth's surface. A logical extension is to inquire into the possible variations of the distribution with height. Such an investigation is undertaken because (1) it provides information on the raindrop-size spectra in regions which are commonly observed by radar, and (2) it contributes to our understanding of the factors affecting the growth and evaporation of raindrops.

Coalescence, accretion, and evaporation processes and their effect on the raindrop-size distribution are considered. Coalescence as used in this study, refers to the collision and joining together of two raindrops. Accretion is the growth of a raindrop by the collision and collection of cloud droplets.[1] Although coalescence and accretion appear to be identical processes, a distinction is made because the effect of the two processes on the raindrop-size distribution is quite different. In addition, the method of investigating the two processes requires a different approach as will be shown in Sections 3.2 and 3.3. The evaporation process

---

[1]The meteorological literature is divided on the use of the word "accretion". Some writers use the definition as given above, whereas others define accretion as the growth of a precipitation particle by the collision of an ice crystal or snowflake with a supercooled liquid droplet which freezes on contact. To clarify this unfortunate situation

refers to the decrease in size of the raindrops as they fall through an atmosphere which is not saturated.

Throughout all the work in this section, it is assumed that at the initial height a constant distribution of raindrops is available (although any initial distribution may be assumed for a given computation). The change in this distribution as it falls to the ground is then determined assuming "steady-state": that is, the change in the distribution with height is considered, but the distribution at each height remains constant with time. In general, the establishment of steady-state conditions requires the length of time it takes for the smallest drop in the distribution to move from the initial top layer to the bottom layer. This time may be in the order of an hour for a fall of 2 km, although if drops of less than 0.4 mm diameter are ignored the time for steady-state to be established is reduced by a factor of about 3. The assumption of steady-state limits the application of the results to those situations in the atmosphere which approximate steady rain over periods of more than an hour.

---

the following definitions of the major processes of growth (excluding condensation and sublimation) are suggested:

coalescence - collision and joining together of two raindrops

accretion - growth of a raindrop by the collision and collection of cloud droplets

coagulation - growth of an ice crystal by the collision of supercooled liquid droplets which freeze on contact

agglomeration-the clustering together of ice crystals or aggregates thereof

These definitions are not wholly different from those in common usage, except that aggomeration as currently applied does not distinguish between the phase of the colliding particle.

Rigby and Marshall (1952) and later Rigby, Marshall and Hitschfeld (1954) investigated the problem of the change in raindrop-size distribution with distance fallen. They started with an initial M-P raindrop-size distribution and considered the changes brought about by collisions among raindrops, by accretion of cloud droplets, and by evaporation, assuming a steady flux of drops at the initial level. They state that they were justified in starting with the M-P distribution within the cloud because "the changes in the form of the distribution are found to be slight: an exponential type of distribution law would seem to be applicable at all heights". They took this result to mean, "that the processes investigated cannot by themselves produce the distributions observed at the ground from distributions of a very different sort, or from the broad distributions of snow".

In considering the coalescence between raindrops, Rigby, et al. derived integral equations for determining the change in drop-size distribution. They obtained the average change in the drop diameter and in the concentration of drops over a fixed height interval and solved the equations graphically. They realized that not all drops of a given diameter would change by this average amount because the number of coalescences between drops of two different diameters is a statistical process. There are also other difficulties with their procedure which will be explained later.

The methods which Rigby et al. used for evaluating the change in the distribution due to accretion of cloud droplets and evaporation are quite standard and will be indicated in Sections 3.3 and 3.4. On the other hand, the distributions

discussed by Rigby, et al. are limited to the exponential ones given by Eq. (4), and the accuracy of their computations depends on the assumption that the slope of the distribution remains constant. This latter assumption usually introduces an error in the final result, but the error is quite small for all processes whenever the distance of fall is less than 1 km and the intensities are less than 25 mm hr^{-1}.

Mason and Ramanadham (1954) have also studied the problem of the modification of the size distribution of raindrops with distance fallen. They similarly treat the coalescence between raindrops, growth through accretion of cloud droplets, and evaporation. They state:

> If a constant flux of raindrops having an exponential size distribution occurs at the level of origin just below the melting level in a layer-cloud to give a steady-state, this initial distribution will undergo considerable modification after a fall of 1 km, the smaller drops being seriously depleted and the larger ones increased.

The method used by Mason and Ramanadham is more realistic than that of Rigby, et al. They considered the change in the drop-size distribution over successive small height intervals. They did not use a computer, and since their method involved a tremendous number of calculations, they were only able to present one complete case. Nevertheless, this one case indicated that important changes in the distribution occurred even over relatively short distances.

In recent years the availability of electronic computers has made possible the solution of many problems which otherwise were much too lengthy to carry out. One such problem is the development or modification of raindrop-size distributions. As will be seen in the following sections this is

a multi-particle problem, the solution of which lends itself to digital methods. The computer provides solutions for any combination of initial conditions, and it therefore becomes very easy to study the influence of a particular variable. The processes of coalescence, accretion, and evaporation are presented separately but in the final computer program they are combined in pairs appropriate to the atmospheric conditions.

3.2 COALESCENCE OF RAINDROPS

3.2.1 Theoretical considerations

Let us consider drops of diameter D_i and D_j ($D_i < D_j$) in concentrations of N_i and N_j and with velocities v_i and v_j respectively. It is assumed that all drops of diameter D_i which collide with the D_j drops are captured. This is assuming a collection efficiency of one, but this value may be altered if better information is available. Consider the drop of diameter D_j in Fig. 7 falling through a layer of thickness Δz in time Δt. During the time Δt, the drops of diameter D_i fall a distance of $v_i \Delta t$. Now $\Delta t = \Delta z / v_j$ and therefore the small drops fall a distance given by $(v_i/v_j)\Delta z$. It is clear from Fig. 7 that all drops of diameter D_i in the cylinder of height $(1 - v_i/v_j)\Delta z$ and diameter $D_i + D_j$ will be picked up by the drop of diameter D_j while it falls a distance of Δz. The volume of this cylinder is given by,

$$(\pi/4)(D_i+D_j)^2(1-v_i/v_j)\Delta z \ . \qquad (9)$$

Now N_i is the number of drops of diameter D_i per unit volume. Therefore, the total number of drops picked up by the single drop of diameter D_j as it falls a distance Δz is

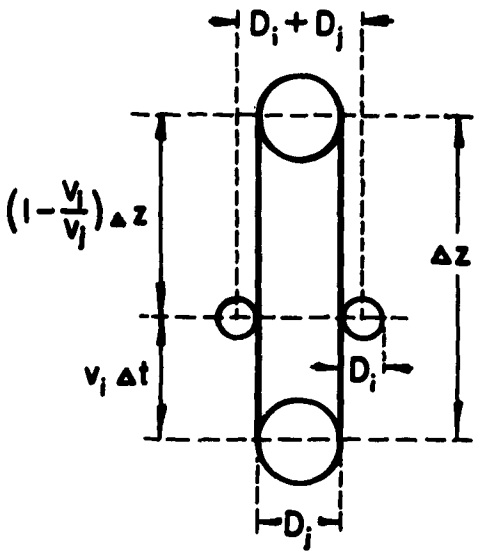

Fig. 7. Coalescence of raindrops

$$(\pi/4)(D_i+D_j)^2(1-v_i/v_j)N_i\Delta z \ , \tag{10}$$

and the number of drops picked up by the N_j drops per unit volume is

$$\Delta N_j = (\pi/4)(D_i+D_j)^2(1-v_i/v_j)N_iN_j\Delta z \ . \tag{11}$$

Eq. (11) which was originally derived by Rigby and Marshall (1952) gives the number of drops of diameter D_j per unit volume which have coalesced with a drop of diameter D_i in time Δt.

Let ΔN_i be the number of drops of diameter D_i per unit volume which are depleted between the top and bottom of the layer of thickness Δz. It is important to realize that ΔN_i is not equal to ΔN_j. Fig. 8 illustrates the derivation of an expression for ΔN_i. The number of drops of diameter D_i

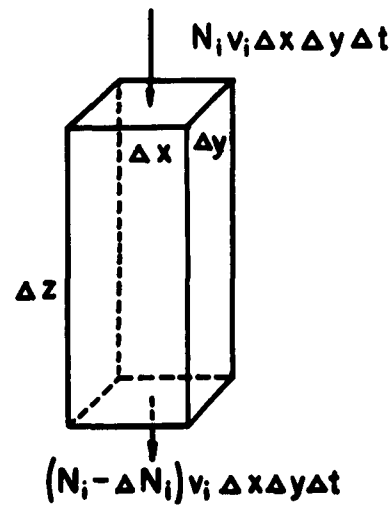

Fig. 8. Flux of drops of diameter D_i.

entering the top surface of the column in time Δt is $N_i v_i \Delta x \Delta y \Delta t$. Similarly the number of drops of diameter D_i leaving the bottom surface of the column in time Δt is $(N_i - \Delta N_i) v_i \Delta x \Delta y \Delta t$. Since $v_j = \Delta z / \Delta t$, it is seen that the number of drops of diameter D_i which are depleted per unit volume in time Δt is given by $(v_i / v_j) \Delta N_i$. But this is identical to ΔN_j, and therefore

$$\Delta N_i = (v_j / v_i) \Delta N_j \quad . \tag{12}$$

By using Eqs. (11) and (12) it is possible to determine the change in distribution throughout the layer Δz.

3.2.2 Computational methods

Although Eqs. (11) and (12) are easily derived, care must be taken in using them in an actual computation. It is clear

that both ΔN_j and ΔN_i are a function of N_j and N_i, and therefore the chosen height interval, Δz, must be small enough that both ΔN_j and ΔN_i are small with respect to N_j and N_i respectively. At the completion of each computation the values of N_j and N_i are appropriately adjusted. Another reason for choosing small height intervals is the requirement that the probability of a particular drop of diameter D_j picking up more than one drop of diameter D_i must be kept small or otherwise the computations would become very complicated. Initially, height intervals as small as 10 m were used, but it was soon found that intervals up to 100 m could be used without affecting the final result. Table 2 gives a few representative values of N_j and $\Delta N_j/Nj$ for various combinations of D_j and D_i and for a height interval of 100 m. The initial distribution is exponential with an intensity of 2.8 mm hr^{-1}. Table 2 shows that the value of $\Delta N_j/N_j$ is small in all cases except when D_i is small and D_j is large. However, the diameter of the combined drop is given by $(D_j^3 + D_i^3)^{1/3}$ which is very nearly equal to D_j whenever $D_j >> D_i$. Therefore, the coalescences between drops of diameter D_i and D_j for $D_j >> D_i$ do not significantly alter the concentration of the larger drops. However, the number of drops of diameter D_i which are depleted by the D_j drops must still be considered.

Fig. 9 shows a typical distribution and the change that is brought about through the coalescence of drops of diameter D_i and D_j. First the values of ΔN_j and ΔN_i are computed from Eqs. (11) and (12) respectively and the new value of N_i is given by $N_i - \Delta N_i$. The drop diameter and velocity after coalescence are designated as D_c and v_c

most sensitive to the shape of the distribution. In view of these results it is seen that the order of the computations does not materially affect the final distribution. In the final program the initial value of i is 1 and j = i+1, i+2, ..., n, then i is changed to 2 and j again varies from j = i+1, i+2,....., n, and so on until i = n-1 and j = n.

The effect of the height interval chosen for the computation is shown in Table 4. The initial distribution is the same as that used in Table 3. Column 3 of this table gives the change in the distribution using 10 height intervals of 10 m each; the fourth column is the distribution after 5 height intervals of 20 m each, and the fifth column gives the distribution after 2 height intefvals of 50 m each. It is clear that for a given distance of fall, the use of 50 m height intervals gives essentially the same change in the distribution as the 10 m height intervals. It was later shown for a different initial distribution that 100 m height intervals do not give significantly different results than the 50 m height intervals, whereas at 200 m intervals larger differences begin to appear. Therefore, 100 m intervals were used in subsequent computations.

Throughout all this work discrete drop diameter intervals are used to describe what is essentially a continuous distribution. In addition it is necessary to maintain these intervals throughout the course of a computation. Reference to Fig. 9, for example, shows that the drop diameter, D_c, lies between two classes, and therefore the $\Delta N'_j$ drops must be appropriately distributed between the classes which it straddles. For most cases D_c is just slightly larger than D_j. Thus, for D_j = 1.0 mm and D_i = 0.2 mm, D_c = 1.024 mm.

Table 4. Coalescence process. Effect of varying the height interval.
R = 2.8 mm hr^{-1} and total fall is 100 m.

Drop Dia. mm	Initial Conc. (m^{-3} 0.1 mm^{-1})	Height Increment (m) 10	20	50
0.1	5690	2676	2662	2619
0.2	3200	2432	2429	2420
0.3	1820	1556	1555	1553
0.4	1010	907	907	906
0.5	569	524	524	524
0.6	320	300	300	300
0.7	182	173	173	174
0.8	101	98	98	98
0.9	56.9	56.3	56.3	56.3
1.0	32.0	32.4	32.4	32.4
1.1	18.2	18.9	18.9	18.9
1.2	10.1	10.8	10.8	10.8
1.3	5.69	6.20	6.19	6.20
1.4	3.20	3.56	3.57	3.57
1.5	1.82	2.05	2.05	2.05
1.6	1.01	1.17	1.17	1.17
1.7	0.569	0.66	0.66	0.66
1.8		0.17	0.17	0.18
1.9		0.03	0.03	0.024

For this case the fraction 0.024/0.1 of $\Delta N_j'$ is taken and added to the class which is centered about D = 1.1 mm. In effect this causes a slight exaggeration to the drop growth. If this is a significant fault, then it should become evident if the class interval is changed. Table 5 shows the effect on the distribution due to the class interval chosen. Columns 3, 4, and 5 are for class intervals of 0.1, 0.05 and 0.025 respectively. Only very minor changes are observed with the change in the class interval, and these are probably caused by inaccurate drop velocity interpolations as the class interval changes. It is concluded from this

Table 5. Coalescence process. Effect of varying the class interval. $R = 2.8$ mm hr^{-1}, and total fall is 1 km using 100 m height intervals.

Drop Dia. (mm)	Initial conc. (m^{-3} 0.1 mm^{-1})	Concentration (m^{-3} 0.1 mm^{-1}) Drop diameter Class interval (mm) 0.1	0.05	0.025
0.1	5690	5.45	6.20	6.20
0.2	3200	250	252	248
0.3	1820	435	431	427
0.4	1010	412	410	414
0.5	569	318	329	321
0.6	320	222	225	226
0.7	182	150	151	150
0.8	101	93.9	97.0	96.8
0.9	56.9	60.8	61.0	61.4
1.0	32	38.1	38.5	38.8
1.1	18.2	24.5	24.4	24.3
1.2	10.1	15.2	15.1	15.1
1.3	5.69	9.26	9.0	9.15
1.4	3.2	5.65	5.40	5.47
1.5	1.82	3.34	3.24	3.22
1.6	1.01	2.02	1.92	1.90
1.7	0.569	1.26	1.19	1.14
1.8		0.89	1.11	0.93
Z ($mm^6 m^{-3}$)	305	436	429	431

table that the 0.1 mm class intervals adequate represent the distribution, and that no significant errors are introduced by the computational methods.

3.2.3 Effect of coalescence on a raindrop-size distribution.

The results of one computation of the effect of coalescence on the distribution are shown in Fig. 10. The initial distribution is one suggested by Mason and Ramanadham, and the new distribution after a fall of 1 km is the one obtained using the methods outlined above. Mason and Ramanadham's result is also shown. Their final distribution indicates less change than that obtained here, although the agreement on the whole is quite good. Their points clearly do not follow a smooth curve, and it may be that their method did not allow them to carry out the computations to the refinement which is obtainable with modern computers. The initial distribution of Mason and Ramanadham extends to a drop diameter of 1.7 mm, and their final distribution to 1.8 mm. Coalescence produces drops of larger diameter, but these are in relatively small concentrations. Further remarks on this point are made later when it is shown that the concentration of larger raindrops observed at the ground must be present in only slightly reduced concentrations 2 km above the ground.

3.3 THE GROWTH OF RAINDROPS THROUGH ACCRETION OF CLOUD DROPLETS

3.3.1 Theory and computational procedure

It is necessary to determine the growth of a raindrop as it falls a distance Δz through a cloud of liquid water content (LWC) equal to M. The volume swept out by the drop in

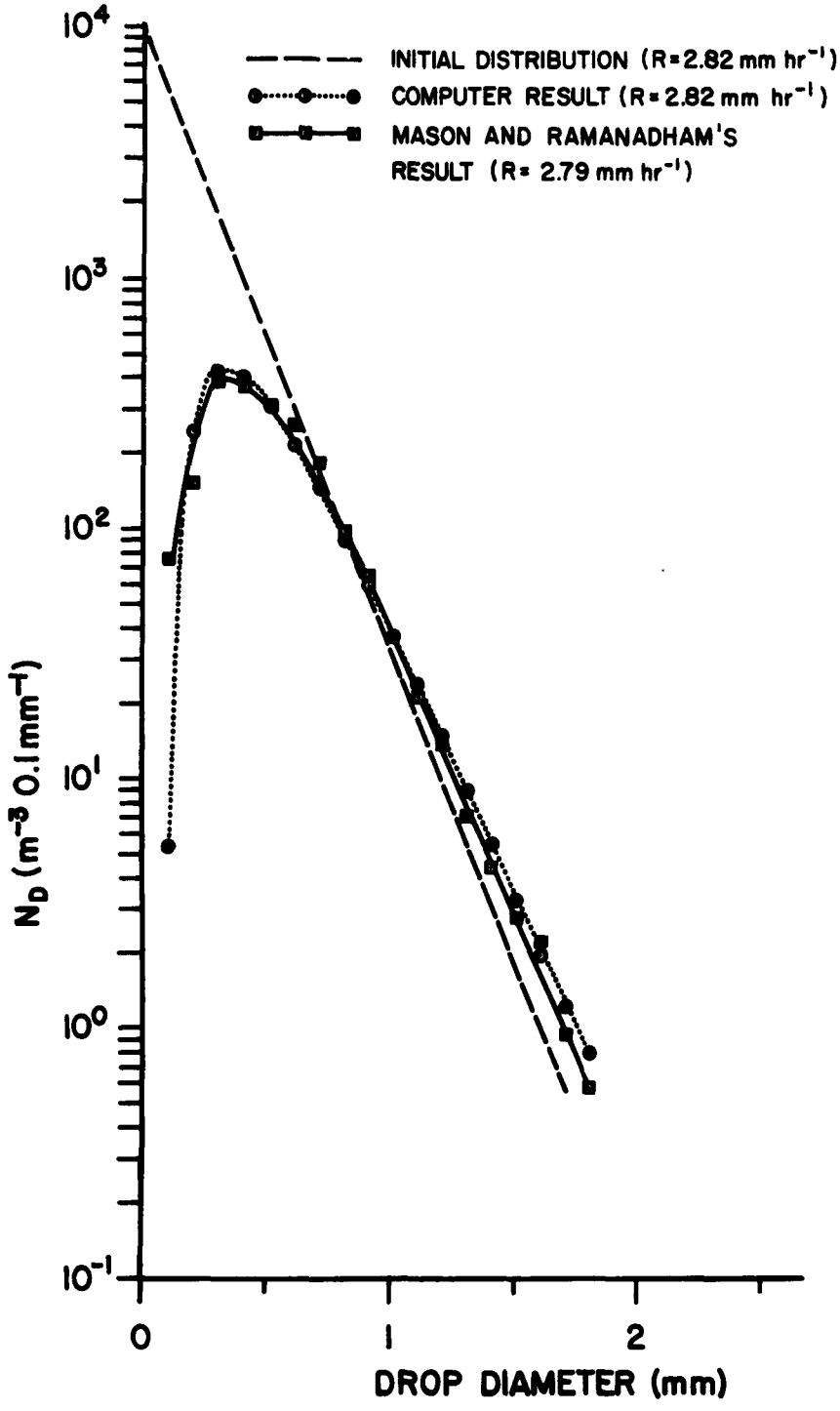

Fig. 10. The modification of the raindrop-size distribution due to coalescence for a fall of 1 km.

falling a distance Δz is $\frac{\pi}{4}D^2\Delta z$. If we assume that the raindrop coalesces with the cloud droplets in its path with an efficiency E and that the cloud droplet velocity is negligible compared with the raindrop velocity, then the total mass of cloud droplets picked up by the raindrop is $EM\frac{\pi}{4}D^2\Delta z$. The mass of the raindrop is given by $\frac{\pi}{6}\rho D^3$, where ρ is the density of water. The change in mass of the drop in falling the distance Δz is $\frac{\pi}{2}\rho D^2\Delta D$. Now the change in mass of the raindrop must equal the mass of cloud droplets which are picked up, and therefore

$$\frac{\pi}{2}\rho D^2\Delta D = EM\frac{\pi}{4}D^2\Delta z \ , \tag{14}$$

or

$$\Delta D = \frac{EM}{2\rho}\Delta z \ . \tag{15}$$

Eq. (15) describes the manner in which the raindrop grows through the process of accretion. The process of growth is caused by many collisions with cloud droplets, and for this reason the treatment of accretion is different than the single collision process considered as coalescence.

The quantity E of (15) is difficult to evaluate. Several investigators have studied the problem over the last 15 years, but the results are not consistent. Langmuir (1948b) first presented comprehensive values of E. He defined E as the ratio of the actual collision cross-section of the droplet to the true cross-section of the raindrop ($\pi a^2/\pi b^2$ in Fig. 11). It can be seen that if the cloud droplet is considered as having a finite diameter, then the value of E could be greater than one. For example, the trajectory to the left in Fig. 11 yields a collision efficiency of $E = c^2/b^2$. Langmuir's values are shown in Fig. 12 for all

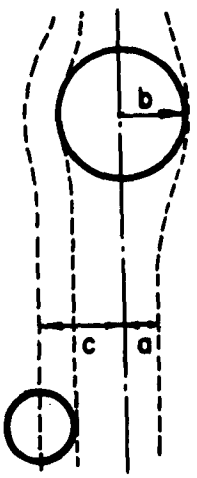

Fig. 11. Representation of the trajectory of a small drop relative to a larger one.

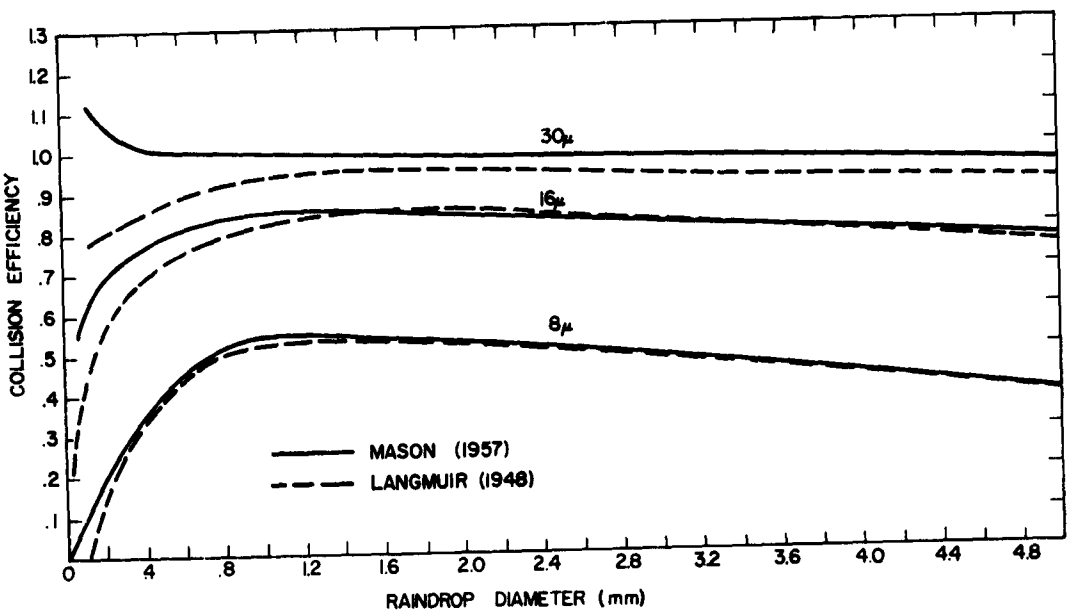

Fig. 12. Collision efficiencies between cloud droplets and raindrops under the force of gravity.

sizes of raindrops and for fixed values of the cloud droplet diameter. Later Mason (1957), making use of the data of Das (1950) and Fonda and Herne (unpublished), presented collision efficiencies computed by assuming more realistically that droplets have a finite size. These are also shown in Fig. 12. For raindrops larger than 1.2 mm diameter there is very good agreement between Langmuir's results and those published by Mason. However, for smaller drops the departure becomes increasingly evident, and for raindrops less than 0.4 mm in diameter there is a wide discrepancy between the results. Of course raindrops with diameters less than 0.4 mm are within a factor of 10 of the diameter of the larger cloud droplets, and it is expected that the trajectories would be influenced by the presence of each drop.

Gunn and Hitschfeld (1951) attempted to determine the collection efficiency[1] between water drops 3.2 mm in diameter and cloud droplets. The cloud droplets were produced by either condensation (diameter = 4-40μ) or atomization (diameter = 14-100μ). Within the limits of experimental error the collection efficiency agreed with Langmuir's calculated values of the collision efficiency which would indicate that every collision resulted in collection.

The values of E as given by Mason for a cloud consisting of droplets of diameter 16μ are used throughout this study. It is seen later that the error in estimating E is compounded by the lack of measurements of M, and it is probable that not much is gained by attempting to obtain more representative values than those given in Fig. 12.

[1]collection efficiency = collision efficiency x fraction of collisions resulting in collection

The evaluation of the change in the raindrop-size distribution due to growth through accretion of cloud droplets is somewhat easier than for the coalescence process. Assuming a certain value of cloud LWC, M, and using the values of E as explained above, ΔD is computed for a fixed height interval Δz from Eq. (15). Each class interval is shifted by an amount ΔD, but because the raindrops increase in size, their fall velocity also increases causing their volumetric concentration to decrease. Provided that such a process is accounted for, the effect of accretion can readily be calculated.

Within a cloud, the raindrop size distribution is modified, both through coalescence between raindrops and through the accretion of cloud droplets. These processes act simultaneously, but because of the discrete nature of the

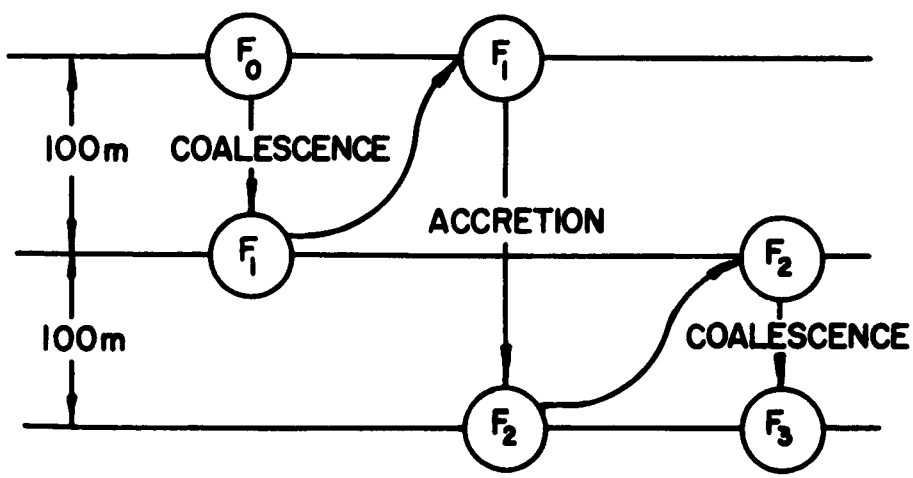

Fig. 13. Illustration of coalescence and accretion computation.

computations used here it is possible only to treat them sequentially. Nevertheless, it is possible to determine their combined effect within a layer of the atmosphere. For reasonable values of M and Δz the change in drop diameter given by (15) is small, and no significant error arises if the effect of accretion on the distribution is computed over a 200 m interval. Thus, the effect on the distribution due both to coalescence and accretion is computed in a manner illustrated in Fig. 13. The initial distribution at the top surface is represented by F_o. The change in this distribution due to coalescence is computed over a 100 m layer producing the distribution F_1. Then the change in F_1 due to accretion over a 200 m layer is computed to give the distribution, F_2. Finally the change in F_2 due to coalescence over the lower 100 m layer is computed. The final distribution, F_3, is assumed to be the result of coalescence and accretion computed over a 200 m layer.

3.3.2 Effect of coalescence and accretion on a raindrop-size distribution

Fig. 14 shows the effect of coalescence and accretion over a distance of 1 km using an initial distribution identical to that of Fig. 10. The assumed cloud LWC is 0.2 g m^{-3}. The effect of including the accretion process is to decrease the slope of the distribution and to reduce the concentration of the smaller drops. Mason and Ramanadham's result is also shown in Fig. 14. Their computation does not indicate such a marked change. The reason may be due to the different method of computing the change due to accretion. Mason and Ramanadham computed the change in drop diameter due to accretion for the full distance of 1 km, whereas the results

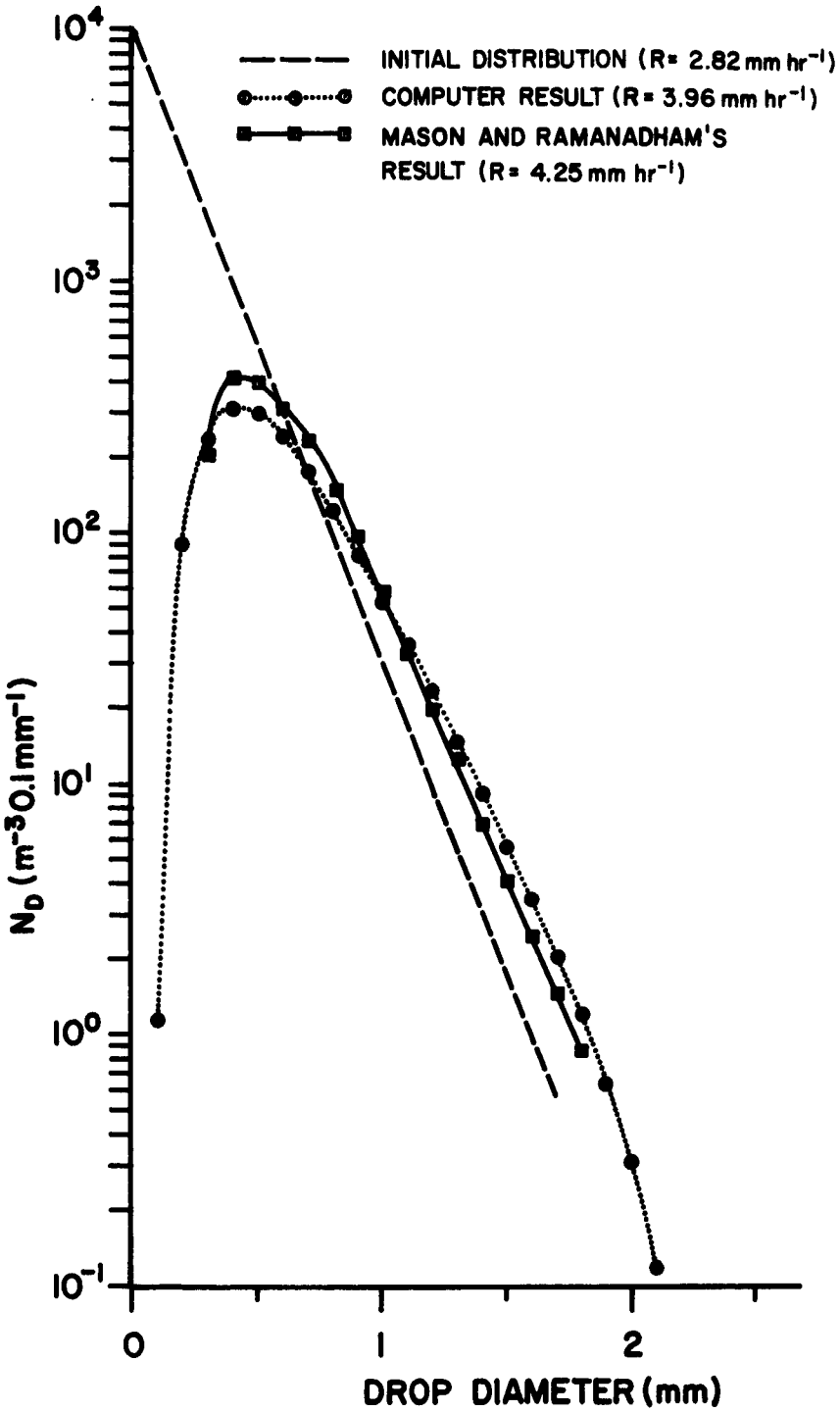

Fig. 14. Modification of the raindrop-size distribution due to coalescence and accretion for a fall of 1 km.

reported here were obtained by computing the accretion effect over 200 m height intervals, and for this reason the latter should be more representative. Fig. 14 also shows that with the computed distribution, drops greater than 1.8 mm appear in fairly high concentrations, whereas Mason and Ramanadham's computation did not indicate drops beyond 1.8 mm. In brief, the distribution obtained with the computer techniques outlined here shows a smaller number of small drops and a larger number of larger drops as compared to the distribution of Mason and Ramanadham. Unfortunately, experimental data for this case are lacking.

The ratio of the Z value of the initial distribution to that of the final distribution indicates a larger value than is normally observed with radar under conditions judged to be comparable. The explanation of this may lie in the unrepresentativeness of the distribution at the top of the layer in which many small drops are assumed to occur. It is the large number of small drops, which are shifted to larger diameters through coalescence and accretion, which produces a marked increase in the value of Z. This work points to the urgent need of measurements of raindrop-size distributions in the cloud and at the ground and also simultaneous radar observations.

3.4 THE EFFECT OF EVAPORATION ON RAINDROP-SIZE DISTRIBUTIONS

The evaporation from a freely falling raindrop depends on the temperature and relative humidity of the atmosphere and the drop diameter. Gunn and Kinzer (1951) have determined values of the change in mass of the raindrop with time $(\frac{dm}{dt})$ as a function of the above three variables. They present their results in two tables. A method to obtain

values of $\frac{dm}{dt}$ for any reasonable combination of temperature, relative humidity (RH), and drop diameter, based on Gunn and Kinzer's tabulated values, is given in Appendix C.

Since the mass of a drop is given by $m = \frac{\pi\rho D^3}{6}$, it is easily shown that

$$\frac{dD}{dt} = \frac{2}{\pi\rho D^2} \frac{dm}{dt} \frac{\Delta z}{v} , \tag{16}$$

or

$$\Delta D = \frac{2}{\pi\rho D^2} \frac{dm}{dt} \frac{\Delta z}{v} , \tag{17}$$

where v is the drop velocity, and Δz is the fall distance in time Δt. Eq. (17) is used to determine the decrease in drop diameter due to evaporation in falling a distance Δz. The mean velocity of the drop within the layer should be used for v, but for normal temperatures and RH, and for a fall distance of 200 m, the value of ΔD is very small, and negligible error arises by using the drop velocity appropriate to the drop diameter at the top of the layer.

The procedure for determining the change in the raindrop-size distribution due to evaporation is quite similar to the procedure described in Section 3.3.1 for the accretion process. The difference is that with accretion the drops increase in diameter, whereas with evaporation the drops decrease. The one difficulty with evaporation is that some of the small drops disappear as they fall through the distance Δz. For these cases the use of Eq. (17) introduces a small error because both $\frac{dm}{dt}$ and v are changing quite rapidly.

The effect of evaporation on the drop-size distribution is calculated starting with the computed distribution shown in Fig. 14. The entire sequence is as follows: first an exponential drop-size distribution is assumed at the top of

a layer of cloud, and the change in this distribution is calculated for a fall of 1 km through a cloud with a LWC of 0.2 g m^{-3}. The resulting distribution is then assumed to be at the base of the cloud, and further modification through coalescence and evaporation is computed over an additional 1 km assuming the atmosphere has a temperature of 15°C and RH of 90%. It is the distribution after 2 km fall that is shown in Fig. 15. The atmospheric conditions used for these computations are identical to those quoted by Mason and Ramanadham, and their final distribution is also shown in Fig. 15. The trend of reduced smaller drops between the computed distribution and that given by Mason and Ramanadham which showed up in Fig. 14 also is present in Fig. 15. The other major difference is that Mason and Ramanadham apparently did not consider the growth of drops beyond 1.8 mm diameter, whereas the computed distribution presented here shows that drops in substantial concentrations can occur even up to 2.2 mm. In spite of the differences between the two curves of Fig. 15, the overall agreement is remarkably close and argues well for the methods of computation presented here and those used by Mason and Ramanadham. The advantage of developing a computer program is that the change in any distribution for any reasonable combination of atmospheric conditions can now be obtained. The time required on an IBM 709 computer is between 2-4 minutes per km of computation depending on the rainfall intensity, or more precisely, on the number of drop-diameter classes which are used.

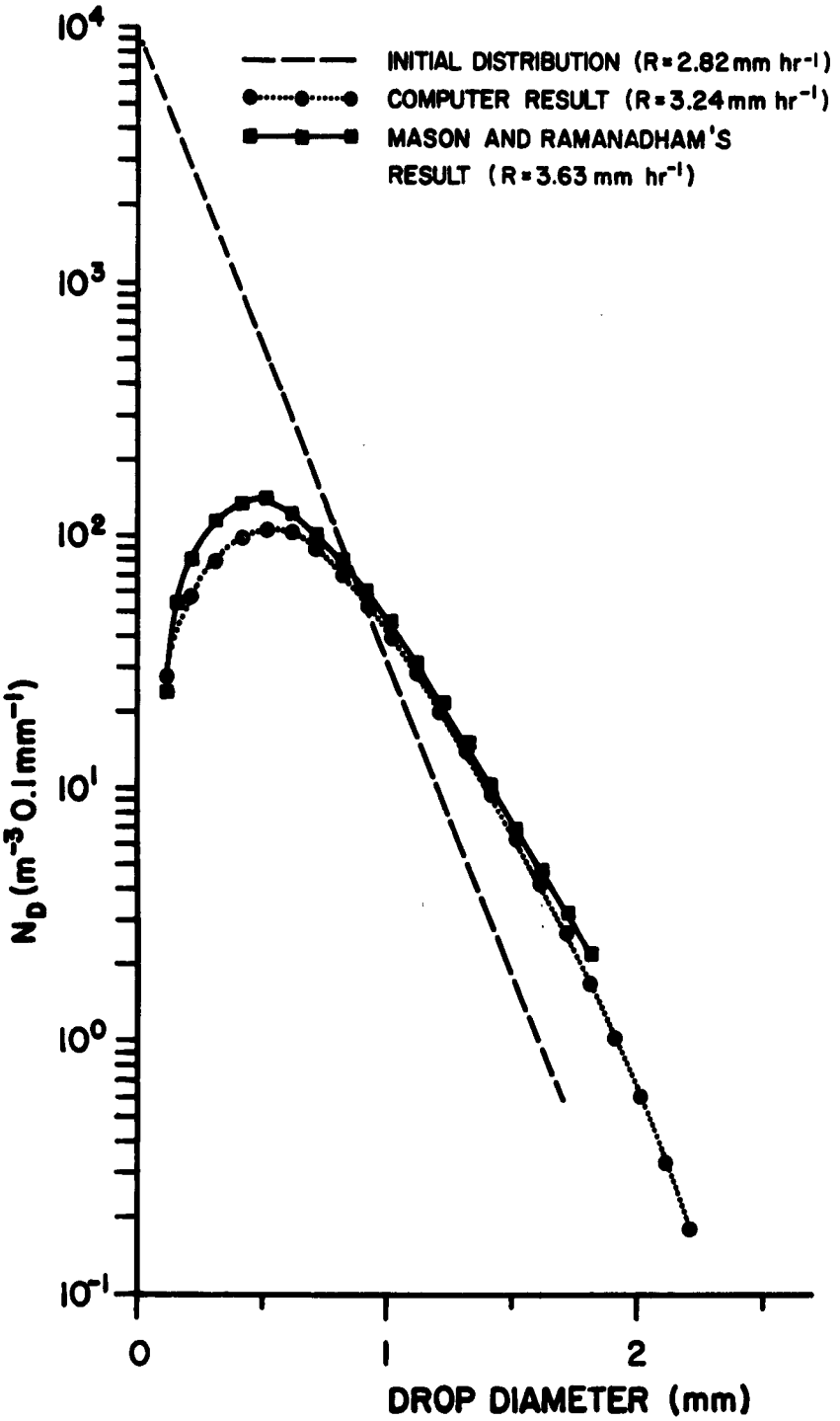

Fig. 15. Final distribution after a 1 km fall through cloud plus a 1 km fall through an atmosphere with a temperature of 15C and RH of 90 per cent.

3.5 THE DEVELOPMENT OF RAINDROP-SIZE DISTRIBUTIONS DURING THE AFTERNOON OF 31 JULY 1961 AT FLAGSTAFF, ARIZONA.

The analysis of the radar data on the afternoon of 31 July (Appendix D) shows that the precipitation originated as snowflakes and was relatively steady. The melting level was at approximately 2400 m and radar echoes were received at altitudes up to 9000 m. Of all periods of observations the data on this day appear to be best suited for a theoretical study since the distributions have a relatively uniform character over a long period of time (Fig. 54).

Using the methods developed in Sections 3.2 - 3.4 an attempt is made to deduce the distribution of raindrop sizes at the melting level on 31 July. The procedure is as follows: (1) assume an initial raindrop-size distribution at the melting level, (2) compute the change that will take place in this distribution in falling to the ground using appropriate values of cloud LWC, temperature and RH, (3) compare the resulting distribution with the observed distribution obtained with the spectrometer, (4) if the computed and observed distributions are similar then the indications are that the assumed distribution at the melting level is representative of the true distribution, and (5) if the computed and observed distributions are dissimilar then steps (1)-(4) are repeated.

The one uncertainty with the above procedure is that it requires a knowledge of the cloud LWC and the temperature and relative humidity below the cloud base. In the computation considered here the temperature and RH between the cloud base and the ground shown in Fig. 16 are estimated from the radiosonde ascent taken at the airport (Fig. 51, Appendix D) and from the hygrothermograph records at Kent

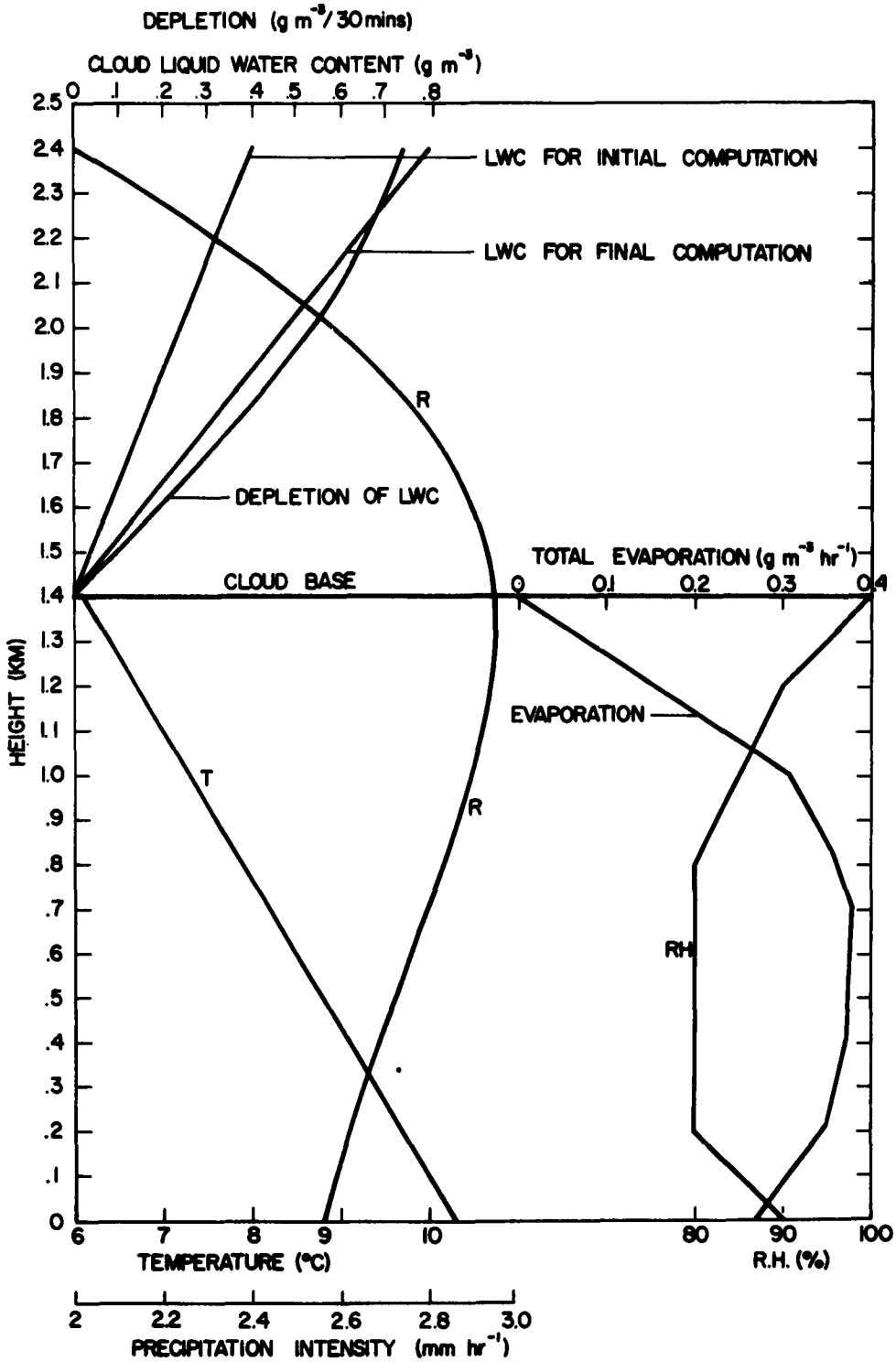

Fig. 16. Vertical profiles for afternoon of 31 July 1961 at Kent Ranch.

Ranch.[1] The cloud LWC is much more difficult to estimate. Probable values for a rain system such as occurred on 31 July are in the range of 0.2-0.4 g m^{-3} (Fletcher, 1962; Warner and Newnham, 1952). Because of the probable structure of the vertical velocity profile and from continuity considerations (Bannon, 1948; Wexler and Atlas, 1957; Kessler, 1959; and Kessler, 1961) it is reasonable to assume that the cloud LWC increases with height at least up to the melting level, and in the present study a linear increase is used.[2]

Curve 2 of Fig. 54 (Appendix D) is chosen as the observed distribution at the ground. The intensity is 2.5 mm hr^{-1}, and an attempt is made to arrive at this distribution through computations on an assumed distribution at the melting level. The results of the work described in Section 3.2 - 3.4 suggest that exponential distributions of the type used by Marshall and Palmer exist at the melting level. Initially then, an M-P distribution with an intensity of 2.8 mm hr^{-1} and a maximum drop diameter of 2.0 mm is assumed at the melting level. This distribution and the distribution with an intensity of 2.5 mm hr^{-1} for 31 July are shown in Fig. 17. The LWC is assumed to increase from zero at the cloud base (1.4 km above ground) to 0.40 g m^{-3} at the melting level (Fig. 16). The computation then proceeds over the height of 2.4 km, coalescence and accretion occurring for the first kilometer and coalescence and evaporation occurring for the latter 1.4 km.

---

[1]The raindrop-size spectrometer was situated at the Kent Ranch (Fig. 41).

[2]Later it was found that a mean LWC for the entire layer of cloud can be used with negligible effect on the final result.

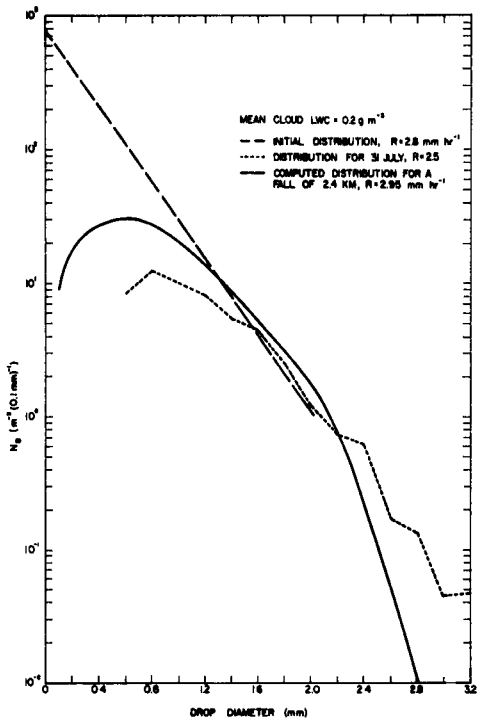

Fig. 17. Comparison of computed and observed distribution for 31 July 1961 - first attempt.

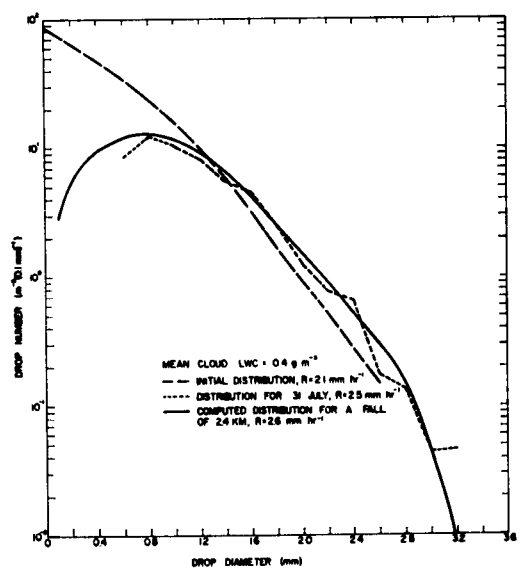

Fig. 18. Comparison of computed and observed distribution for 31 July 1961 - final attempt.

The resulting distribution shown in Fig. 17 is instructive. First, it is clear that the computed distribution has far too many drops at the small end. Secondly, the concentration of large drops falls off too rapidly in the modeled case. The indications are that (1) the M-P distribution does not exist at the melting level in this case, and (2) the concentration of the larger drops at the melting level must not be substantially different from the concentration observed at the ground. By taking these factors into account another initial distribution was chosen (Fig. 18) and the computation repeated. The final computed distribution was found to come much closer to the observed distribution. It failed, however, to show enough growth of the larger drops. Rather than change the form of the initial distribution, the cloud LWC at each level was doubled and the computations repeated. The resulting distribution is shown in Fig. 18. The agreement between the computed and observed distribution is excellent - except perhaps at the smallest drop size. The computed distribution could also be obtained using a different initial distribution and a different LWC. However, if the mean LWC lies between 0.2 and 0.4 g m^{-3}, then the imitial distribution at the melting level must be similar to the one shown in Fig. 18. Thus, the distribution resulting from melted snow flakes cannot be described by the M-P distribution in this case. The requirement is for the distribution to have more drops concentrated in the larger sizes as compared with the M-P distribution. Such a condition is probably characteristic of the raindrop-size distribution resulting from

melted snowflakes which have grown throughout a relatively thick cloud (Gunn and Marshall, 1956).

3.6 THE DEPLETION OF CLOUD LWC BY FALLING RAIN

Gunn (1952) (see also Appendix of Rigby, et al, 1954) studied the depletion of the cloud LWC through accretion by the falling raindrops. He initially assumed that the LWC of the cloud is not replenished by continued condensation or advection. He found that the total LWC of the cloud decreases exponentially for small time increments. For a rainfall intensity of 2.5 mm hr^{-1} Gunn estimates that the cloud will be depleted by 50 per cent in about 11 minutes, whereas for an intensity of 40 mm hr^{-1} the time is reduced to about 2 minutes. Diem (1948) obtained cloud-drop distributions from a precipitating cumulus cloud both before rain and after rain of 3 mm hr^{-1} fell for 20, 80, and 160 minutes. He computed the LWC from the distributions and found that it decreased by a factor of four after 20 min. Such a phenomenon can often be observed when rain begins to fall into fog. When it is not raining and fog is present the visibility is very low indicating the presence of large concentrations of small drops, but after rain has fallen through the fog for a few minutes the visibility is observed to improve markedly because the fog particles are swept out by the falling raindrops.

3.6.1 Depletion of cloud LWC for rain of 31 July.

It is relatively easy to obtain with the computer the total amount of cloud liquid water carried to earth by the falling rain for the cases considered. It is only necessary to keep an account of how much of the cloud LWC is used in furthering the growth of the raindrops. The depletion thus

deduced can also be considered as representing the amount of cloud LWC which must be replenished in order to maintain a constant rainfall intensity. Although it is not known if the cloud LWC remained constant during the rain of 31 July, at least it appears reasonable in view of the steady nature of the rain. The rate of depletion of the cloud LWC for 31 July is given in Fig. 16 in units of g m^{-3} per 30 min. The computation shows that the cloud LWC must be replenished approximately once every 30 minutes if steady state conditions are to persist. The precipitation intensity is also shown in Fig. 16, and it is seen that an increase of 0.94 mm hr^{-1} takes place between the melting level and the cloud base. Of course this increase comes about because of the water which is transferred from the cloud droplets to the raindrops through the accretion process.

It is instructive to determine the updraft velocity which will provide the proper rate of condensation for the replenishment of the cloud LWC. Table 6 gives the rates of condensation for cloud layers 1 km thick assuming a uniform updraft velocity of 14.4 cm sec^{-1} throughout the cloud of 31 July (Fulks, 1935). This updraft velocity was chosen to yield a total rate of condensation of 2.5 mm hr^{-1} which is assumed to be equivalent to the rainfall intensity. The vertical profile of the rate of condensation is such that 29% of the total occurs within the lower kilometer of the cloud. This is in excellent agreement with the increase in the precipitation intensity of 0.94 mm hr^{-1} (32%) that was computed within this layer assuming a mean cloud LWC of 0.4 g m^{-3} (Fig. 16). This suggests that the rain system during the afternoon of 31 July was being maintained in

approximate equilibrium by an updraft of about 14 cm sec^{-1}, although the values of Fulks are admittedly applicable only to an idealized model of the thermodynamic and physical processes that are involved in the precipitation mechanism.

Table 6. Rates of condensation for cloud layers 1 km thick assuming a uniform updraft of 14.4 cm sec^{-1} for cloud of 31 July 1961. (From Fulks, 1935)

Mean height of layer (km)	Mean temp in layer (°C)	Mean pressure (mb)	Rate of condensation (mm $hr^{-1}km^{-1}$)	Per cent in each layer
2.0	3	620	.72	28.8
3	-5	540	.56	22.4
4	-10	480	.45	18.0
5	-16	420	.35	14.0
6	-22	365	.23	9.2
7	-30	320	.13	5.2
8	-38	275	.06	2.4
		Total	2.50	100.0

In the computations of Sections 3.2 - 3.4 it was assumed that there was no vertical air velocity. Although an updraft velocity of 14 cm sec^{-1} is small with respect to the velocity of most raindrops (Fig. 1), it probably should not be neglected. The effect of considering a vertical velocity is to increase the time for the drops to fall a given distance, and, therefore, the residence time of the drops within the cloud is increased. An additional study which includes a consideration of the updraft velocity and the water budget of the cloud system should be highly rewarding and appears to be feasible at this time.

3.6.2 Depletion of cloud LWC and precipitation physics.

The previous section has shown that growth of the raindrops through accretion of cloud droplets produces an increase in the precipitation intensity. Any such increase in rainfall rate must be equivalent to the amount of depletion of the cloud LWC. It can easily be verified that a depletion of the cloud LWC of 1 g m^{-3} hr^{-1} is equivalent to an increase in precipitation intensity of 1 mm hr^{-1} km^{-1}. This section is concerned with some quantitative aspects of the depletion of cloud LWC.

The depletion of cloud LWC per unit time is equal to the total change in mass of the raindrop-size distribution, or

$$\text{Depletion} = \Sigma\Delta M_m = \frac{\pi\rho\Delta D\Sigma D^2}{2} . \qquad (18)$$

Eq. (18) shows that the depletion of cloud LWC is approximately proportional to ΔD (since a given change in ΔD produces a much smaller change in ΣD^2). Eq. (15) shows that ΔD is proportional to the cloud LWC for growth through accretion, and we conclude that the total depletion (and therefore the increase in rainfall intensity) is also approximately linearly related to the cloud LWC. A few computations for the M-P distribution with an intensity of 10 mm hr^{-1} verified the approximately linear relationship between the cloud LWC and the depletion of the cloud.

The depletion of cloud LWC has been calculated for several rainfall intensities (curve (a), Fig. 19) assuming that (1) the cloud LWC is 1.0 g m^{-3}, (2) the collection efficiency of raindrops with cloud droplets is constant and equal to 0.8, and (3) the raindrop-size distribution at the top of the layer is represented by the M-P distribution of

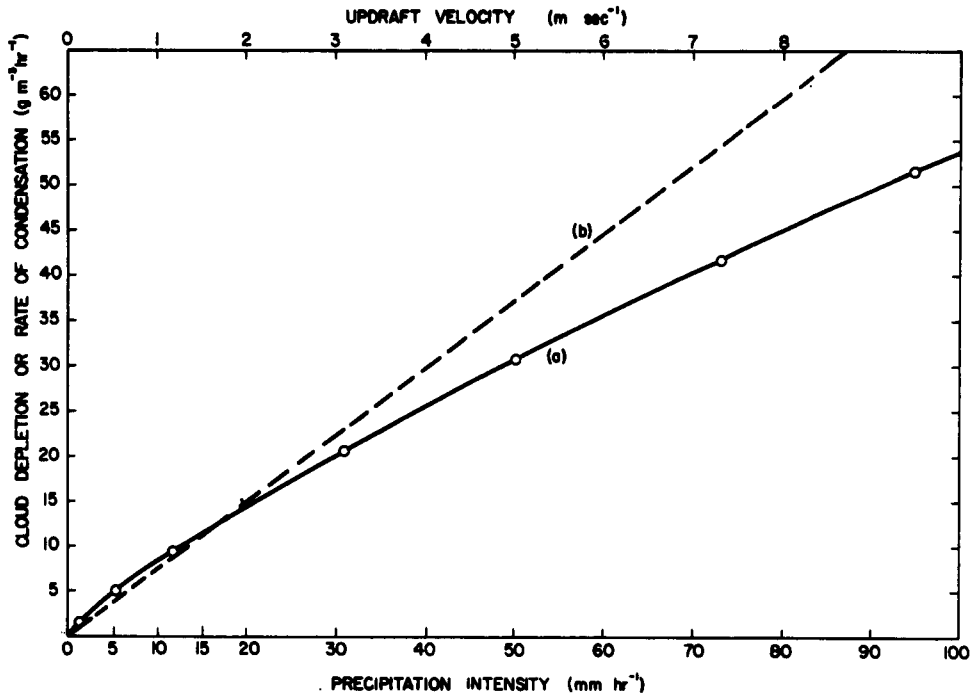

Fig. 19. Curve (a), depletion of cloud LWC for M-P distribution; Curve (b), rate of condensation as a function of updraft velocity.

Eq. (4). The depletion is proportionately greater at low rainfall rates. Curve (b) of Fig. 19 gives the rate of condensation as a function of updraft velocity assuming that the air is saturated at a temperature of 10°C and pressure of 900 mb. The updraft velocity which is required to replenish the cloud LWC depleted by the falling rain can now be determined. For a rainfall rate of 5 mm hr^{-1} (and for the assumptions listed above) the updraft velocity must be about 0.7 m sec^{-1} in order to balance the cloud depleted and the cloud replenished, whereas for a rainfall rate of 50 mm hr^{-1} the corresponding updraft is about 4.1 m sec^{-1}.

Fig. 19 is only applicable for a special set of conditions. Nevertheless, it illustrates a procedure which could lead to a family of cloud depletion curves and rate of condensation curves which are applicable over a wide range of atmospheric conditions. Such curves are not presented here, but, if required, they can be constructed with little error from the information already presented and by reference to Fulks (1935).

The most severe limitation of Fig. 19 is that the results are only valid for the M-P distribution. To partially overcome this difficulty the effect of the raindrop-size distribution on the cloud depletion is also investigated. Fig. 20 shows various raindrop-size distributions, all of which are exponential and have an intensity of 10 mm hr^{-1}. The slopes of the distributions, defined as $\frac{\Delta(\log N_D)}{\Delta D}$ mm^{-1}, are also indicated.[1] The depletion of the cloud (assuming an initial LWC of 1 g m^{-3} and a collection efficiency of 0.8), calculated for each of the distributions of Fig. 20, is shown as curve (a) of Fig. 21. The depletion of the cloud is found to depend markedly on the raindrop-size distribution. For a steep distribution (i.e. slope = -1.39 mm^{-1}) the depletion is more than twice as great as for the distribution with a slope of -0.46 mm^{-1}. Thus, the steep distributions which are common to the rains formed through orographic lifting in Hawaii (Fig. 5) are efficient in

---

[1]The distributions of Fig. 20 are approximations to the distributions which occur naturally. However, if an observed distribution is fitted by an exponential curve, then it is probable that this curve will be encompassed by the curves shown in Fig. 20.

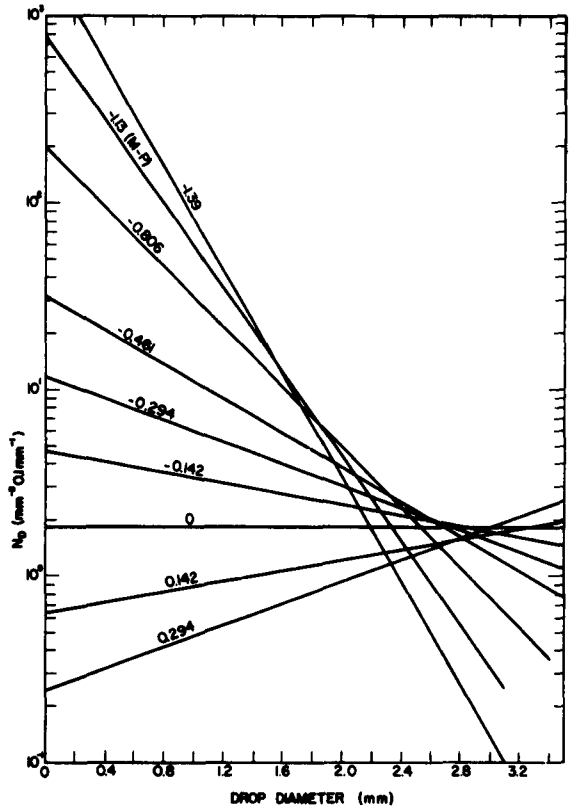

Fig. 20. Exponential raindrop-size distributions with intensities of 10 mm hr^{-1}.

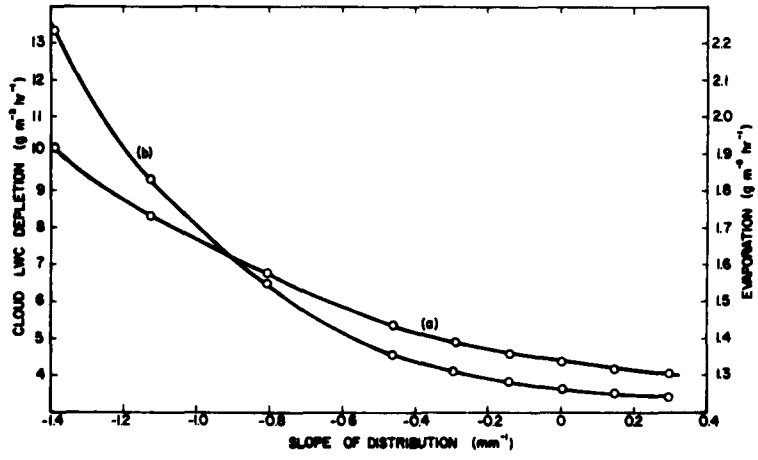

Fig. 21. Depletion of cloud LWC, curve (a); and evaporation, curve (b) for distributions of Fig. 20.

depleting the cloud LWC, and the rainfall intensity in these rains should show a relatively large increase with distance fallen. On the other hand, rains such as those of 31 July at Flagstaff (Fig. 54) are relatively inefficient for depleting the cloud LWC.

The conclusion is that the increase in rainfall intensity caused by accretion of cloud droplets is (1) approximately proportional to the cloud LWC, and (2) strongly dependent on the raindrop-size distribution. However, it should be emphasized that the above conclusion is based on computations which assumed that the collection efficiency is constant for all raindrop sizes. This assumption is not necessarily valid (Fig. 12). Although a knowledge of the actual collection efficiency and cloud droplet spectra would help in a truly quantitative study, it is doubtful whether this information would significantly alter the above conclusion.

3.7 ADDITION OF WATER VAPOR TO THE ATMOSPHERE THROUGH EVAPORATION FROM RAINDROPS

3.7.1 Evaporation for rain of 31 July.

In a manner analogous to that used to compute the depletion of cloud by falling rain it is possible to keep an account of the total amount of water which evaporates from raindrops falling through an unsaturated atmosphere. Fig. 16 shows the rate of evaporation in g m^{-3} hr^{-1} for the rain of 31 July. The amount of evaporation is dependent upon the raindrop-size distribution and the water vapor deficit below saturation. For the first 200 m below the cloud base the water vapor deficit is about 0.5 g m^{-3} (RH = 95% at 6°C). The evaporation from the raindrops corresponding to this

deficit is about 0.1 g m^{-3} hr^{-1} indicating that it would take at least 5 hours for the air to become saturated if the only source of water vapor is the evaporating raindrops and neglecting the lower rate of evaporation as the RH approaches 100 per cent. At a deficit of about 2 g m^{-3} (RH = 80% at 10°C) the evaporation from the raindrops amounts to less than 0.4 g m^{-3} hr^{-1} (Fig. 16). These computations point to the difficulty of saturating the air through the evaporation of falling rain, and in this respect agrees with the relatively rare occurrence of fog formation which is due entirely to this process.

Once the rain has completely wetted the ground a new surface is provided from which evaporation occurs. This results in a relatively moist layer close to the ground. If a warm front is approaching and the initial rain is from a middle cloud layer, then it is often observed that a new cloud layer will form at a much lower altitude. From the above computations it is improbable that this new cloud layer is attributable to the evaporation of the rain falling through the atmosphere. A much more likely explanation is that the moist surface air is eventually lifted either orographically or through convergence associated with the mean flow and condenses at a considerably lower level than the base of the cloud from which the rain is falling.

3.7.2 Evaporation and rainfall intensity

The evaporation which occurs from falling rain affects the atmosphere in two ways: first, it increases the moisture content of the air; secondly, the air is cooled and consequently the stability of the atmosphere is modified. The

evaporation from different raindrop-size distributions falling through air of varying moisture contents is considered in this section.

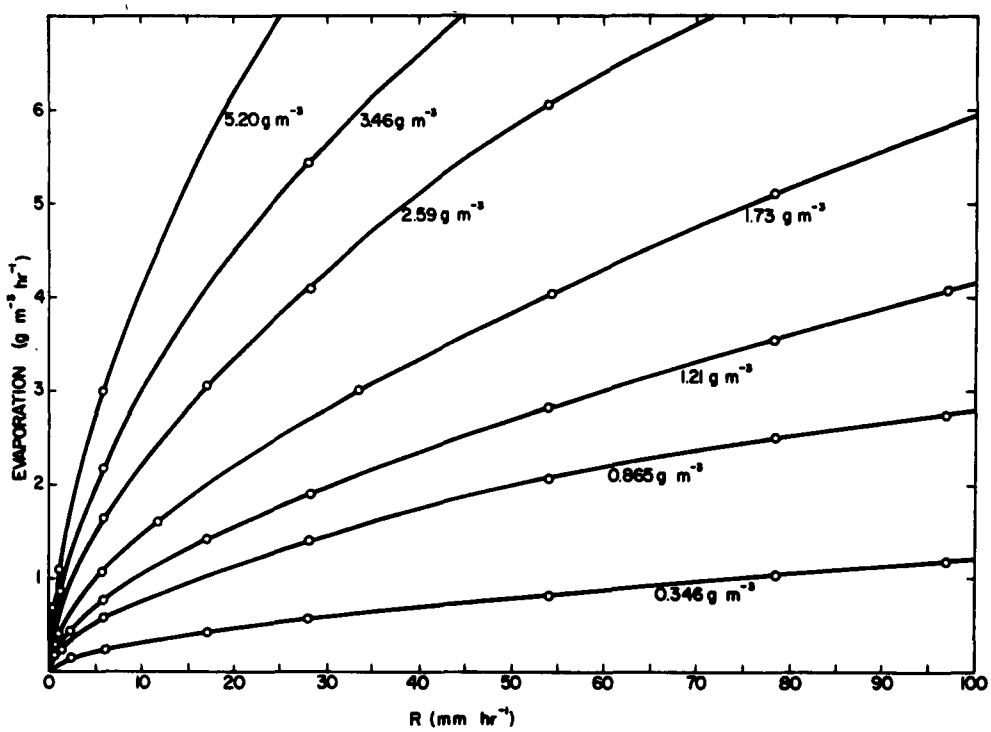

Fig. 22. Evaporation from M-P distributions at several water vapor deficits.

Fig. 22 gives the amount of evaporation from M-P distributions as a function of rainfall intensity. The water vapor deficit, which is used to designate the curves of Fig. 22, is the amount of moisture required to saturate the air. Each deficit corresponds to an infinite number of combinations of temperature and relative humidity. For example, a deficit of 1.73 g m^{-3} is equivalent to the following pairs of values of temperatures and relative humidity: 0.52°C, 80%, 8.6°C, 85%; 20°C, 90%, 26.3°C, 92%. For most rains the air below the

cloud base has a deficit of less than 1.7 g m^{-3}, although for the showers which develop in the southwest United States larger deficits may be observed. Fig. 22 shows a comparatively large amount of evaporation at low rainfall intensities, whereas at high rainfall rates and reasonable water vapor deficits the evaporation is relatively minor. For an intensity of 100 mm hr^{-1} and deficit of 1.7 g m^{-3} the evaporation is only about 6 g m^{-3} hr^{-1}. This, of course, is equivalent to a decrease of 6 mm hr^{-1} km^{-1} in the rainfall intensity.

The amount of evaporation which was calculated for the various raindrop-size distributions of Fig. 20 and using a water vapor deficit of 1.73 gm^{-3} is shown as curve (b) of Fig. 21. Analogous to the depletion of cloud LWC the steeper distributions show greater evaporation than the flatter distributions. The shape of curves (a) and (b) of Fig. 21 is not unexpected, since the greater total raindrop surface area of the steeper distributions is conducive to increased evaporation or increased growth through accretion.

It is concluded that (1) for normal water vapor deficits the amount of evaporation from M-P distributions is relatively small at high rainfall rates but may be quite significant at rainfall rates less than 5 mm hr^{-1}, and (2) for similar rainfall intensities the evaporation increases as the distribution becomes steeper.

3.8 MEAN RAINDROP-SIZE DISTRIBUTIONS FOR THE FLAGSTAFF AREA

The raindrop-size distributions observed in Flagstaff during the summer of 1961 are presented in Appendix D. Generally the rain is characterized by showers of varying intensity. For example, some showers on 3 August had a maximum intensity of about 10 mm hr^{-1} (Fig. 63), whereas the shower on 31 July had intensities greater than 90 mm hr^{-1} (Fig. 52). Usually, wind shear or gravity sorting of the raindrops is most significant during showers (Appendix D), and it is difficult to determine mean distributions for these conditions. On the other hand, the distributions observed during the afternoon of 31 July are the result of continuous and relatively uniform rain (Fig. 52), and, therefore, the mean distributions for this afternoon should not reflect any pronounced effects of sorting due to wind shear or gravity.

The M-P distribution for an intensity of 2.5 mm hr^{-1} and the mean distributions for 31 July are shown in Fig. 54. The observed distribution for 31 July with an intensity of 2.5 mm hr^{-1} has fewer small drops and more large drops than the corresponding M-P distribution. It was shown in Section 3.5 that the M-P distribution is not representative of the rain on this afternoon for any level between the ground and the melting level. It is also known that the rain on this afternoon came from clouds whose tops were at least 6 km above the melting level (Appendix D). This probably is a more favorable condition for growth than are the average growth conditions of the rains from which the M-P distribution was derived. At least on this qualitative basis the distributions of Fig. 54 appear to be justified.

The other distributions for the Flagstaff rains were also compared with the M-P distribution. In practically all the cases (Fig. 59 and curve 7 of Fig. 65 are exceptions) the observed distributions showed more large drops and fewer small drops than those given by the M-P distribution. However, in some instances such a distinction was almost negligible. Nevertheless, we must conclude that conditions in the Flagstaff area during the summer moist period generally promote a greater growth of raindrops than is indicated by the M-P distribution. Possible reasons for this increased growth are (1) the convective activity in the area releases large amounts of water vapor for future growth, (2) a large portion of the cloud system has temperatures below freezing and therefore growth by the Bergeron-Findeisen process is possible, and (3) even during the dissipating stage the clouds are thick and growth may take place place throughout a considerable height.

3.9 THE RELATIONSHIP BETWEEN Z AND R

3.9.1 Observed Z-R relationships

The relationship between the radar reflectivity, Z, and precipitation intensity, R, has been discussed in Section 2.2.1. Since values of Z and R have been computed for every minute of rain observed with the spectrometer, it appears feasible to determine a relationship between these two quantities which has application to the Flagstaff storms. Accordingly, a Z-R relation was obtained for every storm recorded at Flagstaff.

Fig. 23 is a plot of the Z-R values as observed sequentially on 31 July between 1054 and 1118 (Appendix D, Fig. 52).

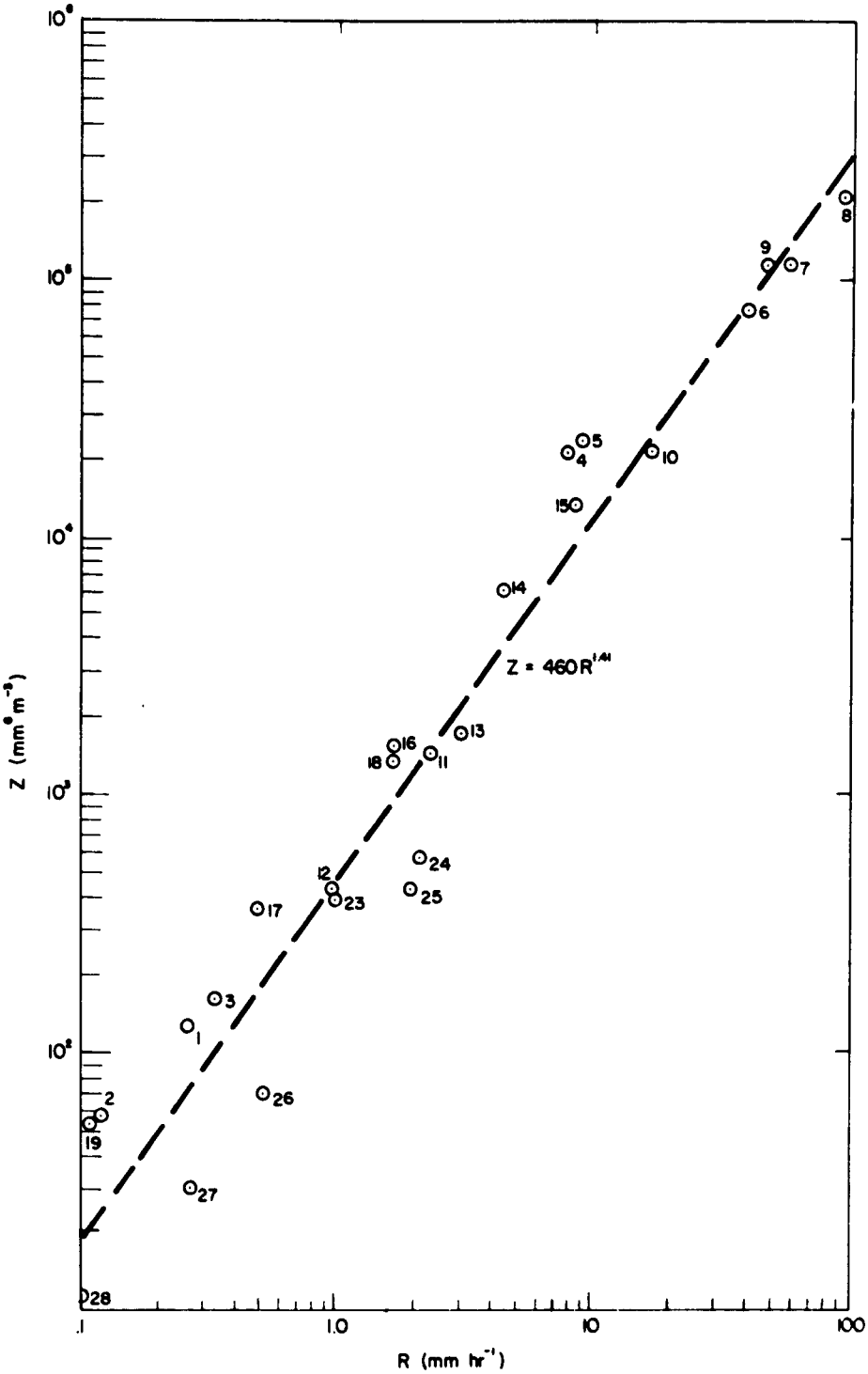

Fig. 23. Sequential values of Z and R from 1054 to 1123, 31 July 1961. Numbers represent succeeding minutes of the shower.

The values show a moderate amount of scatter particularly at low rainfall intensities. The Z-R function for the data of Fig. 23 is given by

$$Z = 460R^{1.41} \tag{19}$$

where R is in mm hr^{-1} and Z is in mm^6 m^{-3}. It is clear that (19) does not represent the observed values at low rainfall rates. The reason is to be found in the radical change that occurs in the raindrop-size distribution as the shower progresses. Relatively high Z values are observed initially for a given R, whereas relatively low values are observed near the end of the shower. For this reason there seems little point in using (19) at low rainfall rates for this shower.

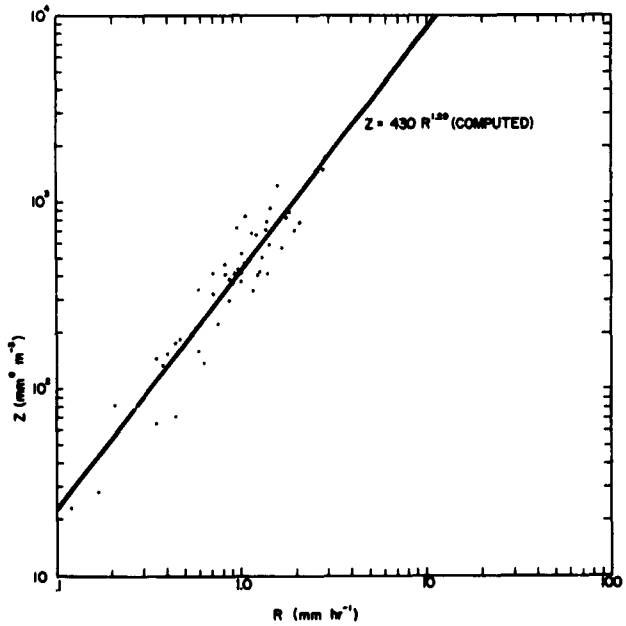

Fig. 24. Z-R relationship for period from 1235 to 1650, 31 July 1961.

The Z-R values computed over 5-min intervals for the period from 1235-1650 on 31 July are shown in Fig. 24. The regression equation of Z on R for this rain is

$$Z = 430R^{1.29} . \qquad (20)$$

There is still a certain degree of scatter in Fig. 24, but it is slightly less than that shown in Fig. 23. However, Eq. 20 is only applicable for a very limited range of rainfall intensities (i.e. approximately 0.1 to 3 mm hr^{-1}).

Figs. 23 and 24 are faily typical of the other storms observed at Flagstaff. Thus, the Z-R data for a complete shower process exhibit a large amount of scatter about the regression equation. On the other hand, the rain near the end of a thunderstorm appears to show a certain degree of consistency. This is shown in Table 7 in which the Z-R relationships and other pertinent data for selected rain situations are listed.

The first three relations of Table 7 are for rains at Flagstaff which occurred after initial thunderstorms. The exponenets are in close agreement, but the coefficient for the rain of 3 August is considerably smaller than that for the rains of 31 July and 1 August. It is possible that the smaller amount of evaporation on 3 August compared with the other two days (Section 3.9.2 and Appendix D) is responsible for the smaller coefficient in this case. The rain on 16 June 1960 at Ann Arbor shows a comparable Z-R relationship. It is also seen that the atmosphere below the cloud base was very dry on 16 June 1960. This may partially account for the similarity between the Z-R relationship for 16 June 1960 and for the three Flagstaff rains mentioned above. The last two Z-R relations given in Table 7 are derived from data

Table 7. Empirical Z-R relationships for selected rain conditions.

Date	7/31/61	8/1/61	8/3/61	6/16/60	10/8/59	12/5/59	12/11/59
Sample Length (min)	5	5	5	1	1	1	1
Number of Samples	50	6	17	26	17	48	25
Range of Intensity (mm hr^{-1})	0.1 - 3	1 - 4	0.1 - 5	0.1 - 7	0.1 - 9	0.8 - 3	1.8 - 4
Melting Level (m)	2400	2600	2600	4000	3650	1200	1800
Cloud Base (m)	1500	2000	1000	1200	900	900	60
Mean Water Vapor Deficit (g m^{-3}) Below Cloud Base	1.24	2.13	1.02	3.86	1.28	0.11	0.12
Bright Band	Yes	No	No	?	No	Yes	Yes
Location	Flagstaff	Flagstaff	Flagstaff	Ann Arbor	Ann Arbor	Ann Arbor	Ann Arbor
Equation ($Z = aR^b$)	$430R^{1.29}$	$378R^{1.39}$	$233R^{1.29}$	$300R^{1.31}$	$198R^{1.40}$	$129R^{1.58}$	$143R^{1.49}$
Remarks	Rain after initial thunder-shower	Rain after initial thunder-shower	Rain after initial thunder-shower and two light showers	Dissipating portion of thunder-shower	Dissipating portion of thunder-shower	Warm frontal rain	Warm frontal rain

observed in warm front rain during December 1959. The cloud base and freezing level were quite low, and the relative humidity below the cloud base was greater than 95 per cent. The Z-R functions have relatively low coefficients and high exponents. The Z-R function for 8 October is approximately intermediate between those for the December rains and those for the rains in Flagstaff. Similarly, the atmospheric conditions on this day are not as extreme as those for the other rains listed in Table 7. The results of this table are investigated further in Section 3.9.2.

The Z-R functions listed in Table 7 have been obtained for rains which, in general, have intensities of less than 5 mm hr^{-1}. These were chosen in an attempt to delineate some of the possible causes which might produce the differences in the observed Z-R relations. The initial minutes of thundershowers have not been considered because they are usually strongly influenced by wind shear or gravity sorting. In addition they represent a relatively small fraction of the period during which rain fell.

It was hoped that the Z-R function at higher rainfall rates would not show as much variation as at the lower rates, but Fig. 25 indicates that this is hardly the case. Every minute of rain observed with the spectrometer which had an intensity greater than 5 mm hr^{-1} is plotted in Fig. 25. The value of Z varies by a factor of 10 near intensities of 10 mm hr^{-1}. This is probably caused by the rainfall near the beginning of the showers when evaporation and wind shear sorting usually combine to produce relatively high Z's for a given R. The least squares regression equation of Z on R for the data of Fig. 25 is

$$Z = 312R^{1.36} \quad . \tag{21}$$

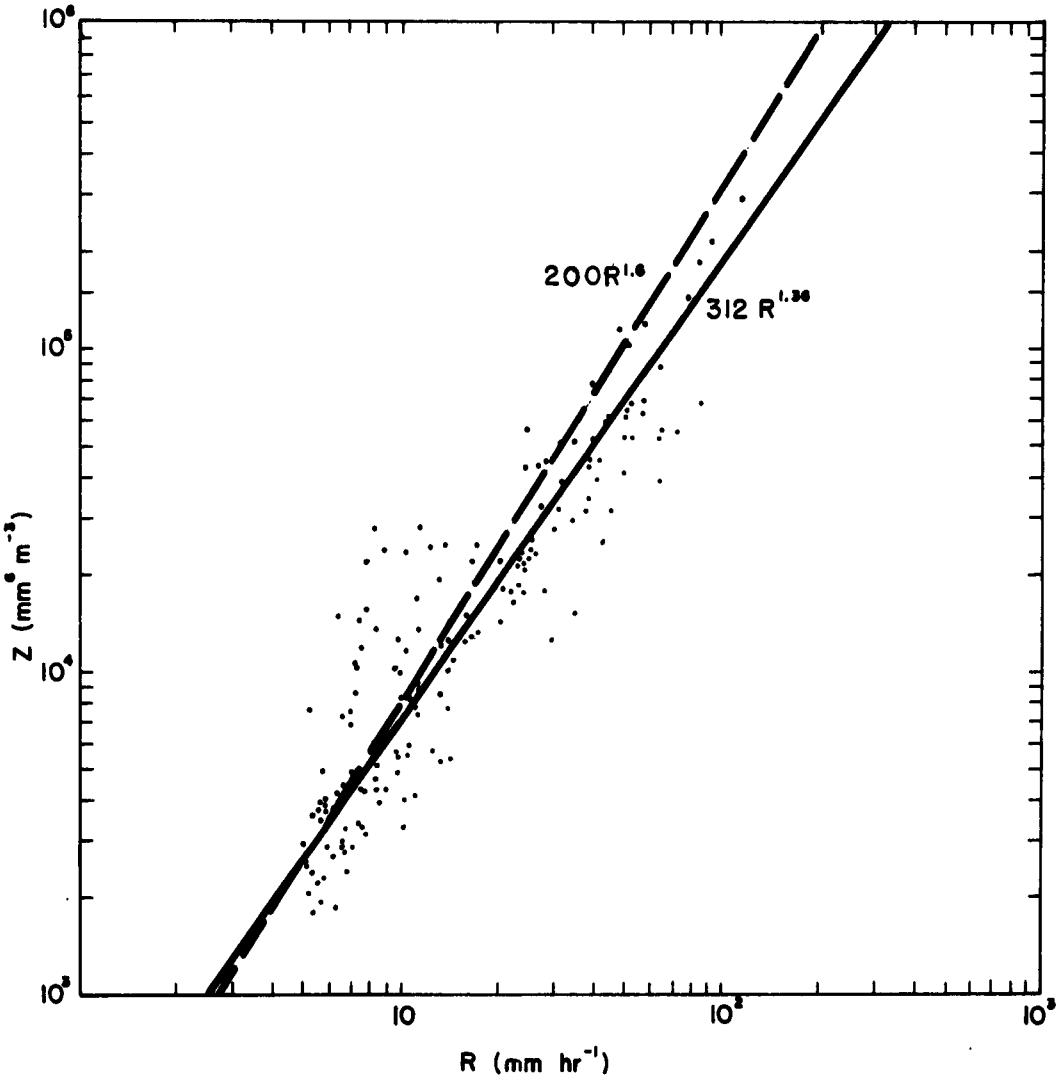

Fig. 25. Z-R relationship for rains with intensities greater than 5 mm hr^{-1}.

This compares with the regression equation of

$$Z = 200R^{1.60}, \qquad (22)$$

which is also shown in Fig. 25. Eq. (22) was suggested by Marshall and Gordon (1957) and was derived from data with rainfall intensities mostly less than 20 mm hr^{-1}. There is close agreement between Eqs. (21) and (22) for rainfall intensities between 5 and 15 mm hr^{-1}. However, at higher intensities Eq. (22) indicates a considerably greater Z for a given R as compared with Eq. (21). Since (21) is based on data which include relatively high rainfall rates, it is suggested that this equation should be used for rainfall rates greater than about 20 mm hr^{-1}.

3.9.2 The effect of accretion and evaporation on the Z-R relationship.

An attempt was made in the previous section to characterize the Z-R relationships on the basis of selected meteorological data. A quantitative evaluation of the effect of evaporation and accretion on the values of Z and R is given in this section.

It is assumed that the M-P distribution described by Eq. (4) is representative of the rain spectra. Changes brought about in this distribution by accretion of cloud droplets in falling through a cloud 1 km thick are determined for various rainfall intensities. The assumed values of the cloud LWC and collection efficiency are 1 g m^{-3} and 0.8 respectively. The values of R and Z calculated from the distribution at the bottom of the layer are then used to establish a new Z-R relationship.

Values of R and Z computed for the M-P distribution are well represented by the equation

$$Z = 234R^{1.48} .^{1} \tag{23}$$

This relation is shown in Fig. 26. Curve (a), described by the equation

$$Z = 169R^{1.51} , \tag{24}$$

relates the Z-R values which result after accretion. The dotted lines indicate the change in the values of Z and R from the top to the bottom of the cloud. The effect of accretion is to decrease the coefficient and increase the exponent of the Z-R relationship. This is expected since accretion causes a greater fractional mass increase of the small drops than the large ones, thus giving the small sizes more weight in the final drop-size distribution than in the initial one.

A similar method is used to determine the effect of evaporation. M-P distributions are assumed to exist at the base of the cloud. The values of R and Z are then calculated from the distributions which are obtained after a fall of 2 km through an atmosphere with a water vapor deficit of 1.73 g m^{-3}. Curve (b) of Fig. 26 shows that after evaporation Z and R are related by

$$Z = 346R^{1.39} . \tag{25}$$

---

[1]Eq. (23) is different from the comparable equation of $Z = 296R^{1.47}$ presented by Marshall and Palmer (1948). However, these authors used observed rainfall intensities rather than the intensities represented strictly by the M-P distribution. This discrepancy is of little significance for our purposes and does not affect the results set forth in this section.

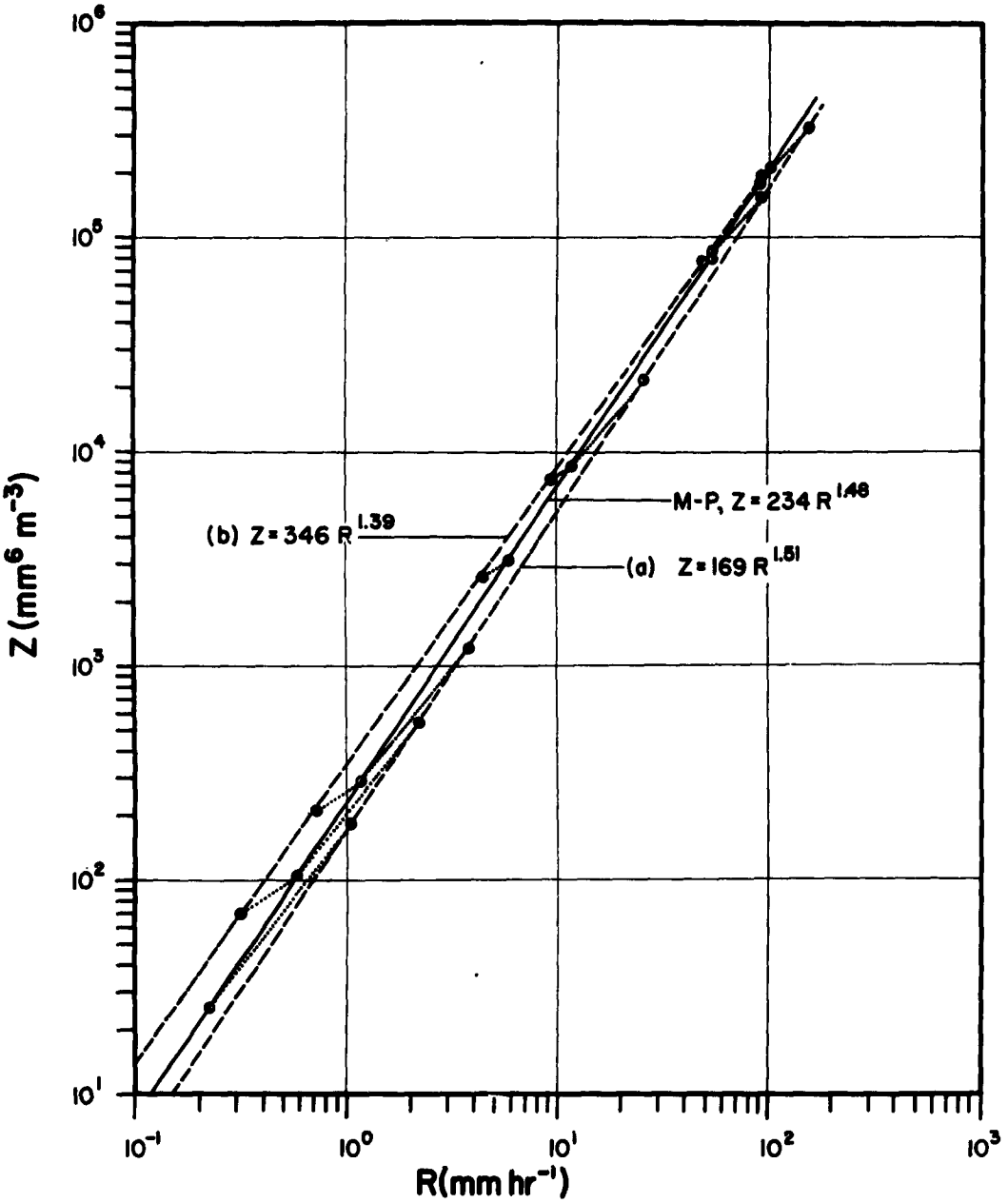

Fig. 26. Effect of accretion and evaporation on the Z-R relationship.

Since evaporation leaves the rain concentrated in the larger drops, the effect of evaporation is to increase the coefficient and decrease the exponent of the Z-R relationship.

The effect of accretion and evaporation on the Z-R relationship was originally studied by Atlas and Chmela (1957). For identical conditions as used above, they found that

$$Z = 70R^{1.73} \tag{26}$$

for the accretion case, and

$$Z = 1270R^{1.12} \tag{27}$$

for the evaporation case. Although a similar trend is shown by Atlas and Chmela's work, the absolute change is much greater than indicated by Eqs. (24) and (25). Hardy (1962) has investigated these differences and concluded that they are probably caused by assumptions made by Atlas and Chmela which tend to overestimate the change in the Z-R relationship.

The Z-R relationships observed at Flagstaff for those days in which evaporation was probably significant do, in fact, show relatively high coefficients and low exponents (Table 7). On the other hand, the days in which there was little or no evaporation are characterized by Z-R relationships with quite small coefficients and high exponents. Although it is tempting to conclude that the effects of accretion and evaporation are reflected in the Z-R relationships, other processes affecting the drop-size distribution should not be overlooked. In particular, it was shown in Section 3.5 that the distributions during the afternoon of 31 July could not be described by the M-P distribution at the melting level. Therefore, the results derived earlier

in this section on the assumption of the M-P distribution initially are not entirely applicable. Nevertheless, regardless of the distribution within the cloud, accretion and evaporation should change the Z-R relationship in a manner similar to that shown in Fig. 26.

3.9.3 The variation of Z with height below the melting level.

If coalescence and accretion are active processes within the cloud, then the radar reflectivity factor should decrease with increasing height above the surface. Harper (1957) has averaged the radar signal intensity of 32 scans which were made on three days with widespread rain. The surface weather reports on these three days suggested that the cloud conditions were rather similar in each steady rain period, with variable amounts of thin fractostratus at 500 to 1000 ft and a main overcast cloud layer with its base at 1500 to 2000 ft (one report of 4000 ft). The relative humidity was between 93 and 99 per cent in each rain period, and it is probable that evaporation of raindrops below the cloudbase was negligible. The mean profile of signal intensity for the 32 scans is shown as the full curve of Fig. 27, and a scale based on the mean rate of rainfall of 2.7 mm hr^{-1} has been added.[1]

The above conditions are almost identical to those assumed for the computation on the effect of accretion and coalescence given in Section 3.3.2: a steady rate of rainfall

---

[1]The abscissa of Fig. 27 is given in decibels (db) defined as 10 log Z/Z_o. A decibel is equivalent to a Z ratio of 1.26. The relationship between rate of rainfall and signal intensity of Fig. 27 is only approximate.

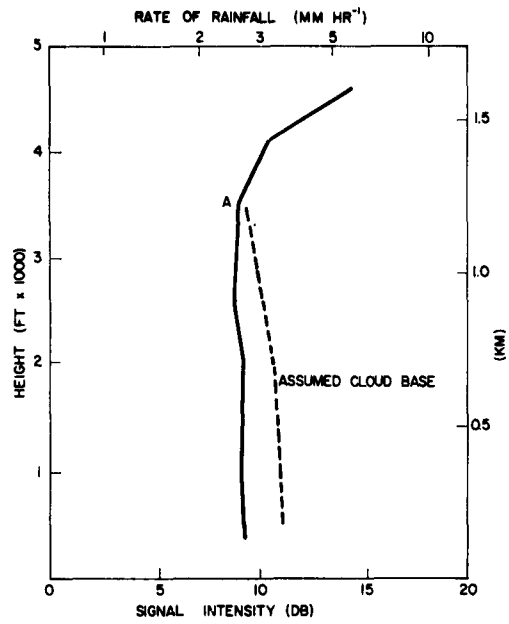

Fig. 27. Average radar signal intensity from 32 scans. The broken line is a computed growth curve. The scale of rate of rainfall does not apply above the point A (From Harper, 1957).

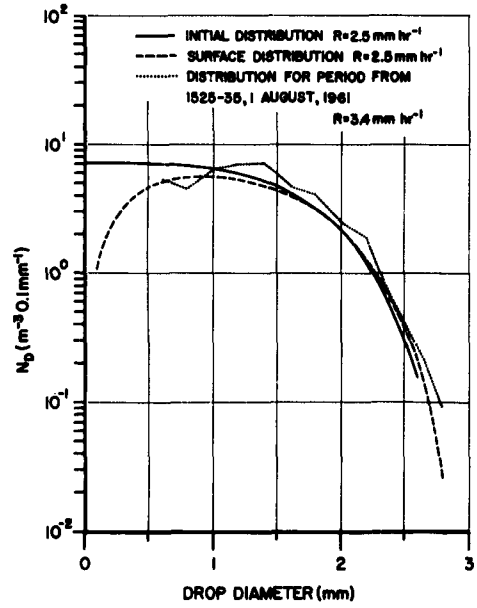

Fig. 28. Effect of growth on a relatively flat raindrop-size distribution.

of 2.8 mm hr^{-1} at the melting level, a 1 km fall through a cloud of LWC 0.2 gm^{-3}, and a cloud base 1 km above the ground. These were originally assumed in the computations made by Mason and Ramanadham (1954). The dashed curve shown in Fig. 27 is the profile of signal intensity obtained from Mason and Ramanadham's computation assuming that evaporation was negligible below the cloud base.

There is seen to be a clear separation between the computed and measured growth curves of Fig. 27. Harper (1957) suggests that the cloud LWC below the melting level was much lower than 0.2 g m^{-3} and that the raindrop-size distribution was unusually narrow during the rains observed by radar. To verify this suggestion a computation has been carried out for a situation considered to be representative for the rains reported by Harper.

Fig. 28 shows an initial distribution which is relatively flat and has most of the rain water content concentrated in drops with diameters between 1.4 and 2.4 mm. The change in this distribution brought about by (1) accretion and coalescence in falling a distance of 0.6 km through a cloud with a LWC of 0.05 g m^{-3}, and (2) coalescence and evaporation for an additional fall of 0.6 km through an atmosphere with a mean water vapor deficit of 0.25 g m^{-3} has been calculated by the methods given in Sections 3.2 - 3.4. The resulting distribution, shown as the dashed curve of Fig. 28, indicates a relatively minor shift of the drops from the low end of the spectrum to the large end. Of greater significance is the fact that the computed increase in signal intensity for the entire fall of 1.2 km amounts to less than 0.4 db. Such a change is barely perceptible on the abscissa of Fig. 27.

Another computation was made, similar in all respects to the one above with the exception of increasing the value of the cloud LWC to 0.2 g m^{-3}. The computed increase in signal intensity for this case amounted to 0.85 db. Such a change might be observed using radar, but it is still much smaller than the change given by the computed growth curve of Fig. 27. The conclusion is that a relatively flat distribution at the melting level is not significantly modified through coalescence or accretion.

One remaining question is whether the initial distribution assumed in Fig. 28 has any counterpart in nature. A similar distribution was observed with the spectrometer for the period from 1525-35[1] 1 August 1961 (dotted curve of Fig. 28). The intensity of this distribution is 3.4 mm hr^{-1}, but the shape is similar to that assumed in the above computations. Although evaporation is probably significant in shaping the distribution of 1 August (Appendix D), the results of Sections 3.4 and 3.7 show that the large drops are not greatly affected in falling through an atmosphere with a reasonable water vapor deficit. In addition, the work in Section 3.5 shows that the concentration of the larger drops at the melting level cannot be substantially different from the distributions observed at the ground. These findings suggest that the initial distribution assumed in Fig. 28 is realistic, and, in fact, it may be typical of the rain whose region of growth is a deep layer of supercooled cloud. Such a region was present on 31 July 1961 (Appendix D). Judging from the low melting level and insignificant growth below the

---

[1]All times refer to local standard time (MST) unless noted.

melting level, it appears certain that the major growth for the rain reported by Harper (1957) also occurred in regions of the cloud which were below freezing.

4. CONCLUSIONS

The chief contribution of this study, in the author's opinion, is the development of a procedure whereby the raindrop-size distribution at the melting level can be deduced. The results of the research contribute to our understanding of the final stage of precipitation growth. In addition, information is provided which is useful in the interpretation of weather radar observations. The conclusions arising from this study are briefly summarized below.

1. An exponential raindrop-size distribution having a relatively large negative slope at the melting level is considerably modified with distance fallen through coalescence among the raindrops, accretion of cloud droplets, and evaporation. Whereas the number of smaller drops is markedly depleted by each process, the number of larger drops is increased by coalescence and accretion but decreased by evaporation. On the other hand, a distribution with a relatively small negative slope at the melting level is only slightly modified by the above three processes.

By considering exponential raindrop-size distributions with various slopes but equal rainfall intensity, it is found that the depletion of cloud liquid water content and the amount of evaporation increase as the slope of the distribution becomes more negative. Since widespread rains often exhibit negligible changes in the radar signal intensity between the ground and the melting level, it is suggested that the raindrop-size distributions in these rains have relatively small negative slopes. It follows that the major growth occurs in regions which are above the melting level

and that the rain water content is concentrated in the larger drop sizes.

2. It is demonstrated that the raindrop-size distributions obtained with the photoelectric raindrop-size spectrometer adequately represent the natural distributions.

3. For the rains observed with the spectrometer, the least squares regression equation of the radar reflectivity factor, Z, on the rainfall rate, R, is

$$Z = 312R^{1.36}$$

provided that R is greater than 5 mm hr^{-1}. The scatter about this regression line is large.

Given the initial Z-R relationship for the Marshall and Palmer distribution, the effect of accretion is to decrease the coefficient and increase the exponent, whereas the effect of evaporation is to increase the coefficient and decrease the exponent. These effects are not as great as was indicated by Atlas and Chmela in an earlier investigation.

4. If the information obtained from the computations of the change in the distribution with height is combined with the observed distributions at the ground, then it is possible to deduce the raindrop-size distribution at the melting level. A study of this type for the light rain on 31 July 1961 at Flagstaff, Arizona shows that at the melting level (1) more large drops must be present than is indicated by the Marshall and Palmer distribution, and (2) the concentration of the larger drops must not be substantially different from their concentration observed at the ground.

5. SUGGESTIONS FOR FUTURE RESEARCH

This study considers the modifications of raindrop-size distributions from the melting level to the ground in the absence of any vertical updraft. One of the first considerations for future work should be the introduction of a vertical velocity profile. The amount of water vapor which condenses for a given updraft may then be considered, and, for a steady-state, this condensed water vapor must be balanced through the depletion of cloud liquid water content by the falling raindrops. By imposing the constraint of a balanced water budget on the processes considered in this study additional information about the precipitation mechanism will be provided.

The process of coalescence has been limited to drops of diameter 0.1 mm and larger. However, similar computations are possible for particles in the cloud droplet range. Although our knowledge of the collection efficiency between cloud droplets is still unsatisfactory (and, therefore, deserving of further study), by using currently available data it is probable that the effect of coalescence on a cloud droplet distribution could be computed. By considering various vertical velocity profiles, it should be possible to determine the conditions which will lead to the formation of precipitation-size particles. It may also be possible to consider the combined effects of condensation and coalescence on the cloud-droplet distribution. However, the initial formation of a cloud droplet distribution through condensation is a complex process and much work remains to be done on this problem.

The general method presented in this study may also be extended to the ice phase. In such an extension the additional problems involving the growth of an ice crystal must be considered, but even with our present relatively sketchy knowledge of the size, shape, and collection efficiency of ice crystals, useful computations should be possible. The problems which arise due to the changes in velocity (and, therefore, concentration) of the snowflakes as they melt, and the effects of a vertical updraft can readily be incorporated in the present computer programs. Such a study would be considerably more complex than the one presented here. Nevertheless, the research reported here suggests that such an extension is feasible, and it would be one of the first attempts to combine the microphysical effects of particle interaction with the large scale dynamics of the cloud system.

APPENDIX A. DESCRIPTION AND CALIBRATION OF A PHOTOELECTRIC RAINDROP-SIZE SPECTROMETER

The photoelectric raindrop-size spectrometer was developed by Dr. A. Nelson Dingle in an effort to improve the accuracy and ease with which raindrop sizes are measured. It was operated successfully in natural rain in August 1959 in Ann Arbor, Michigan. Since that time many different rains have been observed during the various seasons. The most comprehensive measurements were obtained in July and August 1961 at Flagstaff, Arizona.

The spectrometer is described in detail by Dingle and Schulte (1962), and only a brief summary of its essential features is included here. The two basic components of the instrument (Fig. 29) are: (1) a light source which provides a nearly collimated beam 0.5 cm thick by 4.0 cm high, and

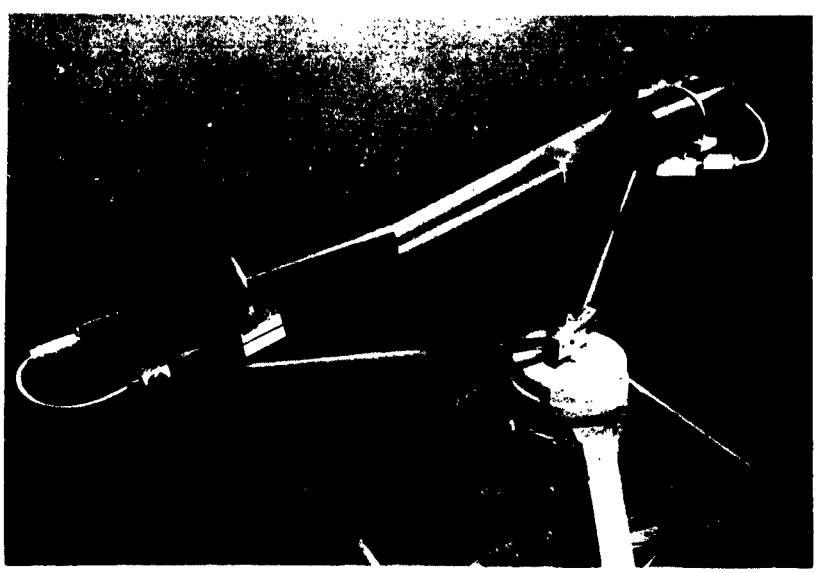

Fig. 29. The photoelectric raindrop-size spectrometer: (A) light source, (B) photometer, (C) vertical shaft and axis of rotation.

(2) a photometer unit which views a segment of the light beam. The sensitive field defined by the intersection of the beam and the optical field of the photometer has dimensions of 10.0 cm by 3.75 cm by 0.5 cm. The unit is rotated about a vertical axis: the volume swept out by the sensitive field being 6.5 liters per revolution. During field use the rotational rate is 120 rpm resulting in a sampling volume of 0.78^3 min^{-1}. Raindrops traversed by the sensitive field scatter light to the photometer in proportion to their surface area. The electronic pulses thus produced are recorded by means of an oscillograph.

SOURCES OF ERROR

The primary advantage of the spectrometer in solving the problem of sizing and counting raindrops is that it provides a continuous record without disturbing the sampling volume. However, errors are still introduced which complicate the interpretation of the data. The purpose of this section is to evaluate the magnitude of some of these errors.

Non-uniform sensitive field

The response from equal sized drops can be constant only if the light intensity within the sensitive field is uniform. However, it is not possible to obtain a uniform sensitive field at the required light intensity with existing lamp sources and within the physical limitations of the spectrometer components. The sensitive field of the present instrument is essentially uniform along a particular line parallel to the beam axis, but it has a less intense center as compared with the portions about 1.5 cm above and below the optical axis. A series of about 80 light intensity

measurements made systematically throughout the sensitive field showed that there was a maximum variation of ±10 per cent from the mean intensity. However, the amount of light scattered by a water drop is proportional to the square of the drop diameter, and therefore the error in the measurement of the drop diameter due to variation of light intensity within the sensitive field amounts to only ±5 per cent.

Scattering angle

The intensity of the scattered light from a given drop decreases as the scattering angle from the forward direction increases (for angles from 0 - 90°). The optical geometry of the sensitive field is so arranged that as the scattering angle to the photometer decreases the distance between the drop and the objective lens increases. This keeps the amount of scattered light gathered by the photometer relatively constant regardless of where the drop is located within the sensitive field. Dingle and Schulte (1962) have shown that with a mean scattering angle of 28.8° (the angle chosen for the spectrometer) the error introduced by variations in the light gathering characteristics of the photometer is about one fifth the error caused by the non-uniformity of the light intensity within the field.

Non-spherical drops

Raindrops less than 1 mm in diameter are essentially spherical. Above 1 mm the shape of a freely falling raindrop in the atmosphere begins to deviate from a sphere, and above 3 mm the drop's lower surface becomes markedly flattened. Jones (1959) has also pointed out that large freely falling raindrops will oscillate between an oblate and prolate shape.

These variations in shape will affect the amount of light scattered toward the photometer. An evaluation of the magnitude of the error introduced by assuming a spherical shape and by neglecting the oscillations of the larger drops has not been made. However, it is probable that such errors are relatively minor below about 2.0 mm diameter. For larger drops the error introduced is combined with that due to other effects described in the next section.

Edge errors

The errors at the edges of the field are of two kinds: (1) the errors at the side edges, and (2) the errors at the upper and lower edge of the sensitive field. The errors at the side edges are due to the raindrops being only partially within the sensitive field and therefore are not completely illuminated. This effectively reduces the area of the sensitive field that will give a normal response for a given sized drop. Thus, the actual area for normal response from a 1 mm diameter drop is reduced by 2 per cent (viz. 1 mm on each side of the 10 cm field). This reduction in area clearly increases for larger drops, becoming about 10 per cent for the maximum sized drops observed.

The errors at the lower and upper edges are of a different order of magnitude, and are caused by the raindrop having a vertical velocity, which for large drops, is about twice that of the tangential velocity of the rotating sensitive field. Fig. 30 is a schematic drawing showing the trajectory of a typical raindrop as the sensitive field sweeps past it. The angle which the falling raindrop makes with the vertical of the sensitive field is given by

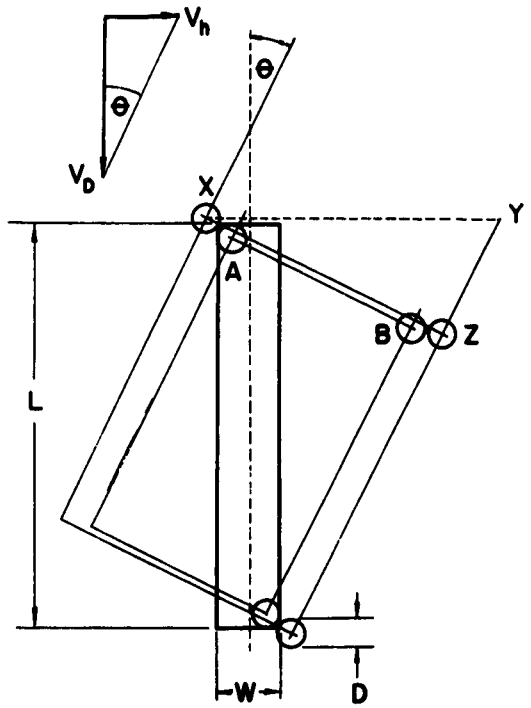

Fig. 30. View of sensitive field along the beam axis showing the trajectory of a drop which will just be completely illuminated.

$\theta = \tan^{-1} v_h/v_D$ where v_h is the linear speed of rotation of the center of the sensitive field and v_D is the fall speed of a drop of diameter D. Since drops of diameter D can occur with equal probability anywhere along the line XY, Fig. 30 shows that the fraction of drops which are not completely illuminated by the sensitive field is given by

$$F = \frac{XZ - AB}{XZ} \qquad \text{(A-1)}$$

It can be shown that

$$AB = \left[L-D + \frac{(W-D)}{\tan \theta}\right] \sin \theta \qquad \text{(A-2)}$$

and

$$XZ = (L - W \tan \theta) \sin \theta + \frac{W}{\cos \theta} + D , \qquad (A-3)$$

where L and W represent the length and width of the sensitive field respectively.

Values of F computed from Eq. (A-1) are shown as a function of drop diameter in Fig. 31. The actual field dimensions of L = 3.75 cm and W = 0.5 cm were used in Eqs. (A-2) and (A-3). The rotational rate was 120 rpm yielding a linear speed of v_h = 382 cm sec^{-1} at the center of the sensitive field. The points plotted in Fig. 31 are the results of the calibration experiment which is described later.

The quantity F gives the fraction of drops which scatters less light than fully illuminated drops and hence the fraction which is not recorded accurately. Fig. 31 shows that the

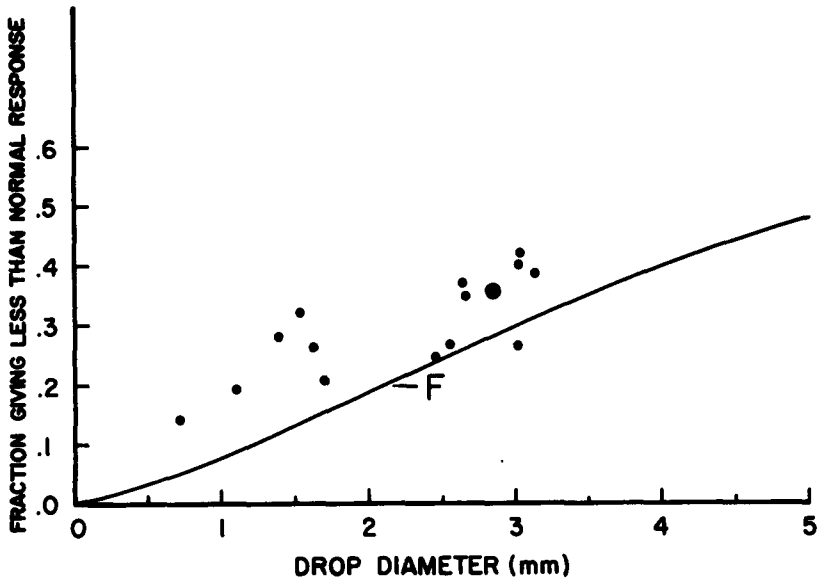

Fig. 31. Fraction of drops giving less than normal response. Curve F gives the values computed from Eq. (A-1). Rotational rate is 120 rpm, and the field dimensions are L = 3.75 cm, and W = 0.50 cm. The points are obtained from the calibration experiment.

fraction incorrectly recorded is quite large, particularly at large drop diameters. If it were possible to determine the amount of light scattered by drops which are only partially illuminated, then an attempt could be made to evaluate the response curve for drops regardless of their trajectory through the sensitive field. Unfortunately, this approach is much too complex and is not presently practical. As an alternative, experimental techniques can be adopted which will provide an overall calibration of the spectrometer and indicate the possible magnitude of some of the errors in the measurement of raindrop sizes.

CALIBRATION EXPERIMENT

Procedure

The purpose of the calibration experiment is to determine a relationship between the magnitude of the recorded pulse height and the drop diameter which produced it. The basic design of the calibration experiment is as follows. Uniformly sized drops of a known diameter are produced and arranged to fall within the volume swept out by the sensitive field. Any drop which is within the sweep of the sensitive field is recorded by the spectrometer. The experiment is continued until about 100 drops have been recorded, and the pulse height from each is measured. If there are no errors in the system, the recorded drops will have a uniform pulse height. However, a distribution of pulse heights is produced because of the errors mentioned earlier. From an analysis of this distribution it is possible to determine the most probable pulse height corresponding to the drop diameter used for the test.

The essential requirement for calibrating the spectrometer is a source of constant sized drops. These are produced at the end of a capillary tube drawn to an outside diameter of about 0.5 mm. The capillary tube is connected to a source of distilled water which is maintained at a constant head throughout an individual test. For the smaller drops the capillary is placed inside a hose of about 5 mm inside diameter. Air is then directed down the tube and past the end of the capillary. This causes a downward force to be applied to the drops forming at the end of the capillary. By this means uniformly sized drops can be produced over long periods of time within a range of 0.7 to 3.0 mm in diameter.

The actual drop diameter is usually obtained by weighing a known number of drops. At least two such measurements are made for each test. If there is a variation of more than 5 per cent in the drop diameter determined from the measurements, then the entire test is discarded. However, drops of less than 1 mm in diameter are produced too rapidly for visual counting. Engelmann (1962) of the Hanford Atomic Products Operation in Richland, Washington has developed a method for measuring these smaller drops. He noted that when the drops are allowed to fall on a special blueprinting paper (referred to as diazo paper), which is then exposed to ammonia fumes, a well defined stain appears. He has determined the relationship between the stain diameter and drop diameters. The samples of small drops that were collected on this paper were sent to Mr. Engelmann, and he determined the required drop diameters. Typical diazo paper samples are shown in Fig. 32. Since the stain diameter depends on the fall velocity of the

water drop, it is necessary to have the drops fall at their terminal velocity. In the laboratory the drops fall through a distance of 310 cm. Drops of 1 mm and less will be within 1 per cent of their terminal velocity in a fall of this magnitude (Laws, 1941). It is for this range of drop diameters that the weighing method is not applicable. Therefore, the diazo paper determination is used primarily for drops of 1 mm and less, while the weighing technique is used for all larger sizes.

Prior to and after each test a 3.18 mm diameter glass bead on the end of a thin rod is rotated through the sensitive field and the pulses recorded while the spectrometer is stationary. This information is used to determine the stability of the light intensity and the electronic components throughout the test or between individual tests.

The recorded pulse height is proportional to the surface area of the drop, but it is desirable to work with a variable which is linearly related to the drop diameter. Therefore, the pulse height of the recorded drop is abstracted in units linearly proportional to the drop diameter. These units are class number, each class representing an increment of about 0.06 mm in drop diameter. Of course the purpose of the calibration experiment is to determine the exact relationship between the particular class number (or fraction thereof) and the drop diameter.

Results

Some of the detailed results from the diazo paper samples are shown in Table 8. The number of stain diameters measured for each sample was about 20. The relationship

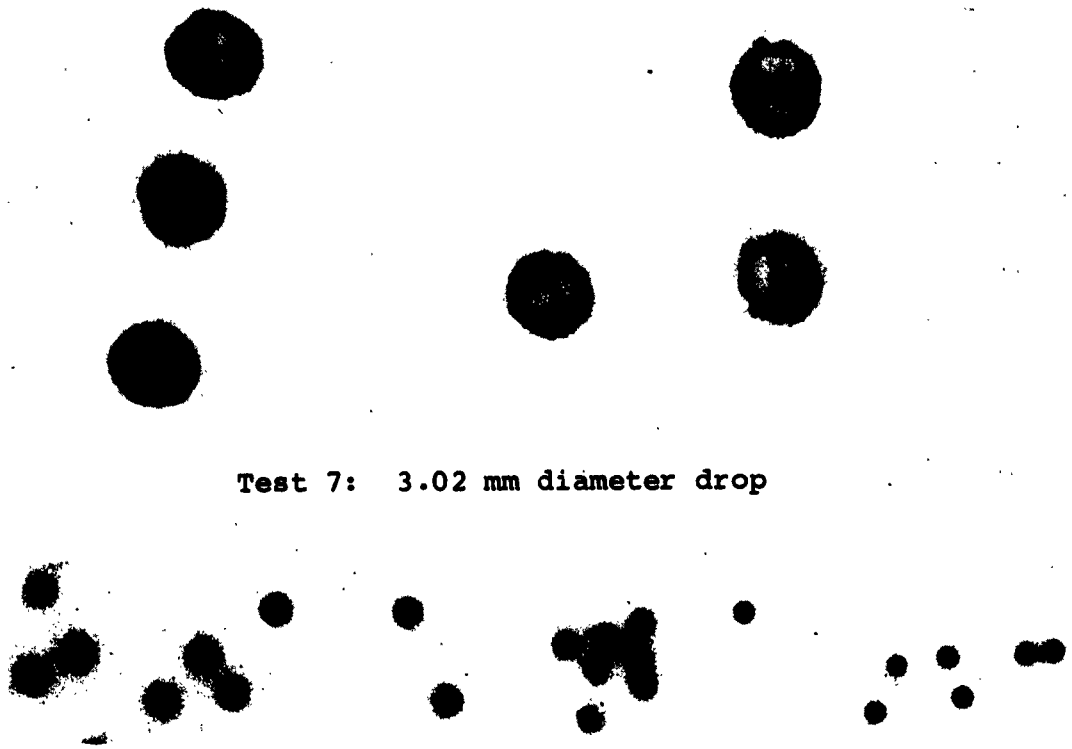

Test 7: 3.02 mm diameter drop

Test 11: 1.01 mm drop

Test 12: 0.76 mm drop

Fig. 32. Diazo paper water drop samples.

between stain diameter, S , and drop diameter, D , given by Engelmann (1962) is

$$S = 3.10\ D^{1.35} \qquad \text{(A-4)}$$

or

$$D = 0.434\ S^{0.741}\ , \qquad \text{(A-5)}$$

for S and D in mm. The mean measured stain diameter, $\bar{S}$, and corresponding mean drop diameter calculated from (A-5), $\bar{D}$, are shown in the 4th and 5th columns of Table 8. Except for Test 11, the values of $\bar{D}$ are fairly constant within each test. The variation within Test 11 is probably caused by unintentional changes in the air flow past the capillary tube. Using (A-5) to compute values of D for each value of S, it becomes possible to calculate the standard deviation of D (σ_D), and this is shown for each test in the 6th column.

Table 8. Drop diameter determinations from diazo paper samples.

Test	Sample	No. in Sample	Mean Stain Dia. ($\bar{S}$) (mm)	Mean Drop Dia. ($\bar{D}$) (mm)	σ_D (mm)	$\sigma_D/\bar{D}$ (%)	Mean $\sigma_D/\bar{D}$ (%)
7	a	22	12.10	3.10	.114	3.7	
	b	20	11.88	3.06	.080	1.9	3.1
	c	20	11.12	2.91	.128	3.9	
11	a	23	3.07	0.99	.046	4.65	
	b	19	2.96	0.965	.041	4.25	4.4
	c	18	3.02	0.98	.036	3.7	
	d	15	3.32	1.10	.054	4.9	
12	a	19	2.15	0.765	.0351	4.6	3.9
	b	19	2.15	0.755	.0245	3.2	

The coefficient of variation, defined as $\sigma_D/\bar{D}$ where σ_D is the standard deviation of D, is presented in the 7th column of Table 8. It is an indication of the percentage variation of the measured drop diameters within each sample.

The mean coefficient of variation for each test is given in column 8. The results of Table 8 show that the coefficient of variation has a range of 3-5 per cent. However, part of this variation in the measured drops is due to the use of the diazo paper rather than an actual variation in the drop diameter.

The responses of the spectrometer to the nearly constant sized drops are shown in Fig. 33 for four of the tests. The class number used for the abscissa of these figures is proportional to the drop diameter. The outstanding characteristics of these response curves are (1) the peak frequency which occurs near the larger observed class numbers, and (2) the much smaller and approximately uniform frequency for all smaller classes. The variation in class number of approximately $\pm$10 per cent about the peak frequency is probably accounted for by the combined errors due to (1) the variation in light intensity throughout the sensitive field, (2) the non-sphericity of the drops, and (3) the use of slightly varying drop diameters during the test. If such is the case then the nearly uniform frequency observed for all smaller classes can be attributed to the edge errors. As a check on this hypothesis the total percentage of drops which had a pulse height greater than class 4 but less than 80 per cent of the maximum class recorded was determined for each test. (The drops in classes 1-4 were assumed to be caused by splash produced by drops which hit parts of the spectrometer and broke up into many small drops - discussed later).

The results of the above calculation are shown in Table 9. The second column of this table gives the actual diameters of the drops used during the test (determined either by weighing

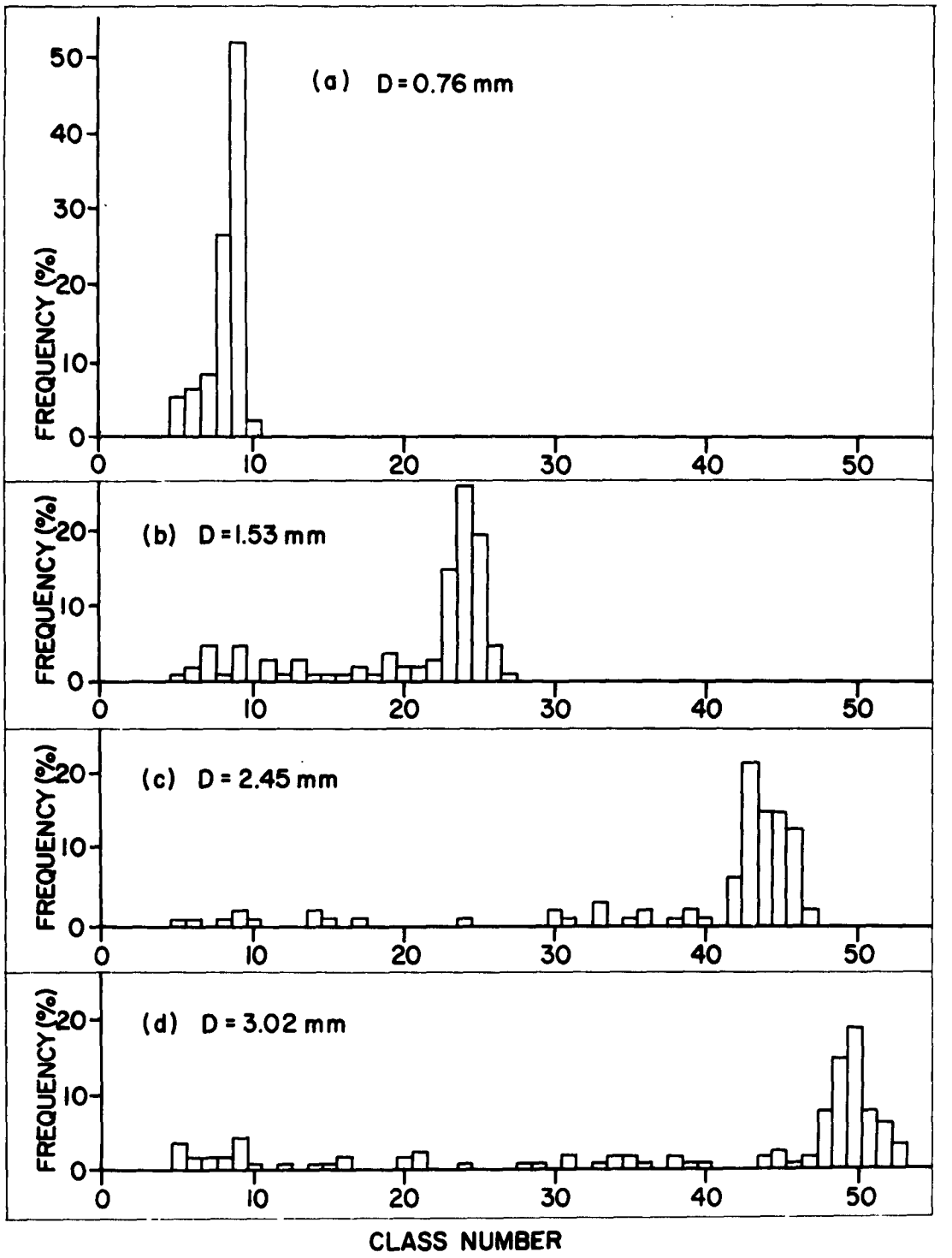

Fig. 33. Response of the spectrometer to nearly constant sized drops. Total frequency is normalized to 100%, and the class number is linearly proportional to the drop diameter.

or with the diazo paper). The third column gives the total number of drops recorded during the test, and the fourth column gives the total fraction of drops which produced a pulse height greater than class 4 but smaller than 80% of the maximum recorded class. This latter fraction is plotted as a function of drop diameter in Fig. 31 in order that a comparison can be made with the theoretical evaluation of the error introduced by drops which are only partially illuminated. In general, the experimental points indicate a greater fraction than that given by the curve for F. This could be due to the inclusion of a few drops produced by splash which are greater than class four. Nevertheless, there is qualitative agreement between the theoretical evaluation of the edge error and the experimental data.

Table 9. Results of the calibration experiment.

Test	Mean Dia (mm)	No. of Drops Recorded	Fraction in Error
1	2.84	70	.357
2	2.84	126	.357
3	2.45	93	.247
5	1.72	53	.207
6	1.53	109	.321
7	3.02	117	.402
8	3.01	135	.267
11	1.01	247	.194
12	0.76	174	.144
15	3.02	78	.423
16	2.64	80	.350
17	1.38	60	.283
18	1.62	140	.264
19	2.64	100	.370
20	2.55	130	.269
24	3.10	155	.387

The value of the class number chosen as best representing the drop diameter used in a test was obtained by taking the mean about the 4-7 class numbers enclosing the peak frequency. The value thus determined was converted to its equivalent pulse height and this was plotted against the square of the drop diameter as shown in Fig. 34. The generally good fit of the data to a straight line confirms the square relationship between drop diameter and output of the photometer. The least squares regression line, restricted to pass through the origin, is

$$H = 13.9\ D^2\ , \qquad \text{(A-6)}$$

where H and D are the pulse height and drop diameter respectively in mm. The above relationship is applicable when the standard 3.18 mm glass bead gives a pulse height of 107.5 mm. The constant of Eq. (A-6) would have to be adjusted if the pulse height for the standard bead changed.

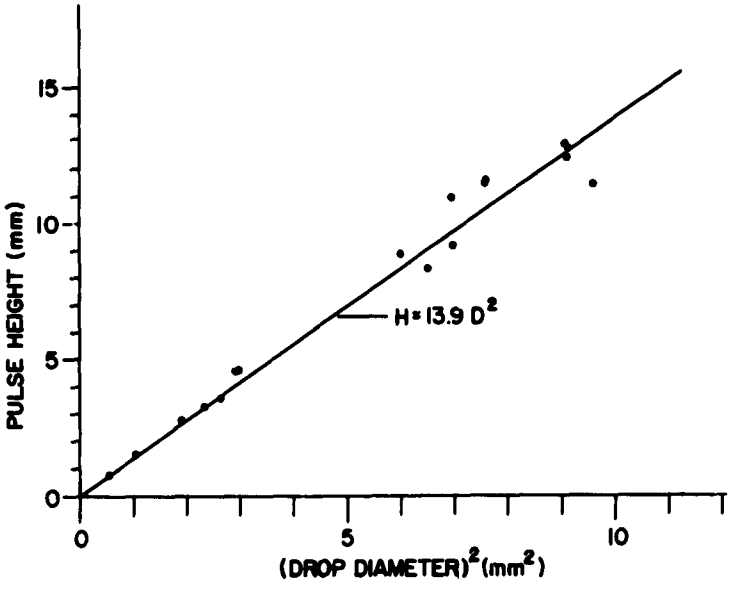

Fig. 34. Results of the spectrometer calibration.

THE EFFECT OF SPLASH

The spectrometer necessarily consists of components which are within 10 to 15 cm of the sensitive field. During natural rains, drops impinge upon the surfaces of these components and produce varying numbers of splash droplets. Some of these droplets may have trajectories which carry them into the path of the sensitive field and are recorded in the same manner as natural raindrops. In an attempt to reduce the splash to a minimum, various materials were tested for their effectiveness in eliminating splash. These materials ranged from window screen placed about ½ in. above the surface to velvet and cheese cloth. The most practical and reasonably effective material was 24 mesh screen. Consequently this screening was mounted ½ - 1 inch above all the exposed spectrometer components. Unfortunately, this did not prove to be entirely satisfactory, but it did reduce the splash markedly. Fig. 35 shows the distribution of splash droplets which were produced by drops of about 6.5 mm

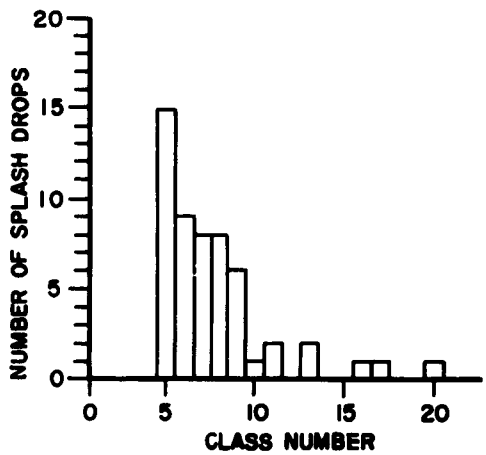

Fig. 35. Splash droplets produced from drops ot about 6.5 mm diameter.

diameter falling at 80 per cent of their terminal velocity and positioned about 42 cm from the center of rotation. This placed the drop outside the region of the sensitive field but still in a position to strike the screen above the photometer sun shield. Approximately 100 drops per minute were produced and the test lasted for 13 min. In this time 54 splash drops were recorded. Only splash drops in class 5 or larger were considered as this represents the lower limit for sizing drops during field operation. Most of the splash drops were less than 0.8 mm diameter, but some were as large as 1.5 mm.

It is nearly impossible to determine the number of splash droplets which are recorded during a natural rain. It depends greatly on the drop-size distribution of the rain; observable splash droplets are seldom produced by drops less than about 2 mm in diameter, but they become quite significant if drops over 3 mm are present. It appears that the number of small drops recorded in the raindrop distribution is somewhat indeterminant, particularly if fairly large drops (which tend to produce splash drops large enough to be recorded) are present in the natural rain.

CORRECTION APPLIED TO THE MEASURED DISTRIBUTIONS

Figs. 31 and 33 illustrate the difficulty in determining drop diameter from a given recorded pulse height. For example, if a drop produced a pulse height within class 24, then Fig. 33b indicates that the drop diameter is about 1.5 mm. However, Figs. 33c and 33d show that there is a certain probability that this pulse height was produced by a drop considerably larger than 1.5 mm. The one certainty is that a pulse height of class 24 could not be produced by drops having a diameter of less than about 1.3 mm.

Let us consider a possible correction to the observed raindrop-size distribution which accounts for the manner in which the spectrometer data is collected. For a given drop diameter, curve F of Fig. 31 can be used to provide an estimate of the fraction of the drop number which is recorded at some smaller drop diameter. This estimate is fairly conservative judging from the experimental data, but its use should avoid the possibility of "over-correcting" the observed distribution. Fig. 36 shows a typical example of a measured raindrop-size distribution. D_n is the largest drop diameter observed and it is assumed that these are not the result of drops which had a diameter greater than D_n. Reference to Fig. 31 gives the correction, F_{D_n}, and the original number of drops of diameter D_n, N_{D_n}, is corrected to $(1 + F_{D_n}) N_{D_n}$. Since $F_{D_n} N_{D_n}$ drops have been added to the drops of diameter D_n, this same number must be subtracted from the remaining distribution. Fig. 33 shows that the probability of a drop of diameter D_n being recorded as a drop of diameter D_i, $i = 1, 2, \ldots n-1$, is essentially constant. Therefore the fraction of drops $F_{D_n} N_{D_n}/n-1$ should be subtracted from each class of drops from D_1 to D_{n-1}. Once this has been done the number of drops of diameter D_{n-1} can be corrected in a similar manner and so on until finally the number of drops of diameter D_2 has been corrected. The resulting distribution is taken to represent the natural distribution.

Fig. 37 shows the effect of the correction on a sample distribution. The number of large drops increase and the number of small drops decrease slightly for the corrected distribution as compared to the original distribution. The

rainfall intensity is increased by about 20 per cent in this case, but the magnitude of the increase is dependent upon the drop-size distribution. Corrected distributions are used in the remainder of this study. The rainfall intensities computed from these distributions agree favorably with the intensities observed with a weighing bucket rain gage (Appendix D).

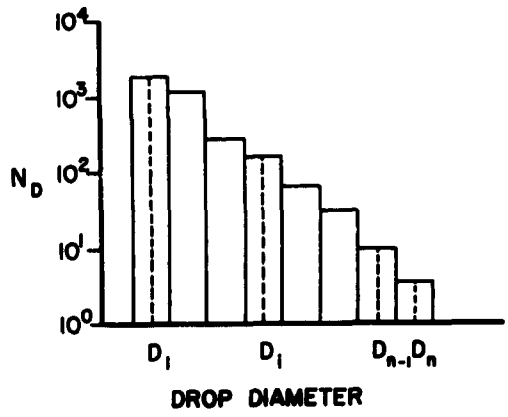

Fig. 36. Illustration of correction to the drop-size distribution.

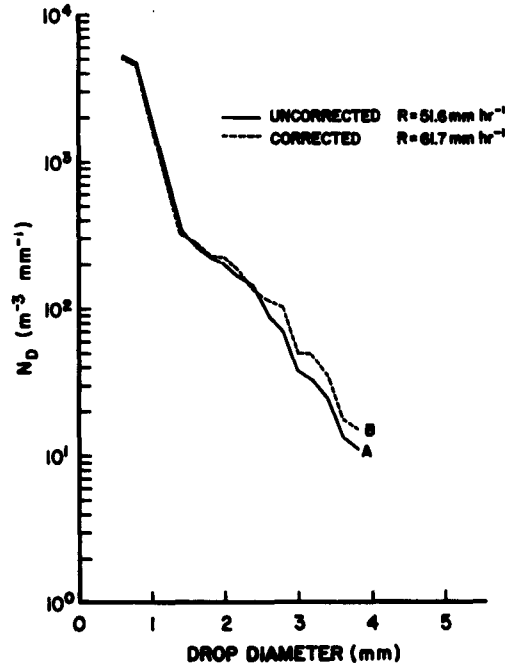

Fig. 37. Curve A, distribution prior to correction; curve B, distribution after correction is applied.

APPENDIX B. CONSTANT FLUX FOR THE PROCESS OF COALESCENCE

It is assumed that at the initial height a distribution of raindrops is available which is invariant with time. For steady-state, the mass flux of raindrops must be constant at all heights, providing the only process acting to modify the distribution is coalescence between the raindrops. Using the notation of Section 3.2 and referring to Fig. 9, it is required to find the concentration of drops $\Delta N_j'$, which form from the ΔN_j coalescences between drops of diameter D_i and D_j.

For the moment, consider the drops of diameter D_i and D_j. The precipitation intensity from the concentration of these two drop sizes is given by

$$R_o = \frac{\pi}{6} (N_i D_i^3 v_i + N_j D_j^3 v_j) \quad . \tag{B-1}$$

Since the concentration of drops of all other diameters remain unchanged, they can be ignored. It is shown in Section 3.2 that over a distance Δz the concentrations of drops of diameter D_i and D_j are reduced by ΔN_i and ΔN_j respectively. Therefore the precipitation intensity at a height Δz below the initial level is given by

$$R_1 = \frac{\pi}{6} \left[(N_i - \Delta N_i) D_i^3 v_i + (N_j - \Delta N_j) D_j^3 v_j + \Delta N_j' D_c^3 v_c \right] \tag{B-2}$$

where $\Delta N_j'$ is the concentration of the drops which formed through coalescence. Now the flux must be constant at each level, and therefore $R_o = R_1$. Equating (B-1) and (B-2), and solving for $\Delta N_j'$ gives

$$\Delta N_j' = (D_i^3 v_i \Delta N_i + D_j^3 v_j \Delta N_j) / (D_c^3 v_c) \quad . \tag{B-3}$$

APPENDIX C. DECREASE IN MASS OF A RAINDROP THROUGH EVAPORATION

The effect of evaporation on freely falling raindrops has been investigated by Kinzer and Gunn (1951). They tabulated the change in mass of the raindrop for selected values of temperature, relative humidity, and drop diameter. The following analysis is based on Kinzer and Gunn's results, but is more general since it allows the evaluation of the effect of evaporation for any reasonable combination of temperature, relative humidity, and drop diameter. In addition, the evaluation is in a form which is readily handled by computer techniques.

Kinzer and Gunn showed that the change in mass with time of a water drop falling at terminal velocity is given by:

$$\frac{dm}{dt} = 4\pi aK(\rho_a - \rho_b)\left[1 + \frac{FRe^{1/2}}{(4\pi\rho K/\eta)^{1/2}}\right] \qquad (C\text{-}1)$$

where a is the drop radius, K is the diffusion coefficient, ρ_a is the saturation vapor density at the temperature of the drop, ρ_b is the water vapor density in the environmental air through which the drop falls, Re is the Reynold's Number, ρ and η are the density and viscosity of the ambient air respectively, and F is a dimensionless number. Frössling (1938) suggests that F is a constant, but Kinzer and Gunn find that F is a function of Re and actually were able to

evaluate it for values of Re up to 2500. The experimental work of Kinzer and Gunn involved careful and brilliantly devised schemes for measuring the evaporation from freely falling drops covering a diameter range of 0.1 to 4.4 mm. The results are presented in the form of two tables. One gives the term

$$4\pi a \left[1 + \frac{FRe^{1/2}}{(4\pi\rho K/\eta)^{1/2}}\right] \qquad (a)$$

for various values of drop diameter and ambient air temperature, whereas the other table gives the term

$$K(\rho_a - \rho_b)X10^{-6} \qquad (b)$$

for various values of relative humidity (RH) and temperature. The rate of evaporation in g sec^{-1} is given by the product of term (a) and (b) as seen from Eq. (C-1).

Fig. 38 is a plot of term (b) against RH for the five temperatures given by Kinzer and Gunn. It is seen that at a constant temperature, there is nearly a linear relationship between the RH and term (b). Values of p are plotted as a function of temperature in Fig. 39, where p is the value of the slope of the lines of Fig. 38. Although this is an odd relationship, relatively little error is introduced if a linear interpolation of p is taken between either 0 and 10C or 10 and 30C. The slope p thus determined is used to compute term (b) for the appropriate relative humidity from Fig. 38.

The values of term (a) are plotted in Fig. 40 as a function of drop diameter for temperatures of 0 and 30C. An analysis of the temperature dependence of term (a) shows that if the value of term (a) is known for 0C, then by multiplying its value by the factor (1 - 0.00264T), where T is the

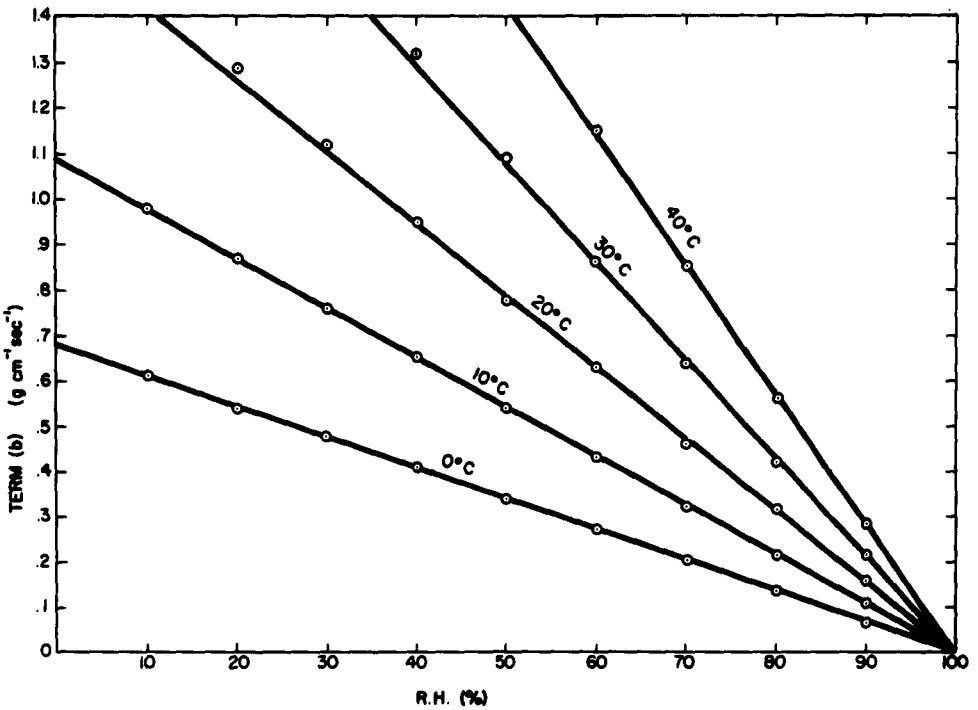

Fig. 38. Plot of term (b) against relative humidity for various temperatures.

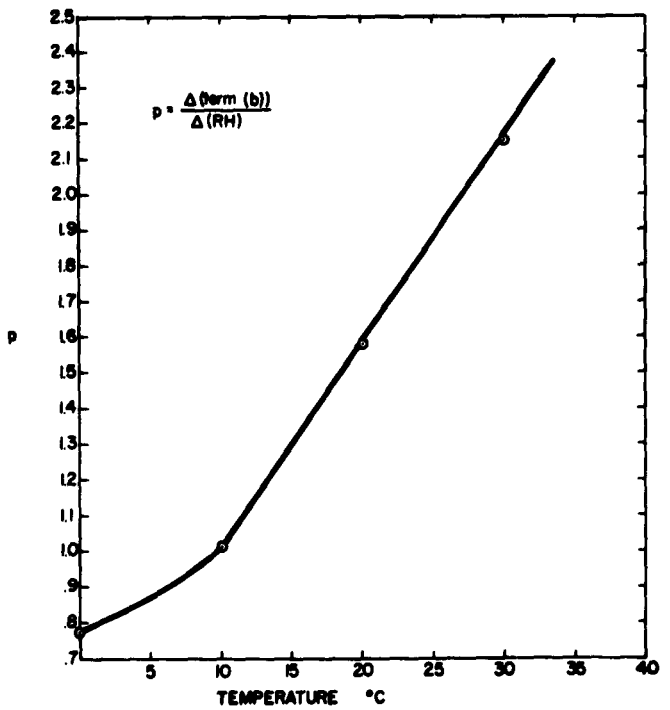

Fig. 39. Values of p as a function of temperature.

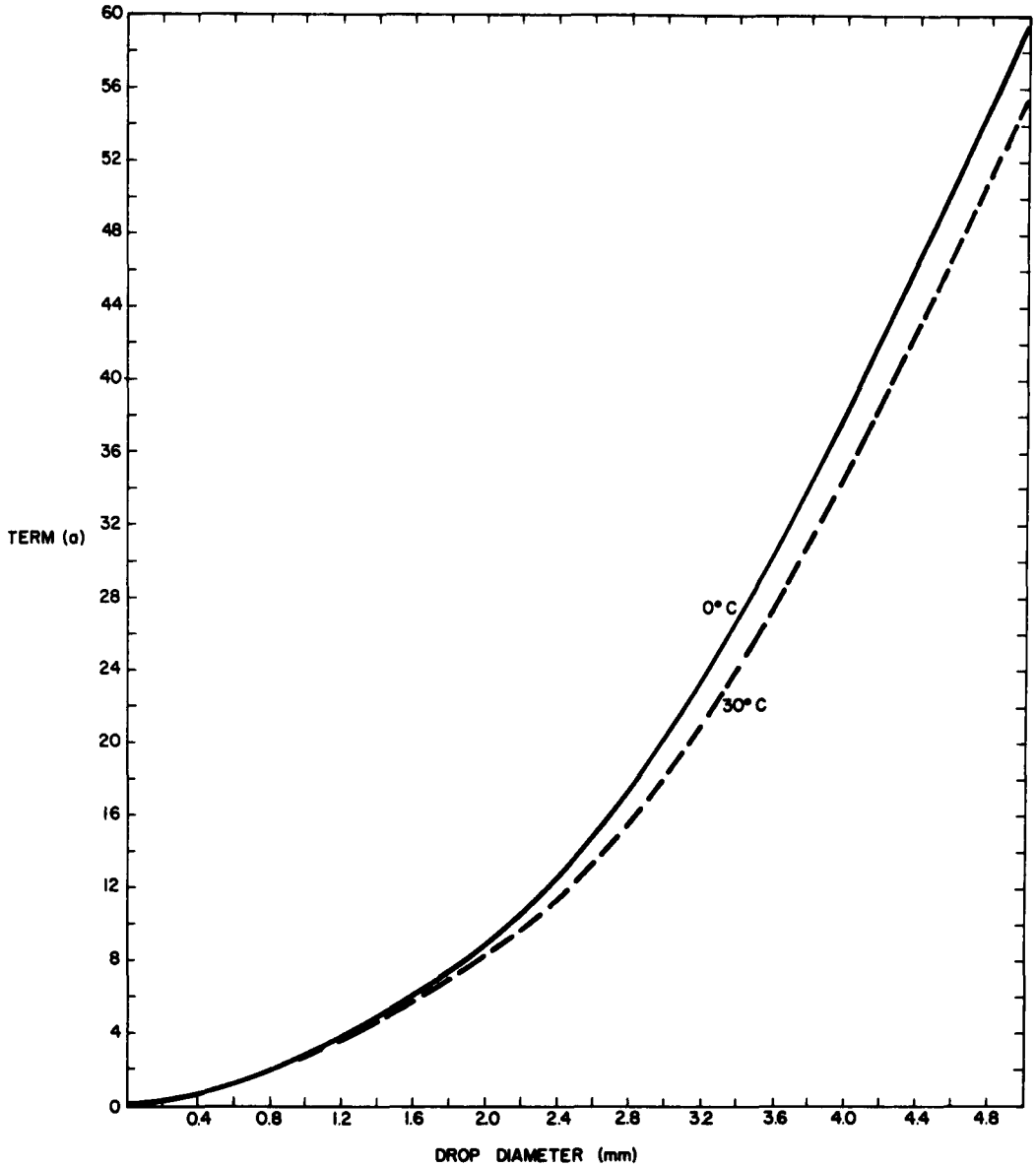

Fig. 40. Plot of term (a) as a function of drop diameter.

temperature in °C, the value of term (a) at the temperature T is evaluated with very little error. In the computer program, E_i is the value of term (a) at 0C obtained from Fig. 40 for a drop diameter of D_i. The change in mass with time of the freely falling drop in g sec^{-1} is given by:

$$\frac{dm}{dt} = p(100 - RH)E_i(1 - .00264T)X10^{-10} , \qquad (C-2)$$

where the units are as follows: p in 10^6 g cm^{-1} sec^{-1}, RH in per cent, E_i in cm, and T in °C. A few test calculations showed that Eq. (C-2) could be used to reproduce the values of Kinzer and Gunn with an error of less than 4 per cent. In addition, Eq. (C-2) is well suited for computer programming and can be used to determine the change in mass with time of freely falling drops for any temperature between 0 and 30C in combination with any RH between 35 and 100 per cent.

APPENDIX D. OBSERVATIONS OF RAINDROP SIZES AT FLAGSTAFF, ARIZONA

GENERAL WEATHER PATTERN

During the summer of 1961, the raindrop-size spectrometer was operated in conjunction with a mesometeorological observational program at Flagstaff, Arizona. The primary aim of the program was to observe and study the life cycle of cumulus clouds. Personnel from The University of Michigan were responsible for observations of raindrop sizes and for the operation of a 3 cm radar. Other participating groups included the University of Chicago (mesometeorological network, electric field measurements), the Geophysics Research Directorate (cloud photography, aircraft measurements and

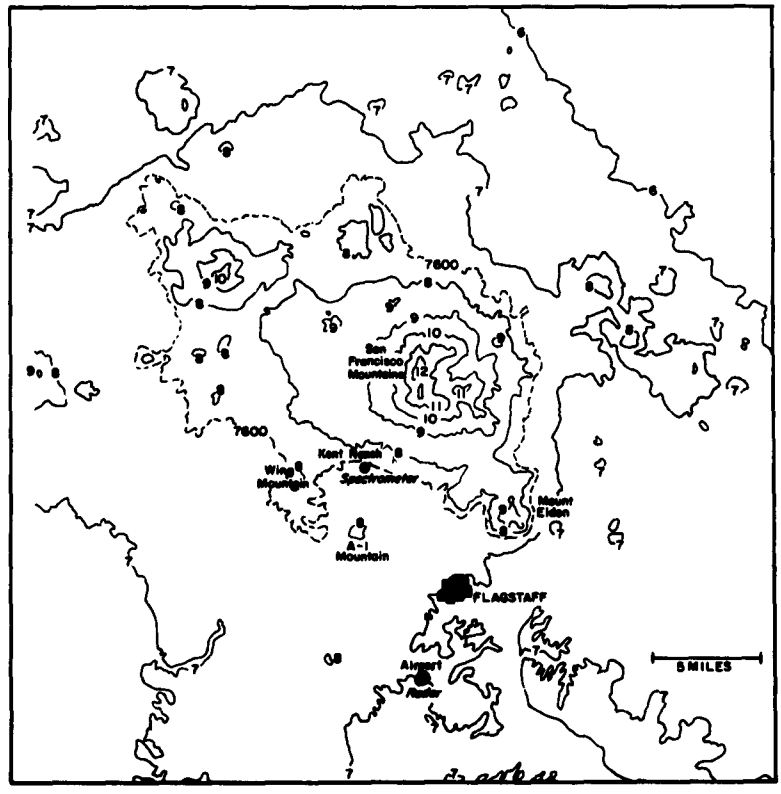

Fig. 41. Topography of the Flagstaff area. Contours are in 1000's of feet.

temperature in °C, the value of term (a) at the temperature T is evaluated with very little error. In the computer program, E_i is the value of term (a) at 0C obtained from Fig. 40 for a drop diameter of D_i. The change in mass with time of the freely falling drop in g sec^{-1} is given by:

$$\frac{dm}{dt} = p(100 - RH)E_i(1 - .00264T)X10^{-10} , \qquad (C-2)$$

where the units are as follows: p in 10^6 g cm^{-1} sec^{-1}, RH in per cent, E_i in cm, and T in °C. A few test calculations showed that Eq. (C-2) could be used to reproduce the values of Kinzer and Gunn with an error of less than 4 per cent. In addition, Eq. (C-2) is well suited for computer programming and can be used to determine the change in mass with time of freely falling drops for any temperature between 0 and 30C in combination with any RH between 35 and 100 per cent.

APPENDIX D. OBSERVATIONS OF RAINDROP SIZES AT FLAGSTAFF, ARIZONA

GENERAL WEATHER PATTERN

During the summer of 1961, the raindrop-size spectrometer was operated in conjunction with a mesometeorological observational program at Flagstaff, Arizona. The primary aim of the program was to observe and study the life cycle of cumulus clouds. Personnel from The University of Michigan were responsible for observations of raindrop sizes and for the operation of a 3 cm radar. Other participating groups included the University of Chicago (mesometeorological network, electric field measurements), the Geophysics Research Directorate (cloud photography, aircraft measurements and

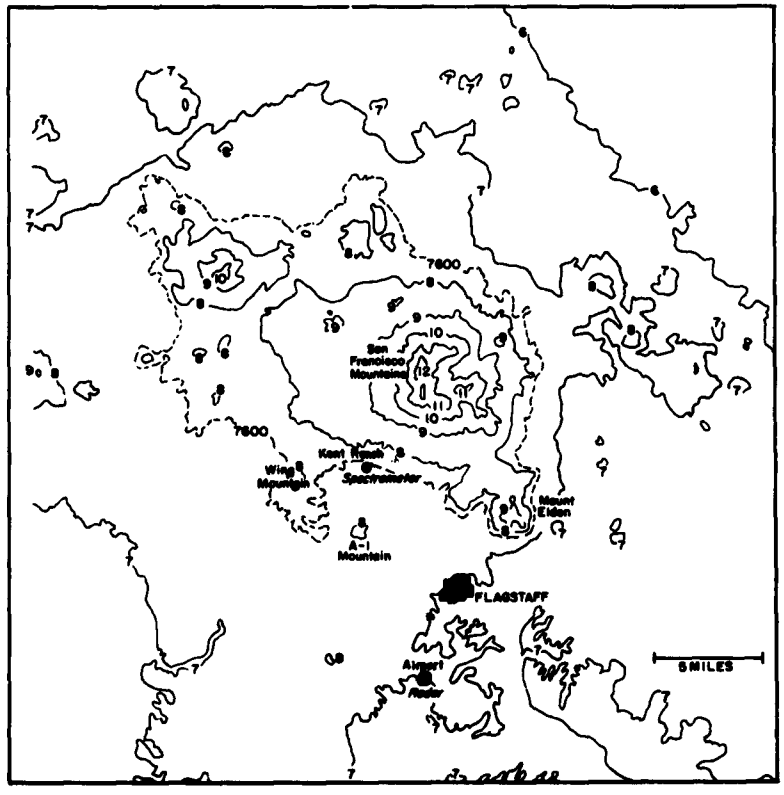

Fig. 41. Topography of the Flagstaff area. Contours are in 1000's of feet.

radar studies), and Meteorology Research, Inc. (aircraft measurements, radar studies, and cloud modification).

Prior to the operational period it was agreed that all observations acquired by one group would be made available to all the other groups upon request. A review of the data revealed that four of the days were particularly promising for further study. The raindrop-size distributions and related information are presented in detail for these four days, and in some cases an explanation of the observed data is given.

The local topography and the location of some of the equipment are shown in Fig. 41. Located approximately 8 miles north of Flagstaff is an isolated group of peaks, volcanic in origin, called the San Francisco mountains. The peaks rise about 1500 m above the relatively level surrounding area. The increased solar energy which is received by the slopes of the mountains facing the sun gives rise to regions of intense local heating (Braham and Dragnis, 1960; Anderson, 1960). During the period from about mid-July to early September a monsoon-like flow of moist tropical air from the Gulf of Mexico extends northwestward into central Arizona. This moist air, which is lifted orographically over 7000 ft before reaching Flagstaff, and the strong heating of the mountain slopes combine to produce intense convective storms. Cumulus clouds form over the mountains every day during this moist period, and thunderstorms, often with hail, are a common occurrence.

In the summer the atmospheric circulation over the southwestern United States is dominated by a thermal (heat) low. The location of the center of the low varies from day to day,

but in general it is slightly to the west of Arizona. The resulting surface flow is nominally from the Gulf of Mexico to northern Arizona, although the circulation around the thermal low is usually weak and diffuse. The dynamics of a thermal low are such that a region of high pressure exists in the upper levels (Willett, 1944, p 151). For our purposes the position and strength of this high is important since it influences the flow from the Gulf of Mexico. Also it affects the upper winds over the peaks and therefore the direction in which the clouds will drift and the area where they will release their rain.

The spectrometer was located southwest of the San Francisco peaks (Fig. 41). It is apparent that a northerly wind component is required if the first showers of the day are to occur over the spectrometer. Unfortunately this did not happen during the observational period. Therefore, the observations of raindrop sizes must be interpreted with particular reference to the history of the rain. Generally the first clouds develop at about 0900. Usually their development is very rapid, and between 1000 and 1100 showers begin in the vicinity of the mountains. Lightning often occurs within the cloud, even during their development stage. The showery regions are initially quite small, but further growth of the rain system usually occurs at least in one or two different areas. Of the four days of rain reported here only one was predominantly showery. The other three days could be described as having a fairly heavy initial shower followed in about half an hour by a relatively steady rain. The duration of this steady rain ranged from less than one hour on 1 August to over three hours on 31 July.

THE EFFECT OF WIND SHEAR ON FALLING RAINDROPS

The raindrop-size distribution may be strongly influenced by variations in the horizontal wind velocity with height (i.e. wind shear). In the Flagstaff area the high cloud base (about 2000 m) and the showery-rain conditions result in complex wind fields between the ground and the cloud. Before considering the observed drop-size distributions it is desirable to understand the effect of wind shear on falling raindrops.

Gunn and Marshall (1955) have presented a comprehensive treatment of the effects of wind shear on falling precipitation. They considered the change in the distribution brought about by a wind speed increasing with height and showed how the Z-R relationship is affected. However, during showery conditions the wind speed may not consistently increase with height but may show a maximum between the cloud base and the ground. The treatment given below is generalized to show the effect of the wind shear on the raindrop-size distribution regardless of how the wind varies with height.

Consider drops at the base of a cloud which is moving with a horizontal velocity of u_h as in Fig. 42. We wish to find the positions of drops of diameter d_1 and d_2 at the ground relative to point P (which is moving with velocity u_h), assuming that sufficient time has elapsed to allow the d_1 and d_2 drops to reach the ground. The required distances are given by x_1 and x_2 respectively. A drop of diameter d_1 with a terminal velocity v_1 at P requires a time $t_1 = H/v_1$ to reach the ground. Similarly $t_2 = H/v_2$. Now the mean wind below the cloud base is given by:

$$u_m = 1/H \int_0^H v\,dz \ . \qquad \text{(D-1)}$$

Thus it is seen that:

$$x_1 = (u_m - u_h)t_1 \ , \qquad \text{(D-2)}$$

$$x_2 = (u_m - u_h)t_2 \ , \qquad \text{(D-3)}$$

and

$$x_1 - x_2 = (t_1 - t_2)(u_m - u_h). \qquad \text{(D-4)}$$

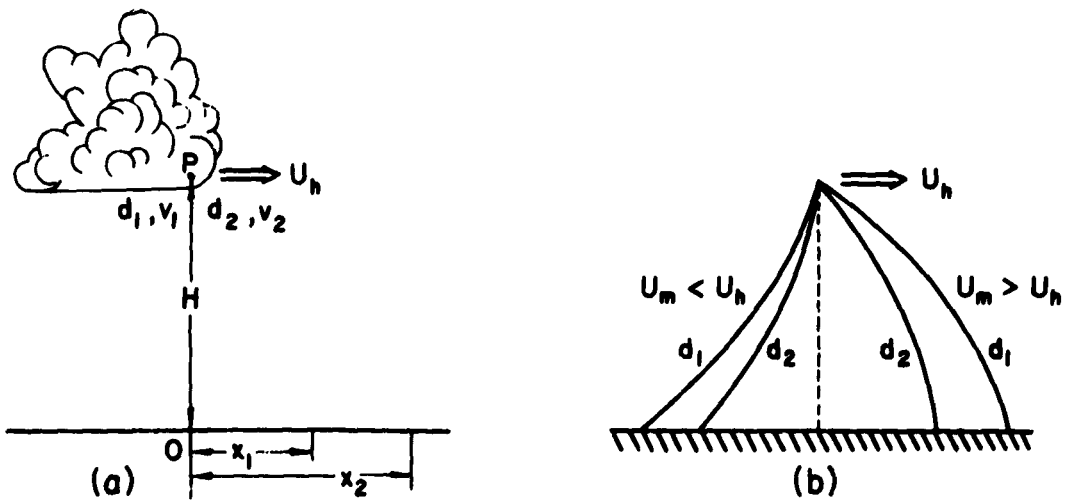

Fig. 42. Effect of wind shear on falling drops; (a) time sequence of drops arriving at the ground, (b) trajectories of drops relative to the cloud base.

If d_1 is less than d_2, then t_1 is greater than t_2. Also if u_m is greater than u_h, then x_1 is greater than x_2, and the smaller drops will be observed at a given site before the

larger ones. Similarly, if u_m is less than u_h, then the larger drops will arrive at a ground location first. For steady-state conditions it is important to realize that in both cases the pattern of raindrop sizes moves along the ground with the velocity of point P (i.e. u_h). An example of drop trajectories relative to the cloud base for both u_m less than u_h and u_m greater than u_h is shown in Fig. 42b.

RAIN OF 27 JULY 1961

Synoptic conditions

Fig. 43 shows the raobs and rawins for 0533 and 1224, 27 July at Flagstaff airport (radar site shown on Fig. 41). The winds as measured by double theodolite pibals are also shown for 1229 and 1415.[1] At 0533 the winds are south-southeasterly up to 5000 m[2] shifting to southwesterly at higher elevations, whereas at 1224 they are south-southeasterly up to 9000 m becoming light westerly at greater heights. Assigning a mean moisture content to the lowest levels, the 0533 sounding indicates that the level of free convection (LFC) is at about 3000 m. The 1224 sounding is very unstable having a superadiabatic lapse rate up to 740 m followed by an approximately dry adiabatic lapse rate up to 2660 m. However the air at that time is very dry and a LFC is not present. The pibal released at 1229 entered the cloud at a height of about 2900 m, whereas the one released at 1415 entered at a height of about 3170 m. It appeared in each case that the pibals did not enter the lowest portion of the cloud. Glass (1962), using stereo photographs, made measurements

[1]The pibals were taken at the spectrometer site.
[2]All heights refer to height above ground in meters unless noted.

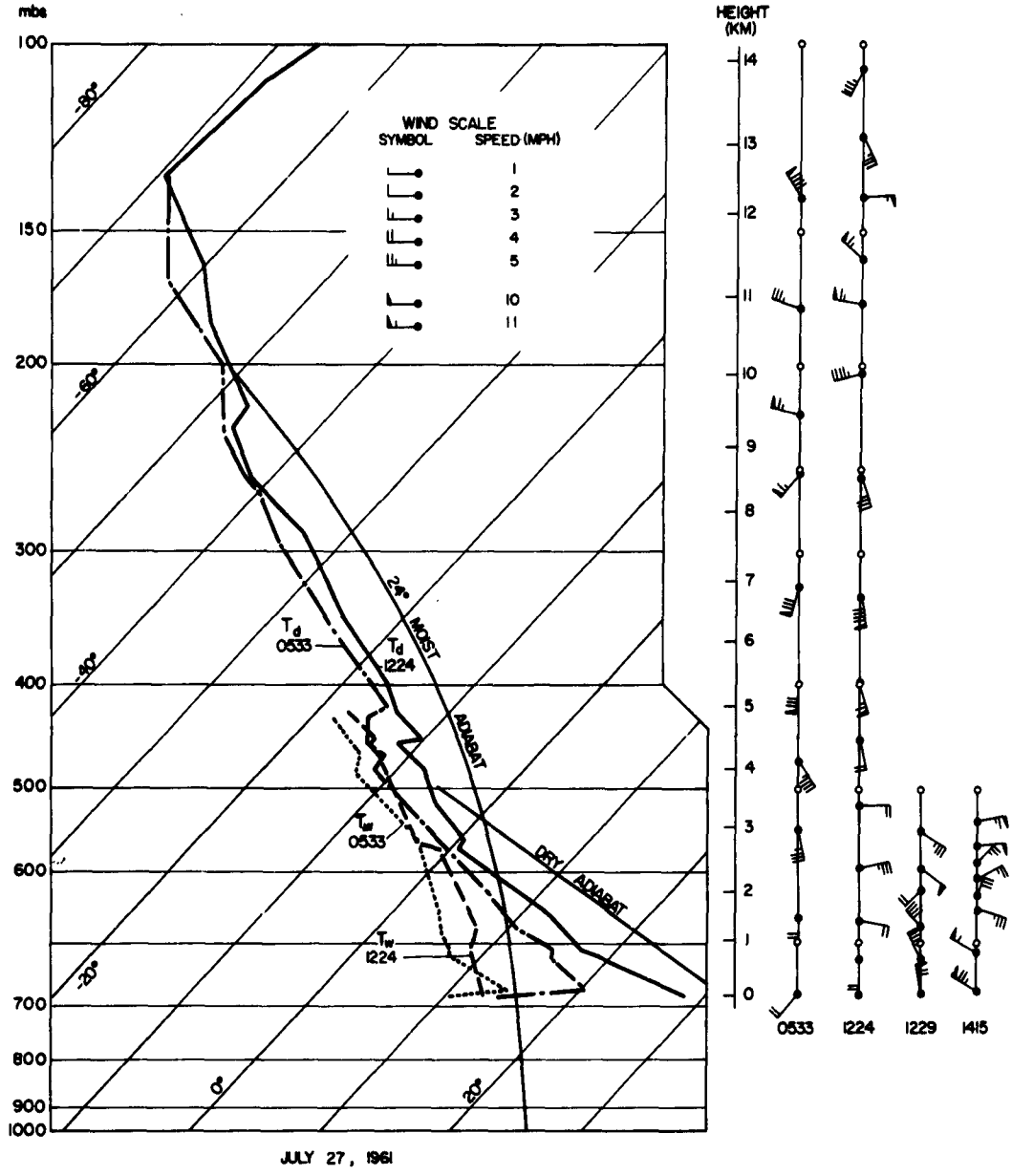

Fig. 43. Raobs, rawins, and pibals for 27 July 1961. The dry bulb temperature soundings for the two ascents are indicated by the solid and broken lines (T_d) and the corresponding wet bulb soundings by the dashed lines (T_w).

between 1254 and 1316 of a cloud about two miles northeast of the spectrometer. The measurements of the cloud base ranged from 2700 to 2760 m, and the cloud top varied from 5340 to 6250 m. However, estimates from an aircraft at 1220 indicated cloud tops which were glaciated and extended to a height of 7500 m.

Fig. 44 is a record of the rainfall intensities computed from the raindrop-size distribution data for 27 July. As a comparison, the intensities obtained from a weighing bucket rain-gage with a 25.3 inch diameter collecting area are also shown. The agreement between these two independent measurements of precipitation intensity is good, particularly since the low resolution of the rain-gage record usually does not allow accurate intensity measurements over periods of less than 2-3 minutes. The maximum raindrop diameter that occurred during each minute of observation is also plotted. The significance of this drop diameter is discussed later, but qualitatively it is seen that (1) the heavier the rainfall is the larger the maximum observed drop diameter becomes, and (2) the largest drop is usually observed during the initial 2-3 minutes of each individual shower.

The first rain of the day fell at the spectrometer at 1221, but lasted only three minutes. At that time the APQ-40 radar[1] was taking PPI data at an elevation of 4° (1040 m above the spectrometer). Fig. 45 shows the pattern of echoes at

---

[1]The APQ-40 radar was operated by personnel from The University of Michigan. Its characteristics are as follows: wavelength, 3 cm; peak power, 250 kw; pulse length, 1 or 5 μ sec; range, 20 or 100 miles; beam width, 1.5° to the half-power points. It is capable of operating in PPI mode (plan-position indicator) or in RHI mode (range-height indicator).

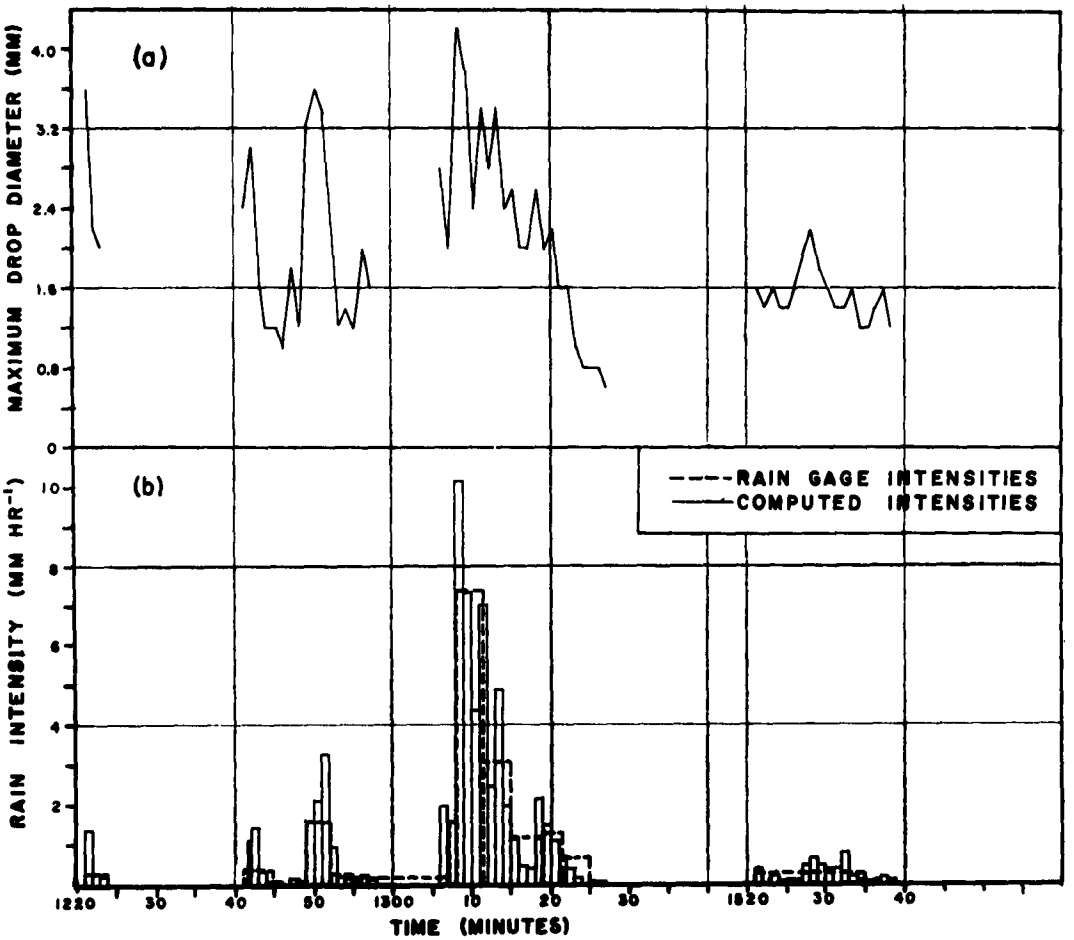

Fig. 44. Observations of rain on 27 July 1961; (a) maximum observed drop diameter, (b) rainfall intensities from rain gage and computed from drop-size data.

Fig. 45. PPI display at 1221, 27 July; gain 1, 20 naut mi range, elevation 4°. Spectrometer located 344° at 8.5 naut mi (marked with an X).

1221. It is seen that the largest echo is mainly west of the spectrometer.

The pibal released at 1229 (Fig. 43) appears to have been caught in a downdraft probably centered to the northwest of the spectrometer. The winds at low level were northerly but shifted to northwesterly above 600 m. The downdraft was apparently strongest in the layer from 900-1200 m since it took the balloon 8 minutes to cover this distance, whereas it traversed the initial 900 m in only 4 minutes. Above 1200 m the winds shifted gradually through the south to the southeasterly.

The wind profile begun at 1229 is typical of that expected through the dome of cold air beneath a thunderstorm as shown in Fig. 46. The actual trajectories of the

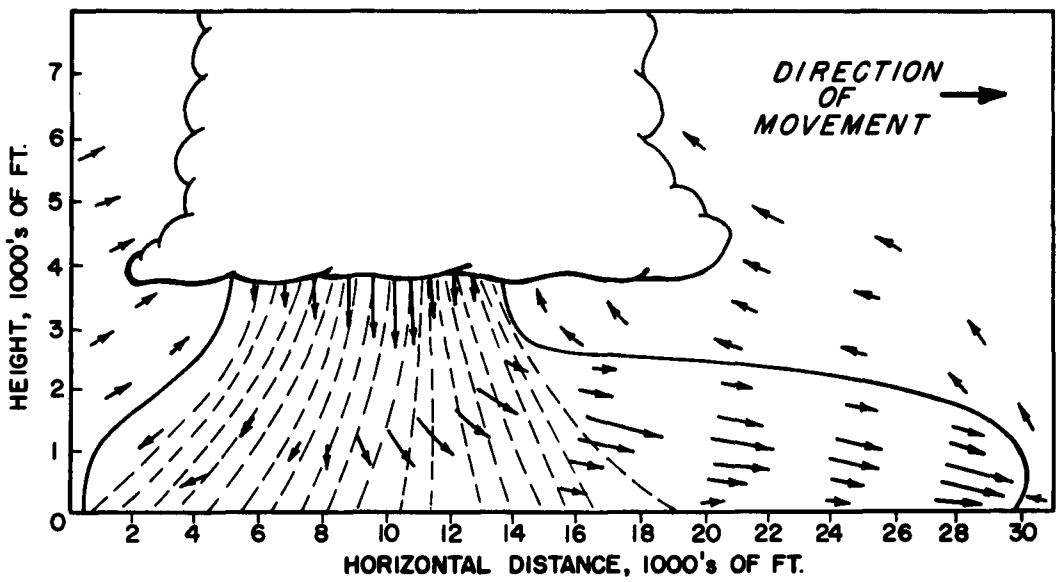

Fig. 46. Cross section through the dome of cold air beneath a thunderstorm cell. (From Byers and Braham, 1949, p 54).

balloon, a 3.5 mm diameter drop, and a 0.6 mm diameter drop are shown in Fig. 47. The drop trajectories are computed on the assumption that the winds obtained from the pibal released at 1229 are applicable during the time the drops fell from the cloud base to the ground.

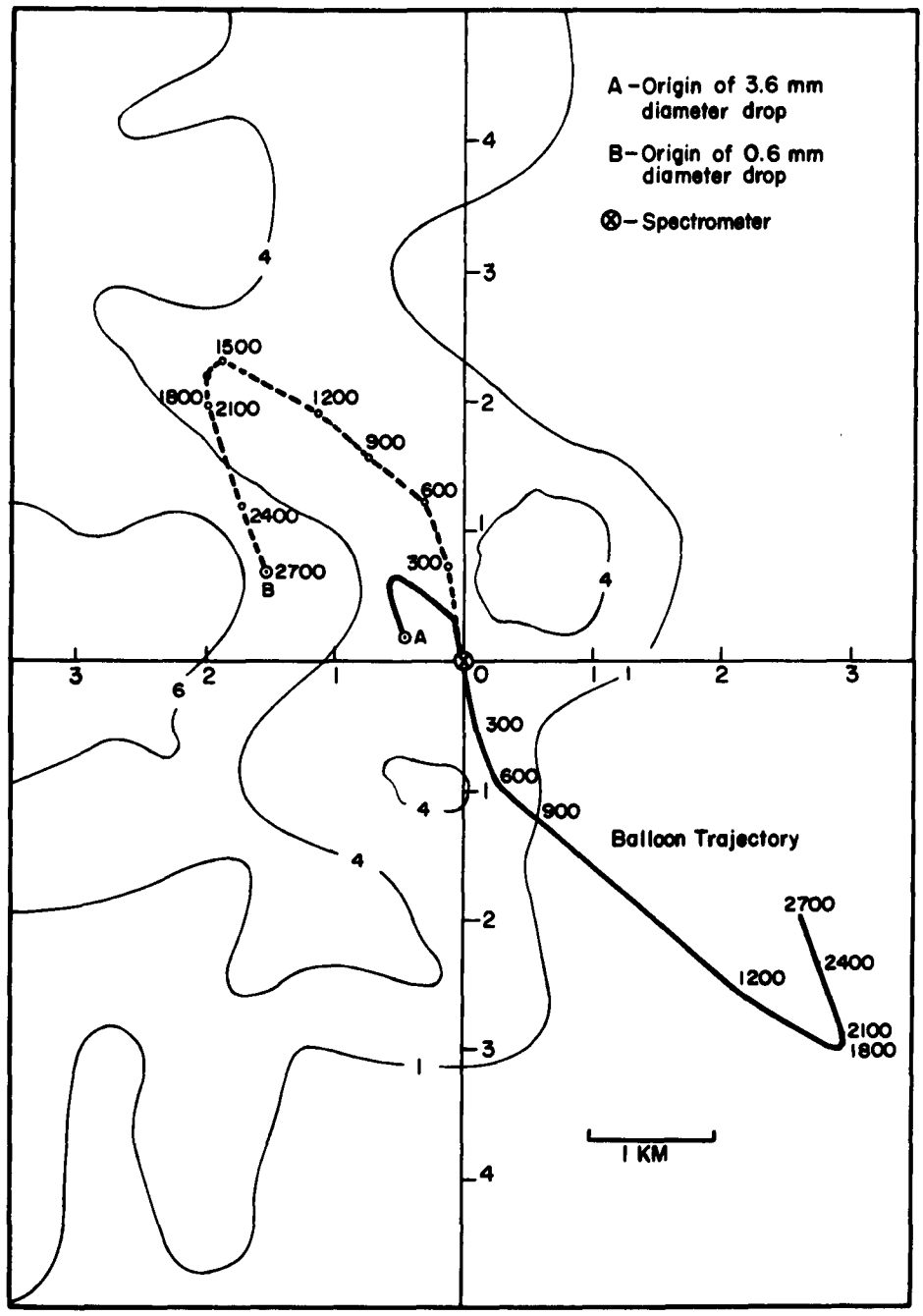

Fig. 47. Trajectories of largest (3.6 mm) and smallest (0.6 mm) drops observed at spectrometer from 1221 to 1223, 27 July 1961. The contours are gain steps at a height of about 1040 m at 1221 (Table 10). Numbers along the trajectories are heights in meters.

The contours shown in Fig. 47 are in terms of gain step. The gain steps are obtained from the radar observations and are related to Z (Table 10). The contours are applicable at 1221 at a height of about 1040 m, whereas the trajectories were computed from wind data obtained after 1229. For this reason the wind field measured by the pibal is probably not applicable for the pattern of radar echoes shown in Fig. 47. However, the fact that the pibal moved considerably east of the weakest radar echo is evidence that the balloon entered the cloud near its periphery.

Table 10. Values of Z at the spectrometer for given gain steps, 27 July 1961.

Gain step	Z at spectrometer location (mm^6m^{-3})	Gain step	Z at spectrometer location (mm^6m^{-3})
1	2.55	6	4.2×10^3
2	36.0	7	1.3×10^4
3	112	8	5.0×10^4
4	405	9	1.37×10^5
5	1.03×10^3	10	5.02×10^5

The effect of wind shear as shown in Fig. 42 is difficult to apply to the period from 1221 to 1223. The pibal released at 1229 indicates that there are southeasterly winds at the cloud base, whereas below the cloud base the mean wind is from the northwest or north. Referring to Fig. 46 and to the notation of Fig. 42 it appears as if u_m is greater than u_h. Since the main precipitation is to the west of the site, the smaller drops would be expected to be observed first. Fig. 44 indicates that quite the opposite occurred. During the first minute the maximum diameter observed was 3.6 mm. However, during the third minute a maximum diameter of only 2.0 mm was

observed. It is possible that at 1221 the smaller drops had not reached the ground and thus the steady state conditions represented in Fig. 42 had not yet been established. This would require the smallest of the observed drops (i.e. 0.6 mm) for each of the three minutes to be the result of either drop break-up or splash. This proposition has a certain amount of merit as is seen in Appendix A.

The next rain that fell at the spectrometer occurred at 1241. Fig. 44 shows that the rain recorded on this day consisted of at least four rainfall intensity maxima. The actual structure of the convective system is difficult to reconstruct from the information available. For example, the pattern shown in Fig. 44 could be due to the development of weak rain cells over the spectrometer. It also could be caused by shifts in the wind field from the cloud base to the ground which at one instance would carry the rain to the site yet a few minutes later would carry the drops short of the site or beyond it. Unfortunately, the available data are not sufficient to resolve this problem.

A series of RHI pictures taken between 1235 and 1241 at an azimuth of 344° (i.e. in line with the spectrometer) shows that the main precipitation was north of the spectrometer. One such RHI picture is shown in Fig. 48 where the echo in the vicinity of the spectrometer spreads southward near the surface. Unfortunately the radar also receives a ground echo which is superposed upon the precipitation echo. This is seen in Fig. 48 as a spreading of the echo slightly above and below the horizontal position of the antenna. The ground echo probably does not extend much above 1000 m and for all practical purposes the echo above this height is due to precipitation alone.

Fig. 48. RHI display at 1240, 27 July; azimuth 344°, 20 naut mi range, gain 2. Vertical scale similar to horizontal scale. Spectrometer located 8.5 naut mi from origin (marked as a short line).

The next burst of precipitation arrived at the spectrometer at 1249. At 1246 the radar record showed a fairly small precipitation region at a height of 1040 m which extended southward from the main precipitation region and which covered the site area. By 1250 the southward extension had broken from the main precipitation region and was centered over the spectrometer. It was during this period that rain was observed at the site (Fig. 44). At 1259 the radar data showed an individual precipitation region centered about 2 naut mi southeast of the spectrometer but not over it. At this time no precipitation was observed at the site.

The most intense rain of the day occurred between 1308 and 1315. Unfortunately the radar was not operating during this period, and it was not until 1318 that a PPI display was obtained. It would seem that the cell which was southeast of the spectrometer at 1259 moved northwestward because by 1318 the strongest echoes were 0.5 naut mi to the west and 1.5 naut mi to the northwest. The echo contours in the vicinity of the spectrometer are shown in Fig. 49 for these two times.

Raindrop-size distributions

The raindrop-size data prior to 1306 do not exhibit any consistent pattern and are not presented. It is probable that the turbulent wind field below the cloud base and the rather low rainfall intensities contribute to the complex distributions observed. The raindrop-size distributions during the period from 1306 to 1327 are shown in Fig. 50. They depict the temporal change that can occur when a cloud releases its rain. At 1306 the distribution is quite narrow with all the drops being between 1.8 and 2.8 mm except a few at 0.6 and 0.8 mm which may be the result of splash. At 1307 (not shown) the distribution is roughly exponential for drops between 0.6 mm and 2.0 mm. The distribution at 1308 has a minor peak at 2.2 mm with a generally exponential curve from 0.6 to 1.8 mm. There are also a few drops as large as 4.2 mm.

The remaining distributions for this day represent averages for three minute intervals. This procedure was adopted since it appears that for the remaining data, the distributions averaged over 3 min are more meaningful than

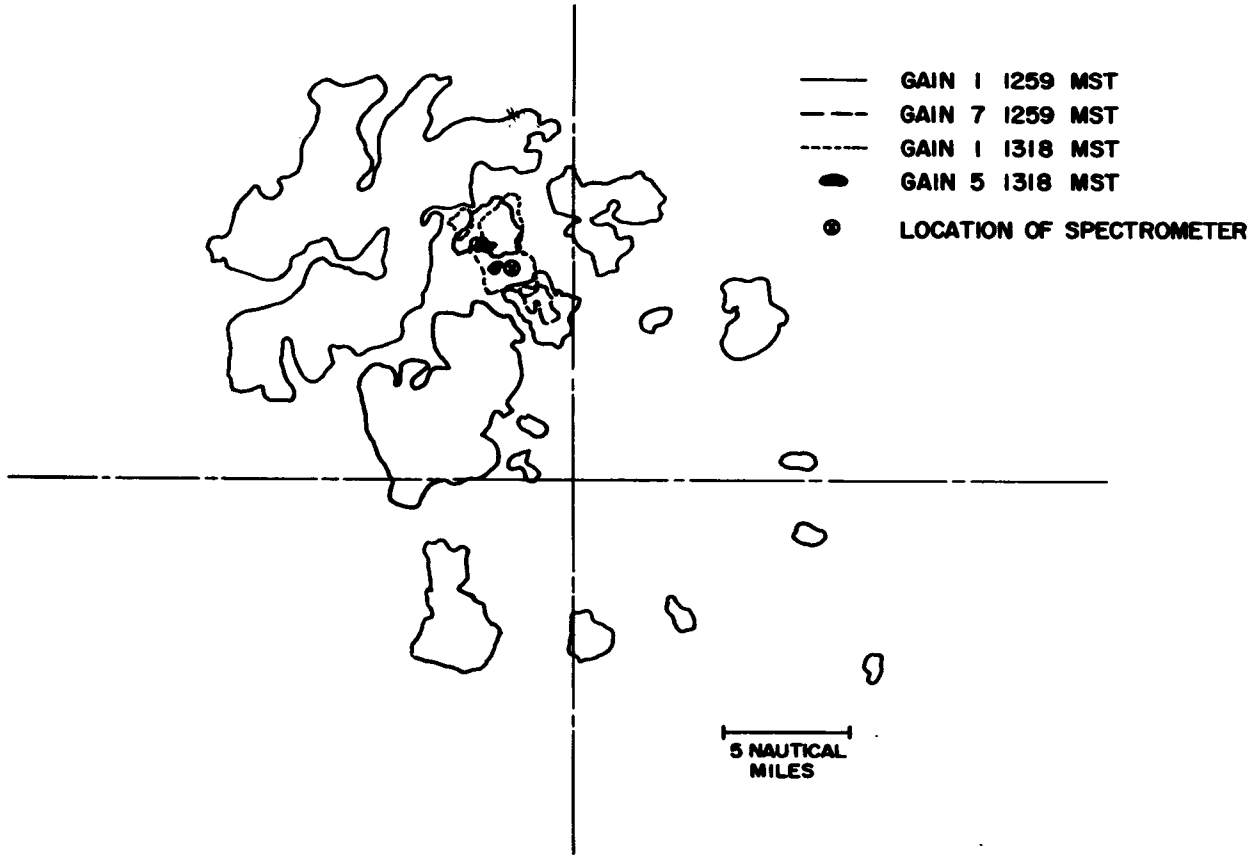

Fig. 49. Stepped gain contours at 1259 and 1318, 27 July. (See Table 10 for values of Z at the spectrometer corresponding to the gain steps.) Only the contours in the vicinity of the spectrometer are shown at 1318.

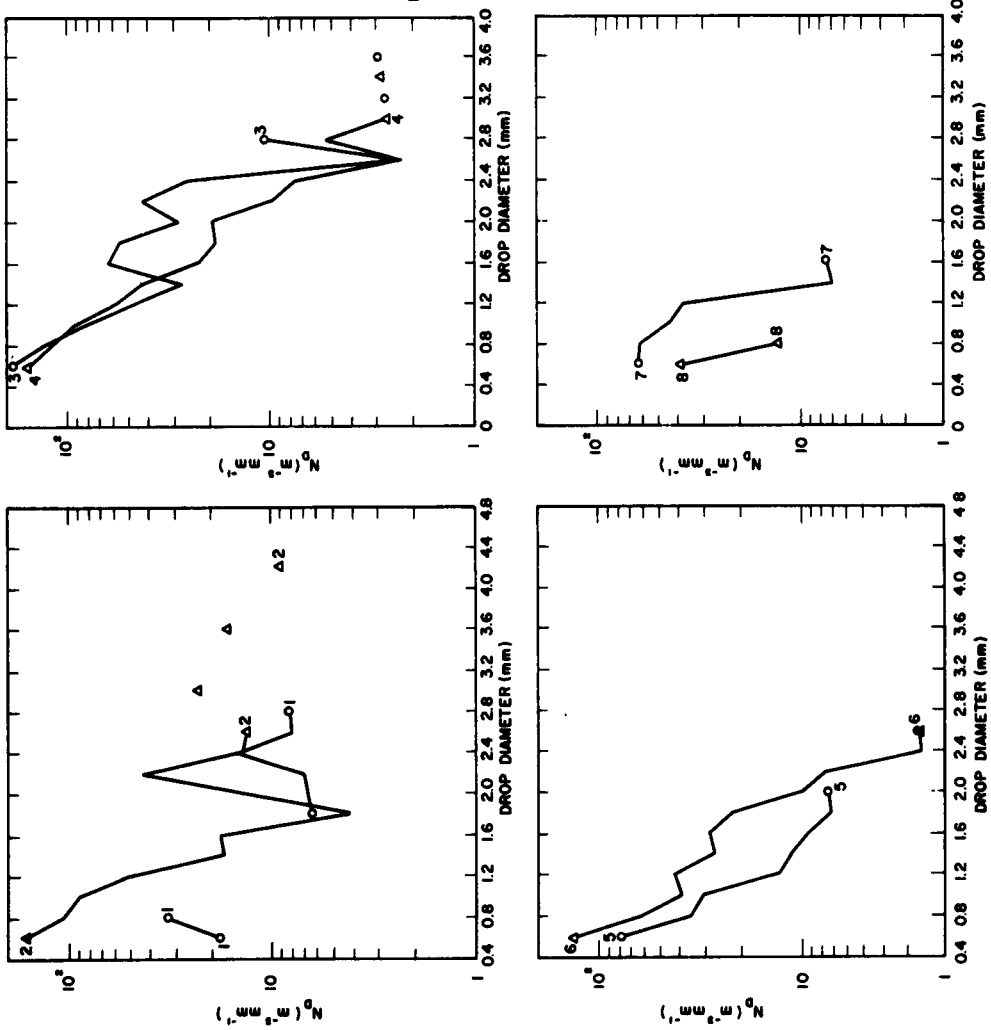

Fig. 50. Raindrop-size distributions for 27 July 1961.

the 1-min data. The changes that occur in the distributions can be seen upon the examination of the remainder of the curves in Fig. 50. In general the distributions are exponential but peaks and troughs do occur. The causes and significance of the details in the distributions are not clear. Some are probably due to the limited sampling volume employed, but on the other hand it is quite possible that the changes could reflect the true changes in the raindrop-size distribution with time.

RAIN OF 31 JULY 1961

Synoptic conditions

The raobs and rawins at Flagstaff airport for 31 July are shown in Fig. 51. Also included are the pibals taken at Kent Ranch. The winds at the airport during the early morning are northwesterly in the low levels shifting to southerly above 1800 m. The pibal taken at Kent Ranch at 0846 also indicates northwesterly winds in the low levels, but the winds shift through the north to the east between 600 and 1500 m. Above 1800 m the winds are southerly.

The temperature curve approximately follows the 22C saturated adiabat up to the tropopause. The lower levels are more moist on 31 July as compared with 27 July, and the LFC is between 1500 and 2000 m. Glass (1962) measured the heights of the cloud bases in the vicinity of the spectrometer between 1045 and 1054 and found they varied from 1235 to 1275 m.[1] He also measured three rain-shafts near the spectrometer at 1056. The shafts were practically adjacent to each other and averaged about 250 m in diameter.

---

[1]The height of the cloud base which is used for the computations of Section 3.5 is 1400 m.

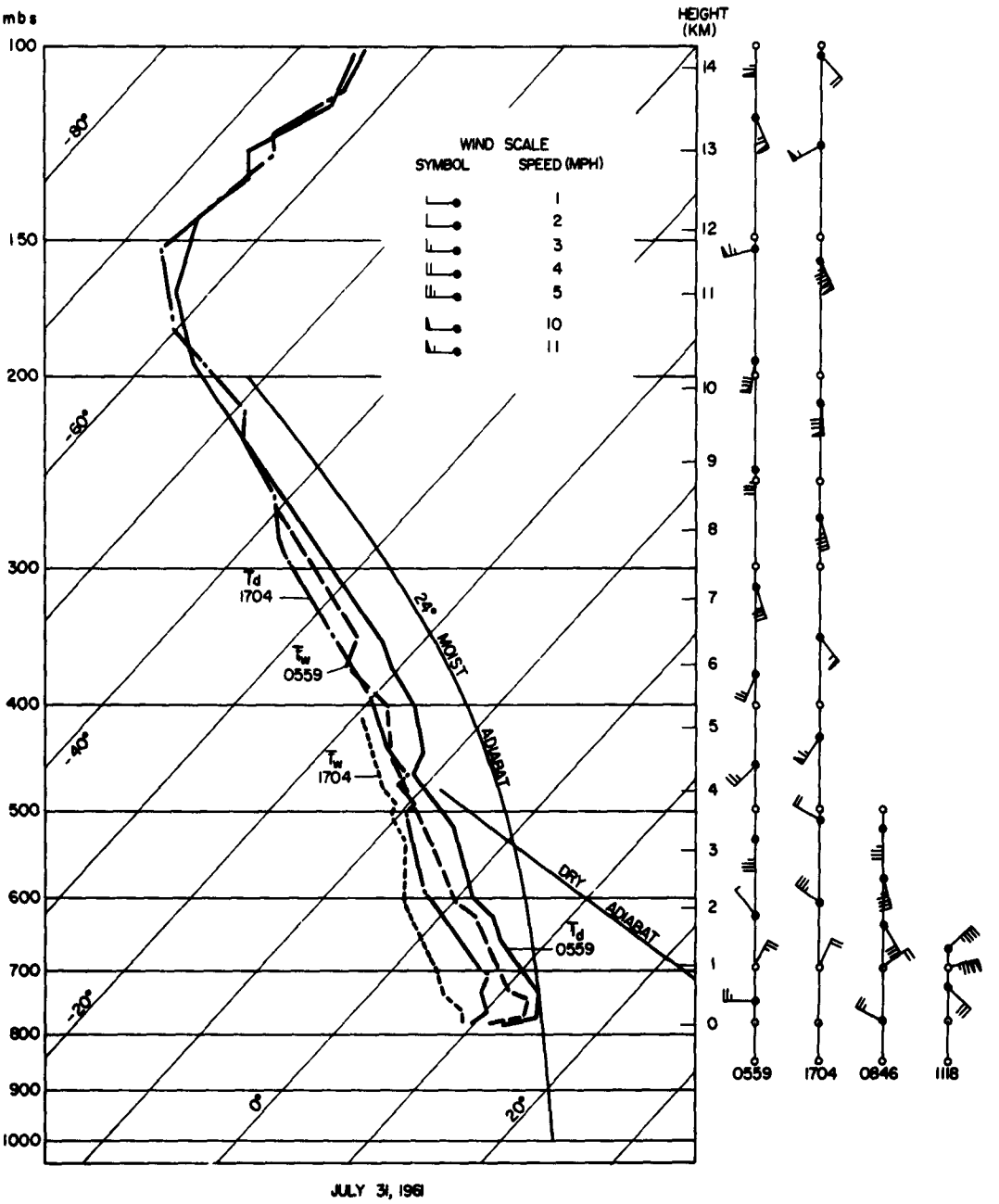

Fig. 51. Raobs, rawins and pibals for 31 July 1961. The dry bulb temperature soundings for the two ascents are indicated by the solid and broken lines (T_d) and the corresponding wet bulb soundings by the dashed lines (T_w).

The rainfall pattern for 31 July is shown in Fig. 52. The first rain arrived at 1054 but only lasted for two minutes. At 1058 heavier rain began which reached a peak intensity of 92 mm hr^{-1} by 1102. Thereafter the rain was of much lower intensity until the time it stopped at 1124. Again the agreement between the rain-gage record and the computed rainfall intensities is quite acceptable.

There was then a period of about one hour in which little or no rain fell at the spectrometer site. However, at 1234 a light rain started which did not stop until 1645. Intensity variations did occur as shown in Fig. 52, but this was the steadiest rain that occurred during the observational period.

The radar data taken in the afternoon showed a definite bright band at a height of about 2500 m. It is thus clear that snow was falling fairly steadily in the upper levels of the cloud and that the atmosphere was relatively stable. Since radar echoes were received from as high as 9000 m, the ice crystals and snow could grow through accretion of sub-cooled cloud droplets or through condensation (sublimation) processes for an effective distance of more than 6000 m. The depletion of the cloud by falling precipitation and the resulting increase in precipitation intensity for this rain are investigated in Section 3.6.

Raindrop-size distributions

The drop-size distributions during the course of the heavy initial shower are shown in Fig. 53. Drops larger than 4 mm diameter are present from 1058-1102,but drops greater than 2.5 mm are rarely present in large enough concentrations

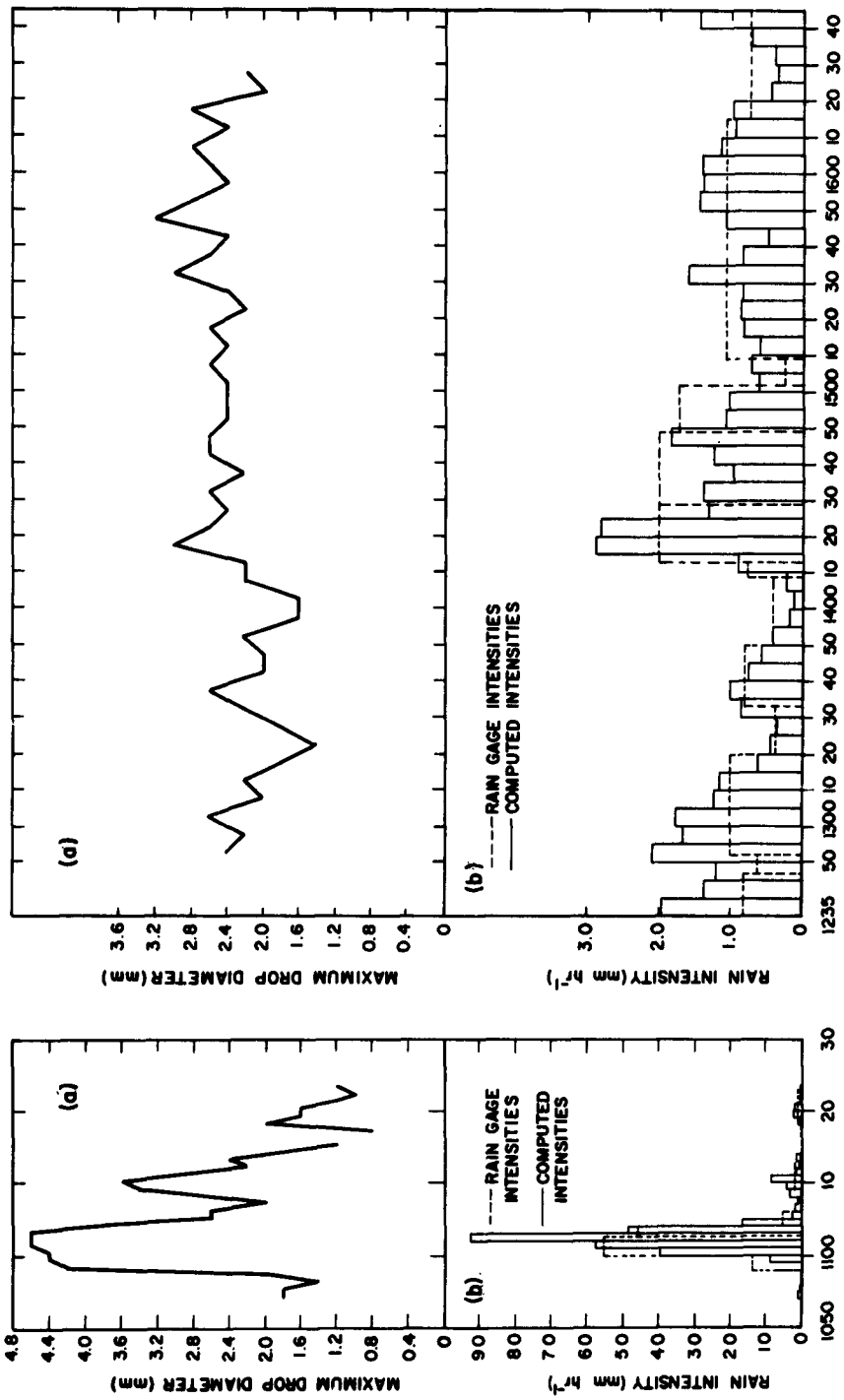

Fig. 52. Observations of rain on 31 July 1961; (a) maximum observed drop diameter, (b) rainfall intensities from rain gage and computed from drop size data.

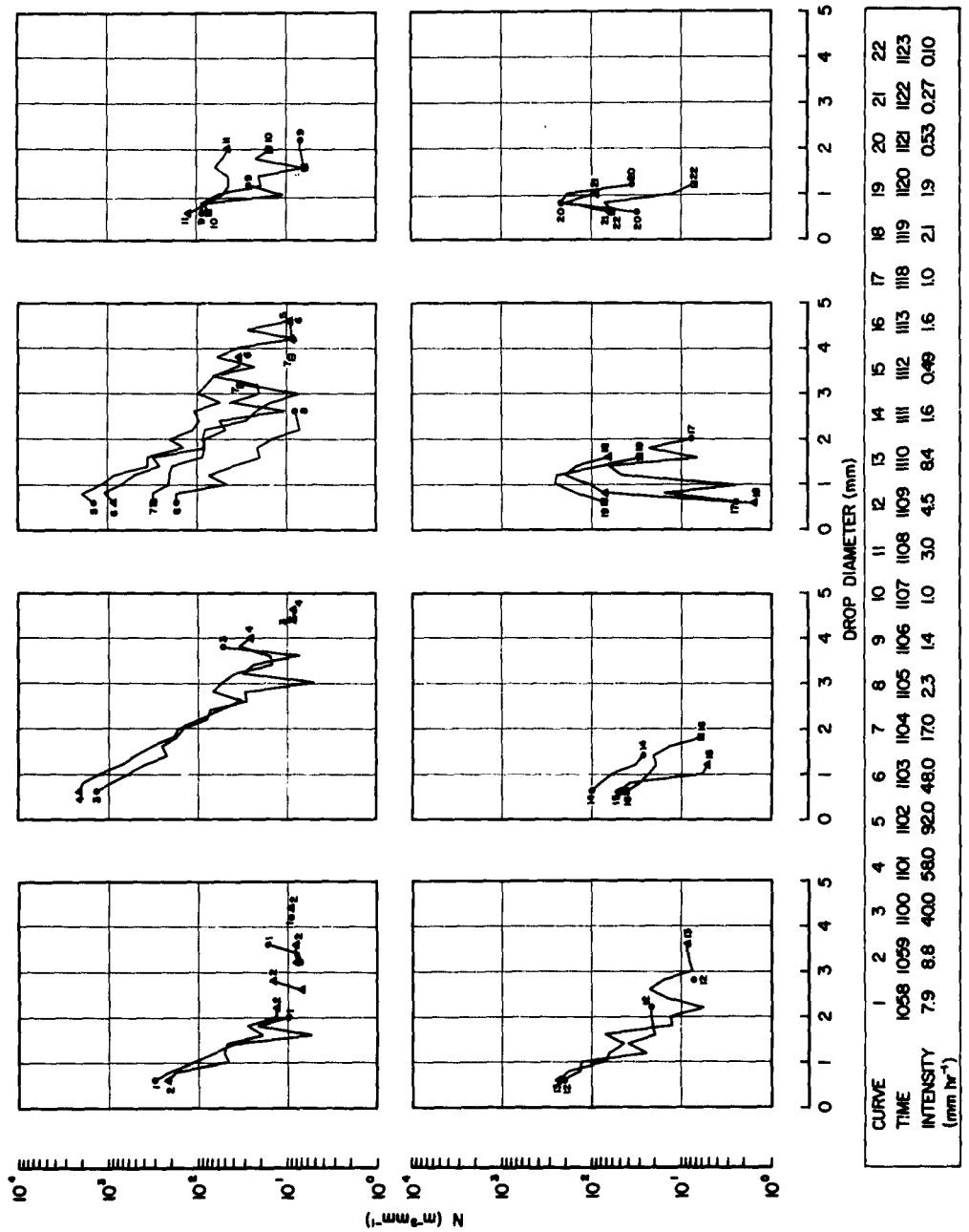

Fig. 53. Raindrop-size distributions for 31 July 1961.

to exhibit a definite pattern as measured with the spectrometer. The 1100 and 1101 distributions are nearly exponential up to 3.2 mm but they flatten out in the largest drop sizes. The 1102 distribution is for an intensity of 92 mm hr^{-1}. It has a dip in its middle size range which is similar to that reported by Dingle and Hardy (1962) for storms in the Ann Arbor region. The distributions from 1103 to 1105 are approximately exponential with the intensity dropping from 48 mm hr^{-1} at 1103 to 2.3 mm hr^{-1} at 1105. The 1106-07 distributions continue to show a decrease in intensity, but drops up to 2.6 mm are still present. The distribution for 1108 is nearly horizontal and appears to combine the dissipating rain from one shower and the initial rain from another. This is partially confirmed in the next two minutes of rain during which the intensity and maximum drop diameter both increase. At 1110 drops up to 3.6 mm are present. The period from 1111-13 does not show any consistent pattern, except for a reduction in the precipitation intensity.

The sequence of distributions from 1118-23 displays some interesting characteristics. The diameter at which the maximum number of drops is found for each successive minute decreases with increasing time. This is the pattern expected for a situation in which the winds increase with increasing height. The pibal released at 1118 (Fig. 51) indicates such a velocity profile. However, the observed pattern could also be due to the variations in the times that are required for drops of different diameter, released at the same time, to reach the spectrometer.

More than 240 minutes of data were obtained between 1235 and 1640. The distributions were originally computed for 1-min intervals but later 5-min intervals were computed. The

precipitation intensities computed using the 5-min intervals are shown in Fig. 52. It is probable that the basic rain-producing mechanism was relatively constant during this prolonged period of light continuous rain. It therefore appears reasonable to average the raindrop-size distributions over fixed intensity intervals. Accordingly, all minutes with intensities over 3 mm hr^{-1} are averaged. Similarly the distributions with intensities from 2-3, 1-2, 0.5-1, 0.25-0.5 and less than 0.25 mm hr^{-1} are averaged. The resulting six distributions are shown in Fig. 54. The distributions have remarkably similar shapes (except perhaps for the distribution with an intensity of 3.4 mm hr^{-1} which is the mean of the six distributions with intensities greater than 3 mm hr^{-1}). The actual character and probable factors shaping these distributions are discussed in Section 3.5. There it is shown that the distributions observed at the surface originate from somewhat different distributions at the melting level.

RAIN OF 1 AUGUST 1961

Synoptic conditions

The raobs and rawins for 0600 and 1646 on 1 August are shown in Fig. 55. Again it is difficult to determine the probable cloud base from these soundings. The 0600 raob indicates that the cloud should be quite low with a LFC of about 1600 m. However, the 1646 ascent indicates a LFC of about 3200 m. The pibals released at the Kent Ranch show a cloud base at about 1700 m at 1500 and at about 3200 m at 1600, but it is not known which of these heights is representative of the general cloud base.

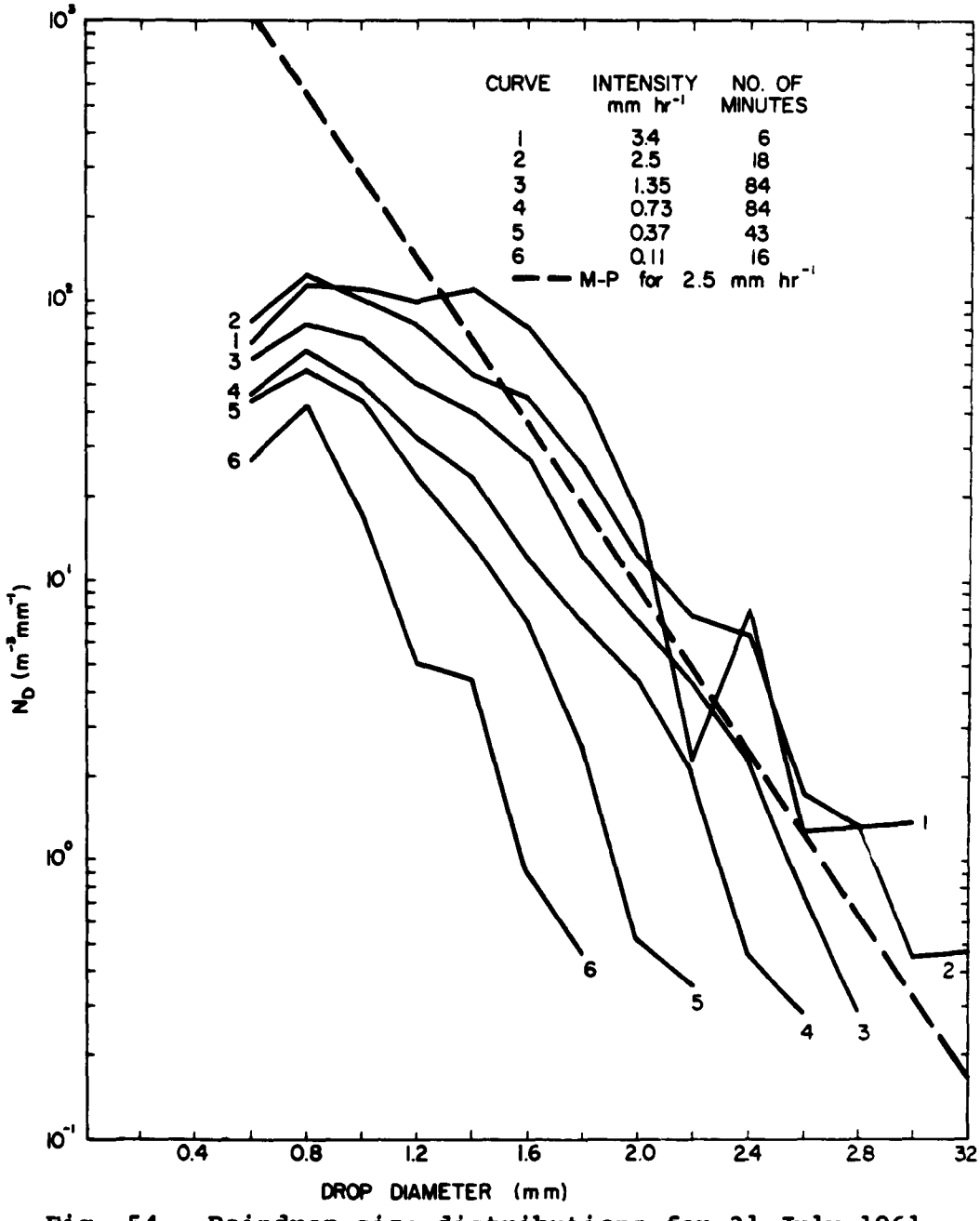

Fig. 54. Raindrop-size distributions for 31 July 1961 for the period 1234 to 1645 and averaged according to precipitation intensity.

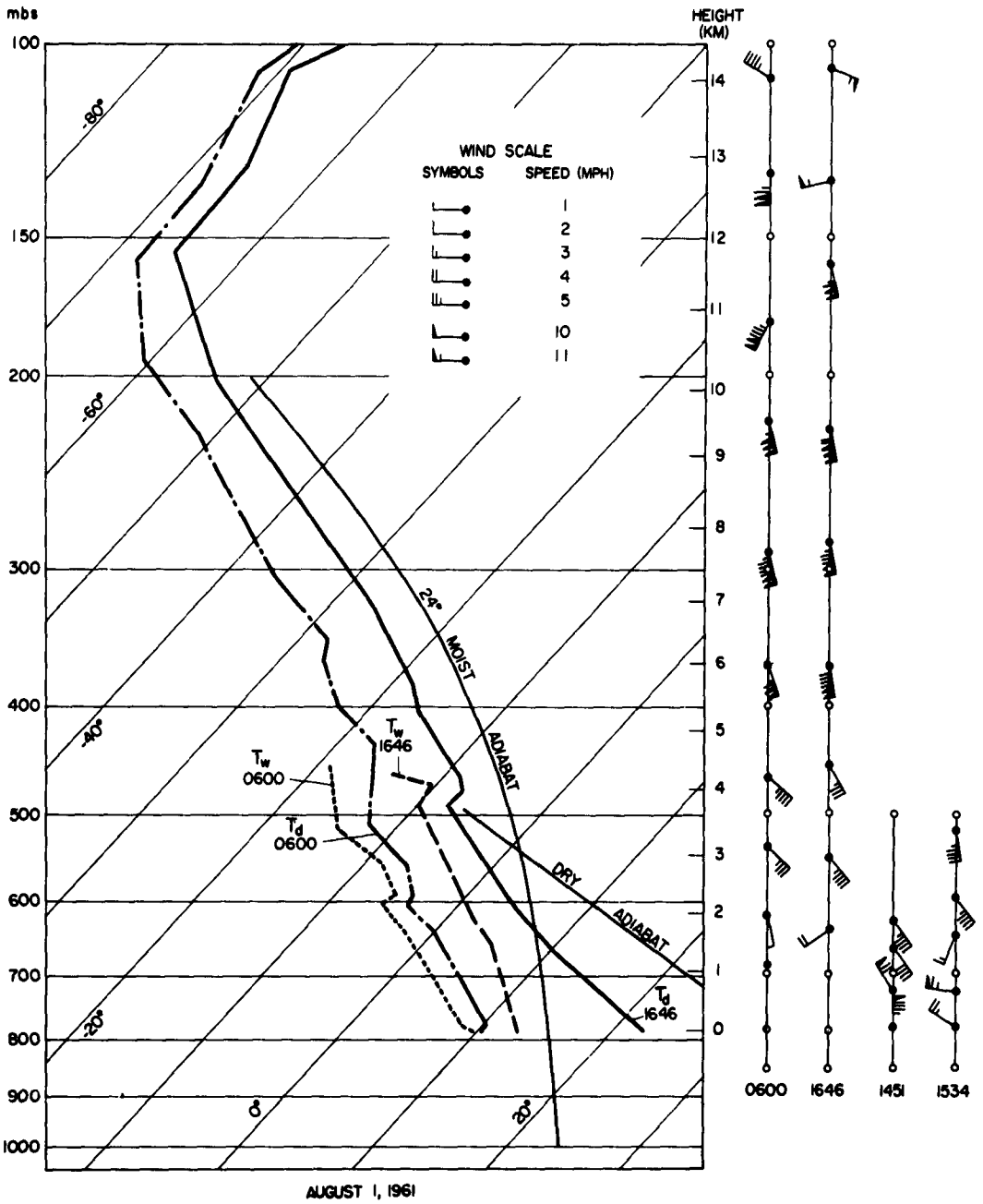

Fig. 55. Raobs, rawins and pibals for 1 August 1961. The dry bulb temperature soundings for the two ascents are indicated by the solid and broken lines (T_d) and the corresponding wet bulb soundings by the dashed lines (T_w).

The upper winds were generally light south-southeasterly between 0600 and 1646. The radar data at 1405 showed isolated echoes averaging about 3 miles in diameter mostly to the west of the San Francisco mountains. By 1425 strong echoes were located both to the north and south of the Kent Ranch. At 1430 rain arrived at the spectrometer site.

Fig. 56 is a record of the rainfall intensity as given by the weighing bucket rain-gage and also as computed from the distribution data. The agreement between these two measurements is not as good as it was for the other storms. This is partially explained by a failure at 1440 in one of

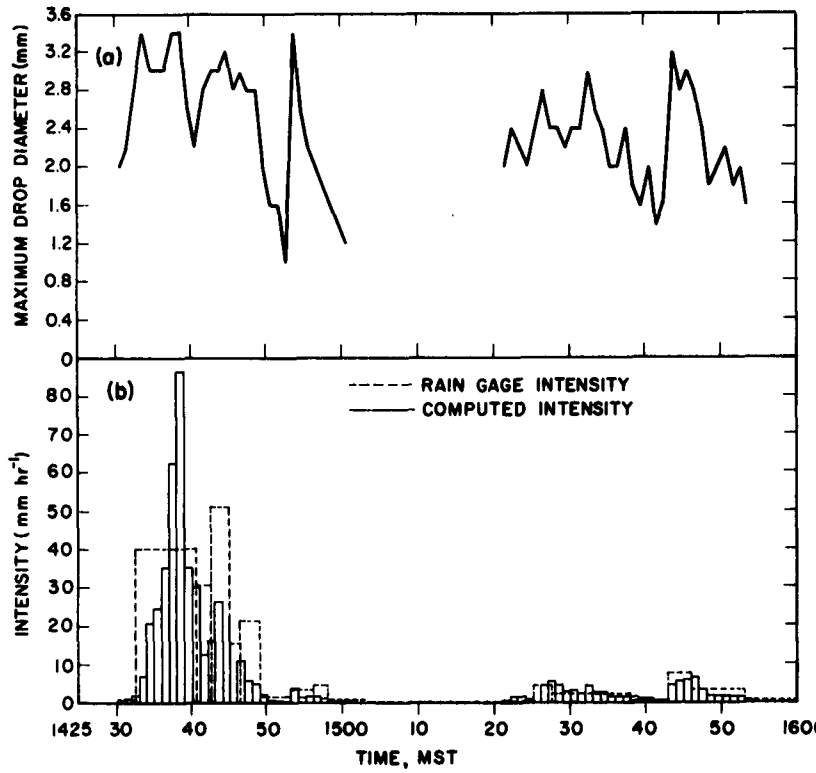

Fig. 56. Observations of rain on 1 August 1961; (a) maximum observed drop diameter, (b) rainfall intensities from rain-gage and computed from drop-size data.

the power supplies for the spectrometer. The net result was a record which did not allow a reliable measure of the larger drops. In fact the recorded signals from many drops were off scale and thus no estimate could be made of the size of these drops except to give their minimum diameters. Therefore, for the period from 1440 to 1500 the rainfall intensities computed from the distributions are considerably too low.

The radar records after 1430 indicated that there was an extensive rain area generally oriented in a north-south direction. The area was about 25 miles in length and about five miles wide. The Z values which were measured by the radar are in quite good agreement with those computed from the drop-size spectra for the higher rainfall intensities. For example a Z profile taken between 1436 and 1440 showed a radar measurement of Z equal to 10^5 mm^6m^{-3} between 400 and 2300 m. The Z values computed from the drop-size data at the surface for this period ranged from $(1.3\text{-}7.0)\times10^4$ mm^6m^{-3}. Fig. 57 is a RHI record at 1436 along an azimuth of 345°. The contours are in gain steps and their corresponding values are given in Table 11. Fig. 57 shows that one of the strongest cells in the area is over the spectrometer. The echo tops at this time are higher to the north, but by 1445 echoes 14 km in height were observed over the spectrometer. Examination of Fig. 57 also indicates that there is a distinct separation between the cell over the spectrometer and the cell centered about 4 miles to the north.

Fig. 58 is a PPI record taken at 1445. The echoes are to the north, west, and south of the spectrometer. A pibal released at 1451 (Fig. 55) indicates that the winds are from the north in the lower levels and shift to the southeast

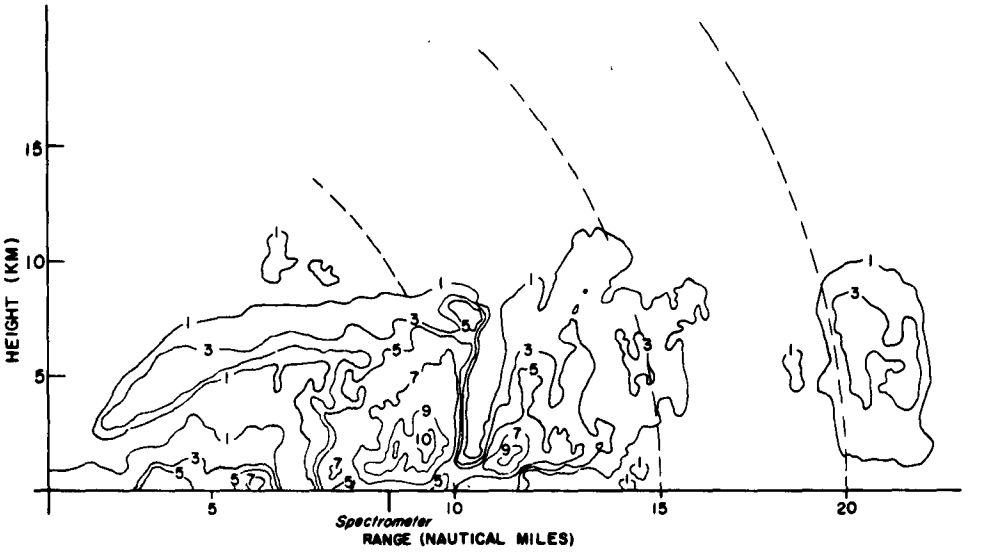

Fig. 57. Stepped-gain contours along an azimuth of 345° at 1436, 1 August 1961. (See Table 11 for values of Z at the spectrometer corresponding to the gain steps.)

Fig. 58. PPI display at 1455, 1 August 1961; 20 mile range, gain 1, elevation 4°. Spectrometer located 344° at 8.5 naut mi (marked with an X).

above 1000 m. The positions of the convective cells relative to the spectrometer are similar to those for 1221, 27 July 1961 (Fig. 45). In addition the 1451 pibal of 1 August

Table 11. Values of Z at the spectrometer for given gain steps, 1 August 1961.

Gain step	Z at spectrometer site (mm^6m^{-3})	Gain step	Z at spectrometer (mm^6m^{-3})
1	1.76	7	9.80×10^3
2	36.0	8	3.80×10^4
3	116	9	1.04×10^5
4	445	10	3.65×10^5
5	1.00×10^3	11	7.80×10^5
6	4.20×10^3		

exhibits some of the same characteristics as that released at 1221 on 27 July (Fig. 43). These two cases show that a preferred region for the convective cells during their precipitating stage is downwind from the peaks. This observation might well be taken into account in the future when a spectrometer site is to be chosen.

Raindrop-size distributions

The drop-size distributions for this rain display the usual characteristics of a shower, with generally large drops but low intensities during the initial minutes of rain followed by a gradual shifting to an exponential type distribution and heavier precipitation. Fig. 56 shows that the maximum drop diameter is 3.4 mm. This is considerably less than the maximum drop diameter observed on either 27 or 31 July. We know that up to 1440 the observations are considered reliable and are not influenced by the power failure mentioned previously. Therefore, there must be some physical

reason for the absence of large drops. A possible explanation is given by Dingle and Hardy (1962) for the absence of large drops in a thunderstorm. This is that small scale turbulence breaks up the large drops, thereby causing a larger fraction of small and medium-sized drops to be present. The average distribution for the four most intense minutes of rain is shown in Fig. 59. It exhibits slightly more medium-sized drops than a strictly exponential type distribution. Dingle and Hardy (1962) reported that this also was the case for some distributions observed under turbulent conditions. However, a study of the wind records

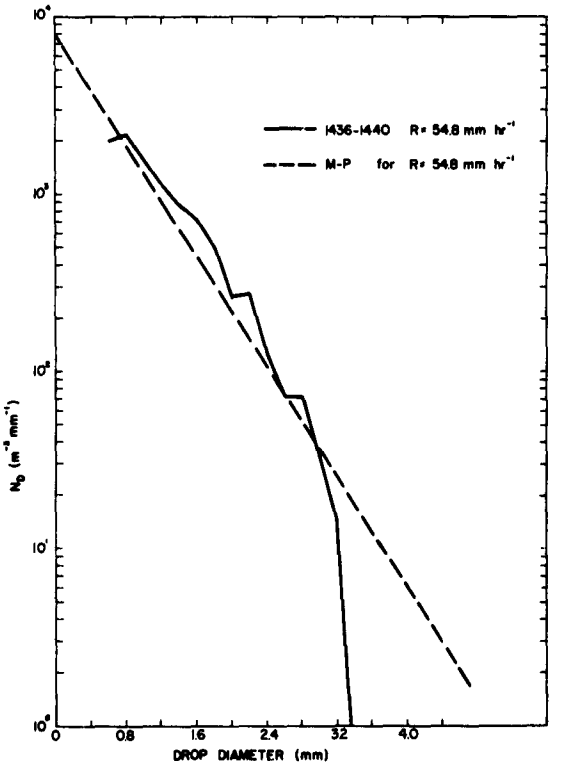

Fig. 59. Average distribution of the four most intense minutes of rain for 1 August 1961.

did not reveal any strong evidence that the turbulence on 1 August was significantly greater than that on 27 and 31 July, although the wind speed on 1 August did show more variation than on either of the other two days. Another possible explanation is that offered by Gunn and Marshall (1955). They reason that for a finite source area, a shift in wind direction with height between the cloud base and the ground results in a limited drop diameter range being observed at a given site at the ground. This may be illustrated with the use of Fig. 47. In this figure the trajectory of a 3.6 mm drop is such that it will arrive at the spectrometer. Now suppose that 5 mm drops are also present at the position occupied by the 3.6 mm drop at 2700 m. It is clear that these 5 mm drops will not strike the surface at the spectrometer but will fall somewhere between A and O. If this larger drop was observed at O it would have to originate toward the spectrometer from A. The wind shift for the occurrence of only a limited diameter range was present on 1 August as evidenced by the pibal winds shown in Fig. 55. However, the dimensions of the source regions are unknown so that it is difficult to know whether a limited range would be observed on this account.

The distributions from 1441-1500 on 1 August will not be presented because they are thought to be unrepresentative of the natural spectra. By 1500 the region had become practically overcast and radar echoes extended to the north and south in a broad zone. RHI data taken along 344° at 1518 are shown in Fig. 60. Surface precipitation is shown to exist both to the north and to the south of the spectrometer at this time but over the spectrometer the base of the echo is 4600 m.

However, by 1521 rain was observed at the spectrometer. This rain could not have come from the echo region which was directly above the spectrometer at 1518, as some of the observed drops would not have had sufficient time to fall to the ground. At 1534 the winds below the cloud base were southerly. This suggests that the downward projection of the echo which was to the south of the spectrometer at 1518 may be responsible for the rain observed at the spectrometer three minutes later. Another possibility is that the rain reaching the spectrometer at 1521 was advected over the spectrometer from outside the region covered by the RHI record of Fig. 60.

Fig. 56 shows that negligible rain fell at the spectrometer site from 1500 to 1520. After 1520 a light rain

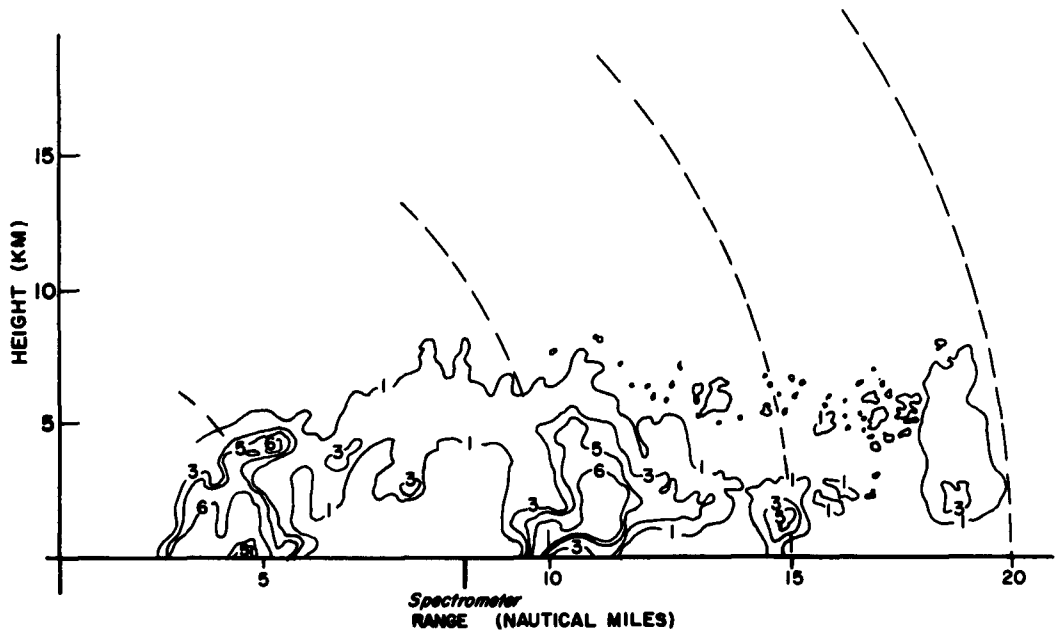

Fig. 60. RHI display at 1518, 1 August 1961; 20 mile range, azimuth 344°. (See Table 11 for values of Z corresponding to the gain steps.)

occurred in rather regular intensity intervals. For this reason, consecutive 1-min raindrop-size distributions which have approximately the same intensity and similar characteristics are averaged. The resulting distributions are shown in Fig. 61. Curve 1 of this figure is for the first four minutes of rain and the distribution is relatively flat, particularly at drop diameters of less than 1.2 mm. Curve 2, the average of 10 minutes of rain from 1525 to 1535, is one of the flattest distributions observed for such an extended period. It is possible (as is shown in Section 3.9.3) that the distribution represented by curve 2 is the result of rain whose region of growth is primarily limited to heights

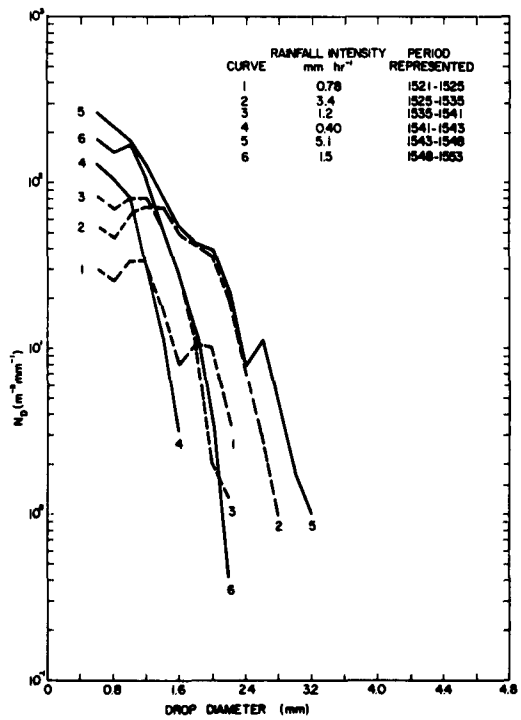

Fig. 61. Raindrop-size distributions for period from 1521 to 1553, 1 August 1961.

above the melting level. Curve 3 is the mean distribution of 6 minutes of rain and has fewer large drops than Curve 2. Curve 4 continues to show a reduction in rainfall rate and a steepening of the slope of the distribution, whereas curve 5 indicates a greatly increased rainfall rate. Curve 6 (for the period from 1548-1553) has a very steep slope and represents the distribution near the end of the rain. The rain ended at the spectrometer site at 1555.

It is interesting to note that the number of smaller drops continues to increase from 1521 to 1548, and it is only during the latter minutes of the rain that a decrease in the number of these drops occurs. The distributions are in fact indicative of a complete shower process at very low intensity. That is, the drop sizes show relatively flat distributions initially, but change gradually to distributions with markedly steep slopes. The other feature is the very close agreement between curves 2 and 5 and between curves 3 and 6 for drop diameters from 1.2 to 2.4 mm. This indicates that two weak cells are represented by the distributions of Fig. 61 and that gravity sorting (i.e. drops arrive at the surface in times which are inversely proportional to their diameter) may be responsible for the difference between the above two pairs of curves at the smaller drop sizes.

RAIN OF 3 AUGUST 1961

Synoptic conditions

The raobs and rawins for 0606 and 1234 on 3 August are shown in Fig. 62. The 0606 ascent indicates a LFC at about 2800 m, but by 1234 the LFC has dropped to about 1200 m. This rather marked change in the LFC could be due to the

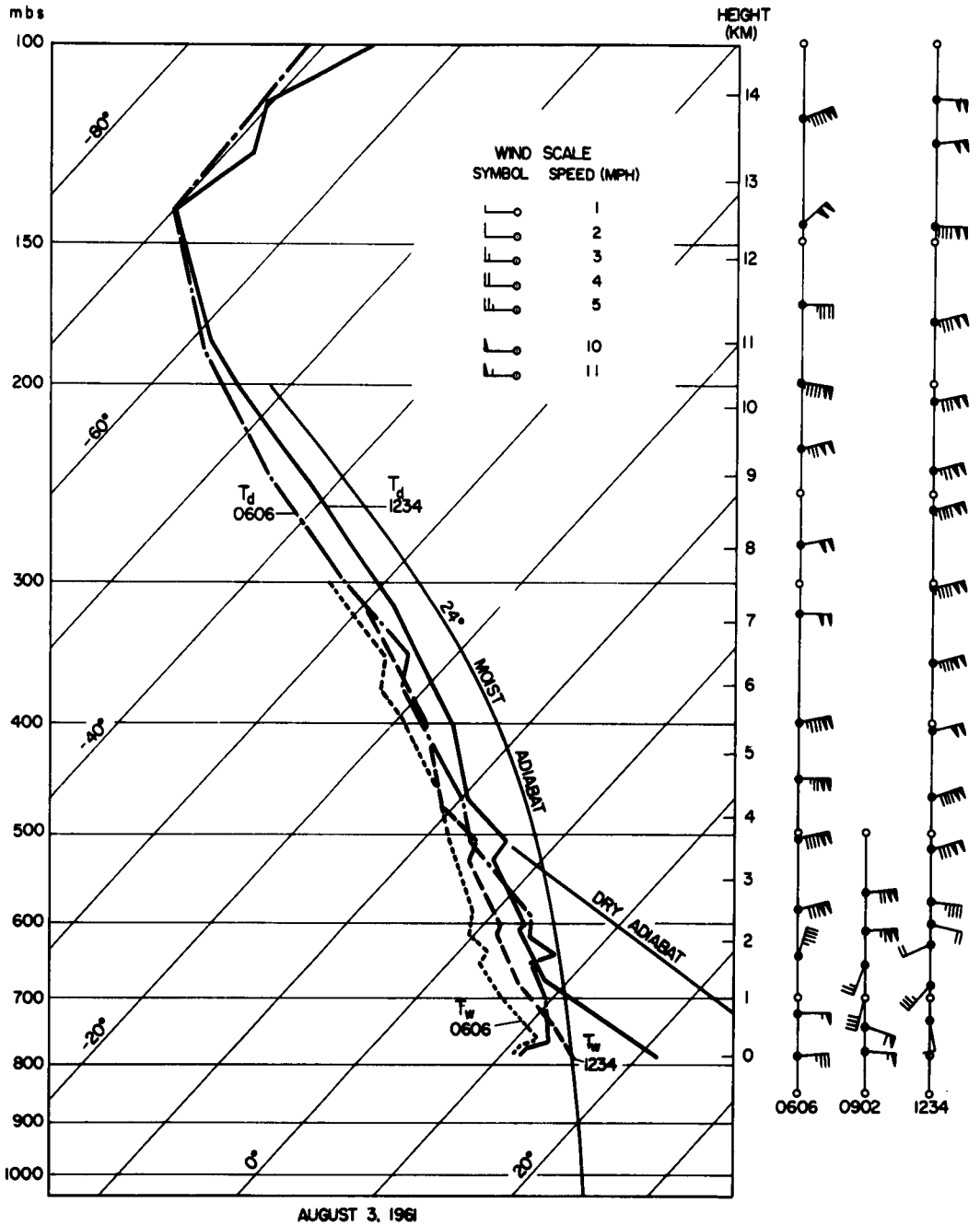

Fig. 62. Raobs, rawins, and pibals for 3 August 1961. The dry bulb temperature soundings for the two ascents are indicated by the solid and broken lines (T_d) and the corresponding wet bulb soundings by the dashed lines (T_w).

influx of small amounts of moisture in the lower levels accompanied by strong surface heating. The low level of condensation observed at 1234 is partially born out by the rainfall during the afternoon, since the cloud base after 1500 is well below the mountain peaks (i.e. much below 1500 m).

The winds at the airport at 0606 are generally easterly from the surface to 14 km, whereas at the Kent Ranch the 0902 pibal indicates a layer of southerly winds from 600-1600 m with easterly winds both above and below this layer.

By 1345 the radar indicated large echoes to the north and south of the spectrometer. Lightning and thunder were present in the immediate vicinity of the Kent Ranch as early as 1320. Rain showers were evident over both the San Francisco mountains and A-1 mountain (Fig. 41) at 1338. At this time the surface wind shifted to southerly which indicated that the downdraft from the A-1 shower had reached the spectrometer. Unfortunately a total power failure occurred at 1410, and power was not restored until 1429. Observations of drop sizes began at 1429 after having missed the first eight minutes of the rain. At 1419 the radar showed that the precipitation was fairly extensive. From visual observations and radar data it was evident that the rain reaching the spectrometer on this day fell from cells which originated to the northeast or east of the spectrometer.

The precipitation pattern observed on 3 August is unique. It is shown in Fig. 63 and consists of a series of fairly light showers (although the heaviest one reached an intensity of 40 mm hr^{-1} for a period of two minutes). The rather regular shower interval which existed is best indicated by the plot of the maximum drop diameters (Fig. 63).

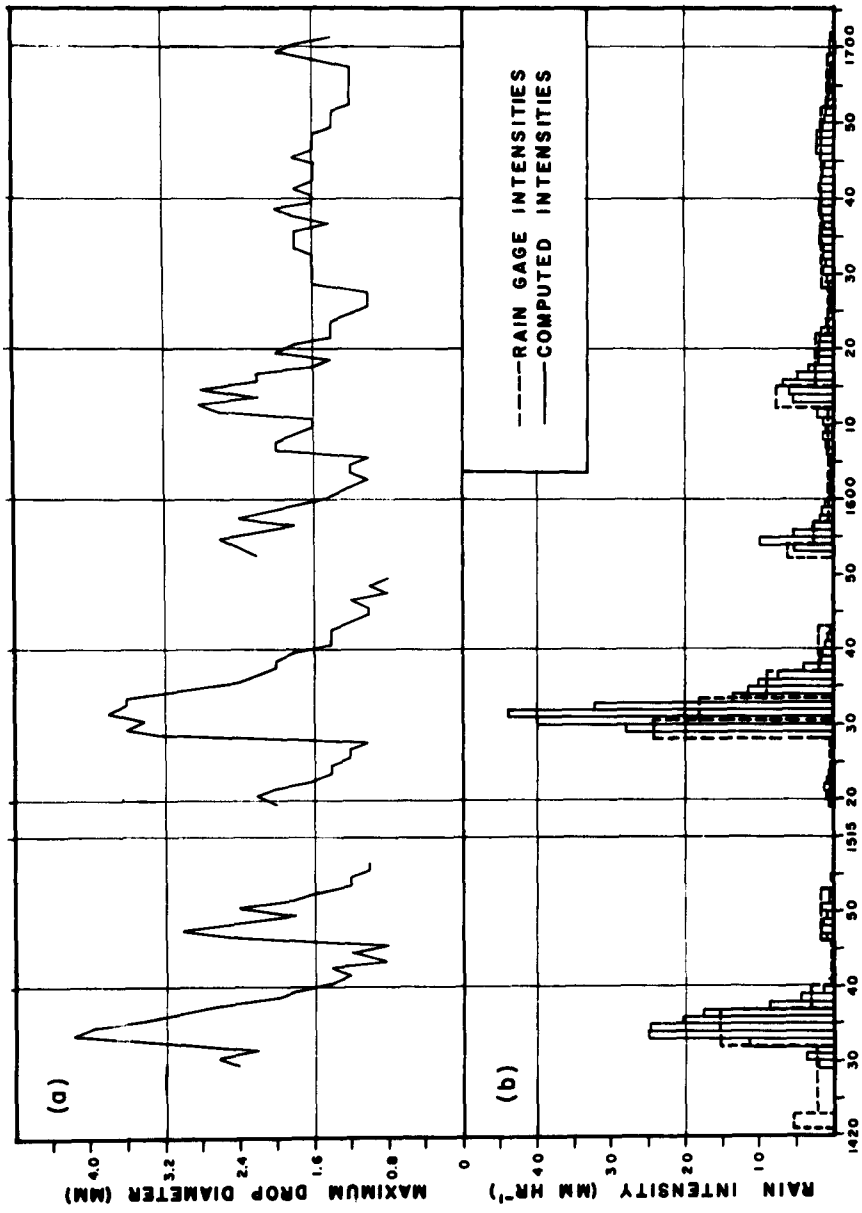

Fig. 63. Observations of rain on 3 August 1961; (a) maximum observed drop diameter, (b) rainfall intensities from rain gage and computed from drop-size data.

Upon inspection it is seen that the time interval between the peaks of the maximum drop diameter varies from 9 to 38 minutes. With a moderate wind from the east, Mount Elden acts as an orographic barrier (Fig. 41). It is possible that small cells developed rather regularly over Mount Elden, and then were carried over the spectrometer during their precipitating stages.

Fig. 64 is a RHI record of the step gain contours along an azimuth of 344° at 1558. The values of Z for each gain step are given in Table 12. Fig. 64 shows evidence of the cellular structure, the largest buildup occurring in the vicinity of Humphrey's mountain[1], the lesser in the vicinity

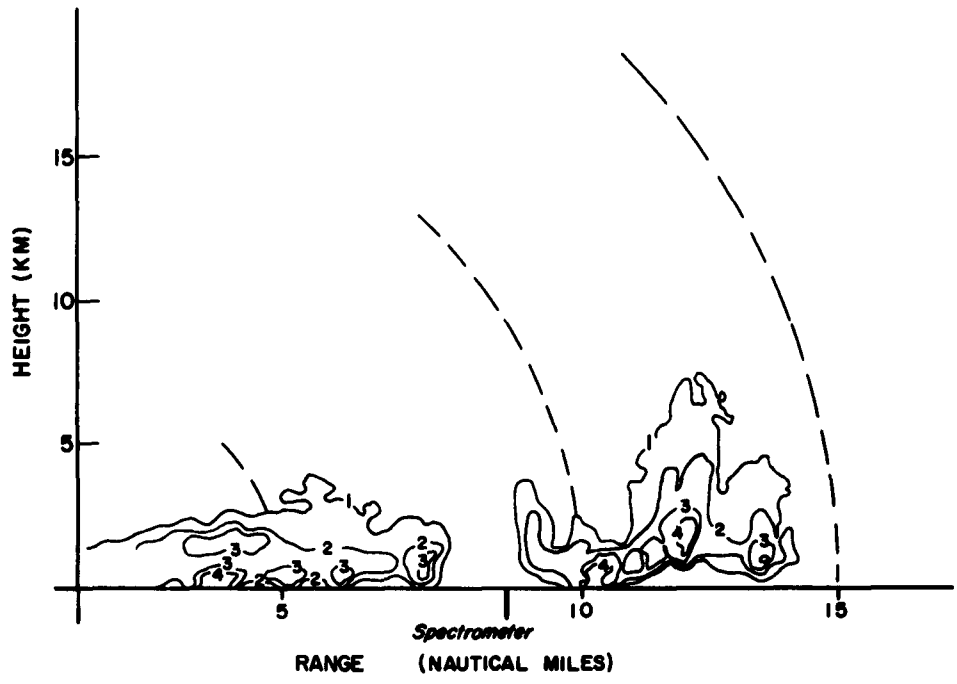

Fig. 64. RHI display at 1558, 3 August 1961; 20 mile range, azimuth 344°. (See Table 12 for values of Z corresponding to the gain steps.)

[1] Mount Humphrey is the highest of the San Francisco peaks.

Table 12. Values of Z at the spectrometer for given gain steps, 3 August 1961.

Gain step	Z at spectrometer site (mm^6m^{-3})	Gain step	Z at spectrometer site (mm^6m^{-3})
1	1.72	7	1.12×10^4
2	31.0	8	3.70×10^4
3	94.0	9	1.04×10^5
4	324	10	3.19×10^5
5	1.06×10^3	11	9.65×10^5
6	3.20×10^3		

Mount Elden. Since the radar was only operating intermittently on this day, it is difficult to study the actual development of these rather small convective cells.

Raindrop-size distributions

The initial shower that occurred on 3 August is not analyzed because the data are incomplete. The distributions for the shower from 1519 to 1543 are also not presented because of their similarity to the distributions from 1058 to 1118 on 31 July 1961 (Fig. 53). However, the two showers which occurred from 1553 to 1625 are of particular interest.

The distributions for the period from 1553 to 1625 were treated in the same manner as those for 1 August (i.e. consecutive distributions with approximately the same intensity and character were averaged). The distributions thus obtained are shown in Fig. 65. Curve 1 is the mean of the first three minutes of the shower and shows a peak number of drops at 1.2 mm diameter. Curves 2 and 3 show a tendency for the peak number of drops to occur at smaller drop diameters as the shower progresses. Curves 4 and 5 probably reflect the beginning of another shower which is fully

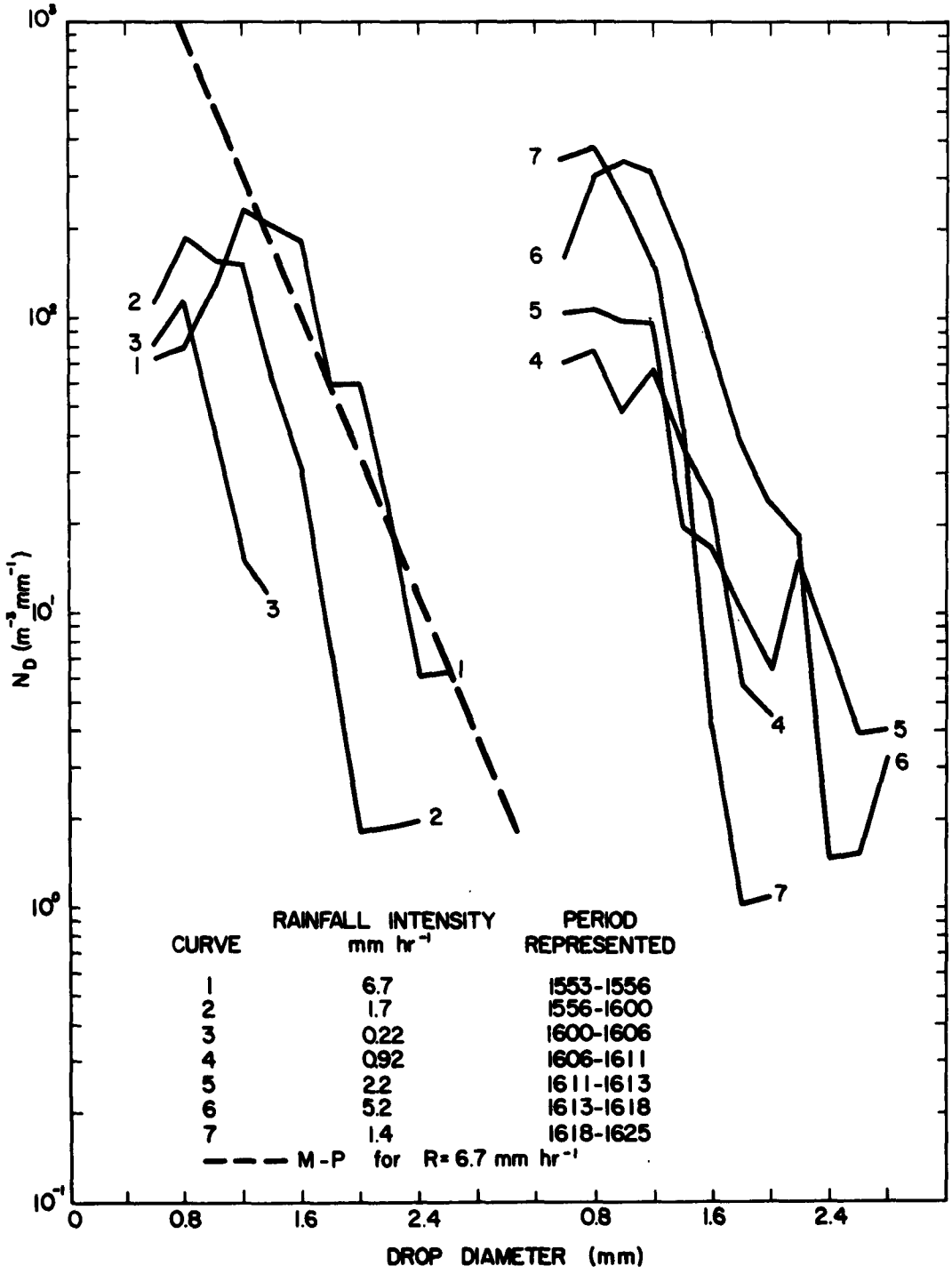

Fig. 65. Raindrop-size distributions for period from 1553 to 1625, 3 August 1961.

realized in curve 6. Curves 1 and 6 are similar except that curve 6 has considerably more drops which have diameters smaller than 1.2 mm. Curve 7 represents the latter part of the shower for which the slope of the distribution is quite steep.

REFERENCES

Anderson, C.E., 1960: A study of the pulsating growth of cumulus clouds. Geophys. Res. Paper, No. 72, Geophys. Res. Directorate, Bedford, Mass., 136 pp.

Atlas, D., 1954: The estimation of cloud parameters by radar. J. Meteor., 11, 309-317.

————, 1962: Indirect probing techniques. Bull. Amer. meteor. Soc., 43, 457-466.

————, and S. Bartnoff, 1953: Cloud visibility, radar reflectivity, and drop-size distribution. J. Meteor., 10, 143-148.

————, and A.C. Chmela, 1957: Physical-synoptic variations of raindrop-size parameters. Proc. 6th Weather Radar Conf., Cambridge, Mass., (Boston: Amer. meteor. Soc.), 21-29.

aufm Kampe, H.J., and H.K. Weickmann, 1957: Physics of clouds. Meteor. Monographs, 3 No. 18. ed. A.K. Blackadar (Boston: Amer. meteor. Soc.).

Austin, P.M., and S. Geotis, 1960: The radar equation parameters. Proc. Eighth Wea. Radar Conf., San Francisco, Calif. (Boston: Amer. meteor. Soc.), 15-22.

————, and E.L. Williams, Jr., 1951: Comparison of radar signal intensity with precipitation rate. Tech. Report No. 14, Wea. Radar Res., M.I.T., Cambridge, Mass.

Bannon, J.K., 1948. The estimation of large-scale vertical currents from the rate of rainfall. Quart. J.R. meteor. Soc., 74, 57-66.

Bartnoff, S., and D. Atlas, 1951: Microwave determination of particle-size distribution. J. Meteor., 8, 130-131.

Battan, L.J., 1959: Radar meteorology, Chicago, The Univ. of Chicago Press, 161 pp.

Becker, A., 1907: Zur Messung der Tropfengrössen bei Regenfällen nach der Absorptionsmethode. Meteor. Z., 24, 247-261.

Bentley, W.A., 1904: Studies of raindrops and raindrop phenomena. Mon. Wea. Rev., 32, 450-456.

Bergeron, T., 1935: On the physics of clouds and precipitation. International Geodetic Geophys. Union, Fifth General Assembly, Sept. 1933, Lisbon, Verbal Proc., Part II, 156-175.

Best, A.C., 1950: The size distribution of raindrops. Quart. J. R. meteor. Soc. 76, 16-36.

————, 1952: Effect of turbulence and condensation on drop-size distribution in cloud. Quart. J. R. meteor. Soc. 78, 28-36.

Blanchard, D.C., 1953: Raindrop-size distribution in Hawaiian rains. J. Meteor. 10, 457-473.

Boucher, R.J., 1951: Results of measurements of raindrop size. Proc. Conf. on Water Resources (Illinois State Water Survey), Bull. 41 [Urbana, Ill.], 293-297.

Bowen, E.G., 1950: The formation of rain by coalescence. Aust. J. Sci. Res., Ser. A. 3, 193-213.

————, and K.A. Davidson, 1951: A raindrop spectrograph. Quart. J. R. meteor. Soc., 77, 445-449.

Braham, R.R., Jr., and M. Dragnis, 1960: Roots of orographic cumuli. J. Meteor. 17, 214-226.

Byers, H.R., and R.R. Braham, Jr., 1949: The thunderstorm, U.S. Govt. Print. Off., Washington, D.C., 287 pp.

Chapman, G., 1948: Size of raindrops and their striking force at the soil surface in a red pine plantation. Trans. Amer. Geophys. Un., 29, 664-670.

Cooper, B.F., 1951: A balloon-borne instrument for telemetering raindrop-size distribution and rainwater content of cloud. Aust. J. Appl. Sci., 2, 43-55.

Das, P.K., 1950: The growth of cloud droplets by coalescence, Ind. J. Meteor. and Geophys. 1, 137.

Defant, A., 1905: Gesetzmässigkeiten in der Verteilung der verschiedenen Tropfengrössen bei Regenfällen. Akademic d. Wissenschaften, Vienna, Math. - Naturwiss, Klasse, Sitzungberichte, 114, 585-646.

Diem, M., 1948: Messungen der Grösse von Wolkenelementen II. Meteor. Rundschan, 1, 261-273.

Dingle, A.N., and K.R. Hardy, 1962: The description of rain by means of sequential raindrop-size distributions. Quart. J. R. meteor. Soc., 88, 301-314.

————————, and J.F. Schulte, Jr., 1962: A research instrument for the study of raindrop-size spectra. J. Appl. Meteor., 1, 48-59.

East, T.W.R., 1957: An inherent precipitation mechanism in cumulus clouds. Quart. J. R. meteor. Soc., 83, 61-76.

Ekern, P.C., 1950: Raindrop impact as the force initiating soil erosion. Ph.D. thesis, Univ. of Wisconsin.

Ellison, W.D., 1944: Studies of raindrop erosion. Agri. Engr., 25, 131-136 and 181-182.

————————, 1949: Protecting the land against the raindrop's blast. Sci. Monthly, 68, #4, 241-251.

Engelmann, R.J., 1962: The Hanford raindrop sampler and selected spectra. Hanford Atomic Products Operation, Richmond, Wash. Available from O.T.S., Washington 25, D.C.

Findeisen, W., 1938: Die kolloid-meteorologischen Vorgänge bei der Niederschlagsbildung. Met. Z., 55, 121-135.

Fletcher, N.H., 1962: The physics of rainclouds. Cambridge University Press, Cambridge, 386 pp.

Frössling, N., 1938: Über die Verdunstung fallenden Tropfen. Gerlands Beitr. Geophysik, 52, 170-216.

Fulks, J.R., 1935: Rate of precipitation from adiabatically ascending air. Mon. Wea. Rev., 63, 291-294.

Gerhardt, J.R., and C.W. Tolbert, 1957: Rain attenuation and back-scattering measurements at 4.3 millimeter wavelength. Proc. Sixth Wea. Radar Conf., M.I.T., Cambridge, Mass., (Boston: Amer. meteor. Soc.), 243-252.

Glass, M., 1962: Personal letter giving data on clouds at Flagstaff, Arizona for 27 and 31 July 1961.

Gunn, K.L.S., 1952: The effect of accretion on cloud through which rain is falling. Geophys. Res. Pap., No. 13, Geophys. Res. Directorate, Bedford, Mass., 65-69.

————————, and T.W.R. East, 1954: The microwave properties of precipitation particles. Quart. J. R. meteor. Soc., 80, 522-545.

Gunn, K.L.S., and W. Hitschfeld, 1951: A laboratory investigation of the coalescence between large and small water-drops. J. Meteor., 8, 7-16.

————, and J.S. Marshall, 1955: The effect of wind shear on falling precipitation, J. Meteor., 12, 339-349.

————, 1956: The distribution with size of aggregate snowflakes. Proc. Sixth Wea. Radar Conf., M.I.T., Cambridge, Mass., (Boston: Amer. meteor. Soc.), 37-41.

Gunn, R., and G.D. Kinzer, 1949: The terminal velocity of fall for water droplets in stagnant air. J. Meteor., 6, 243-248.

Hardy, K.R., 1962: Note on the effect of accretion and evaporation on the Z-R relationship. Unpublished report to Dr. D. Atlas.

————, and A.N. Dingle, 1960: Raindrop-size distribution in a cold frontal shower. Proc. Eighth Wea. Radar Conf., San Francisco, Calif., (Boston: Amer. meteor. Soc.), 179-186.

Harper, W.G., 1957: Variation with height of rainfall below the melting level. Quart. J. R. meteor. Soc., 83, 368-371.

Horton, R.E., 1948: Statistical distribution of drop sizes and the occurrence of dominant drop sizes in rain. Trans. Amer. Geophys. Un., 29, 624-630.

Houghton, H.G., 1950: A preliminary quantitative analysis of precipitation mechanisms. J. Meteor., 7, 363-369.

Imai, I., 1960: Raindrop-size distributions and Z-R relationships. Proc. Eighth Wea. Radar Conf., San Francisco, Calif., (Boston: Amer. Meteor. Soc.), 211-218.

Johnson, J.C., 1954: Physical meteorology, John Wiley and Sons Inc. and The Technology Press of M.I.T., Boston, Mass., 393 pp.

Jones, D.M.A., 1955: 3-cm and 10-cm wavelength radiation back-scatter from rain. Proc. Fifth Radar Wea. Conf., Fort Monmouth, N.J., (Boston: Amer. meteor. Soc.), 281-285.

————, 1959: The shape of raindrops. J. Meteor., 16, 504-510.

Jones, D.M.A., and L.A. Dean, 1953: A raindrop camera. Res. Rep. No. 3 under Contract No. DH-36-039-42446, Illinois Water Survey, Urbana, Ill.

————————, and E.A. Mueller: Z-R relationships from drop-size data. Proc. Eighth Wea. Radar Conf., San Francisco, Calif., (Boston: Amer. meteor. Soc.), 498-504.

Kessler, E., III, 1959: Kinematical relations between wind and precipitation distributions. J. Meteor., 16, 630-637.

————————, 1961: Kinematical relations between wind and precipitation distributions, II. J. Meteor., 18, 510-525.

Kinzer, G.D., and R. Gunn, 1951: The evaporation, temperature and thermal relaxation time of freely-falling water drops. J. Meteor., 8, 71-83.

Kohler, H., 1925: Über Tropfengruppen und einige Bermerkungen zur Genauigkeit der Tropfenmessungen besonders mit Rücksicht auf Untersuchungen von Richardson. Meteor. Z., 42, 463-467.

Landsberg, H., and H. Neuberger, 1938: On the frequency distribution of drop sizes in a sleet storm. Bull. Amer. meteor. Soc., 19, 354-356.

Langmuir, I., 1948a: The growth of particles in smokes and clouds and the production of snow from supercooled clouds. Proc. Amer. Phil. Soc., 92, 167-185.

————————, 1948b: Production of rain by a chain reaction in cumulus clouds at temperatures above freezing. J. Meteor., 5, 175-192.

Laws, J.O., 1941: Measurements of the fall-velocity of water-drops and raindrops. Trans. Amer. Geophys. Un., 22, 709-721.

————————, and D.A. Parsons, 1943: The relation of raindrop size to intensity. Trans. Amer. Geophy. Un., 24, Part II, 452-460.

Lenard, P., 1904: Über Regen. Meteor. Z., 21, 249-262.

Levin, L.M., 1954: Size distribution function for cloud droplets and rain drops. Dok. Akad. Nauk SSSR, 94, 1045. Trans. T263r of D.R.B., Ottawa, Can.

Ligda, M.G.H., 1951: Radar storm observation. In Comp. of Meteor., ed. T.F. Malone (Boston: Amer. Met. Soc.), 1265-1282.

Lowe, E.J., 1892: Rain drops. Quart. J. R. meteor. Soc., 18, 242-243.

McDonald, J.E., 1954: The shape and aerodynamics of large raindrops. J. Meteor., 11,478-494.

Magono, C., 1954: On the shape of water drops falling in stagnant air. J. Meteor., 11, 77-79.

Marshall, J.S., and W.E. Gordon, 1957: Radiometeorology. Meteor. Monographs, 3, No. 14, ed. A.K. Blackadar (Boston: Amer. meteor. Soc.)

————————, R.C. Langille, and W. McK. Palmer, 1947: Measurement of rainfall by radar, J. Meteor., 4, 186-192.

————————, and W. McK. Palmer,1948: The distribution of raindrops with size. J. Meteor., 5, 165-166.

Mason, B.J., 1952: Production of rain and drizzle by coalescence in stratiform clouds. Quart. J. R. meteor. Soc., 78, 377-386.

————————, 1957: The physics of clouds. London, Oxford Univ. Press. 481 pp.

————————, and J.B. Andrews, 1960: Drop-size distributions from various types of rain. Quart. J. R. meteor. Soc., 86, 346-353.

————————, and F.H. Ludlam, 1951: The microphysics of clouds. Phy. Soc., London, 14, 147-195.

————————, and R. Ramanadham, 1953: A photoelectric raindrop spectrometer. Quart. J. R. meteor. Soc., 79, 490-495.

————————————————, 1954: Modification of the size distribution of falling raindrops by coalescence. Quart. J. R. meteor. Soc., 80, 388-394.

Niederdorfer, E., 1932: Messungen der Grosse der Regentropfen. Met. Z., 49, 1-14.

Probert-Jones, J.R., 1962: The radar equation in meteorology Quart. J. R. meteor. Soc., 88, 485-495.

Ramana Murty, Bh.V., and S.C. Gupta, 1958: Precipitation characteristics based on raindrop-size measurements at Delhi and Khandala during south-west monsoon. J. Sci. Industi. Res., 18A, 352-371.

Rigby, E.C., and J.S. Marshall, 1952: The modification of rain with distance fallen. 'Stormy Weather', Res. Rep., McGill Univ., MW-3., 51 pp.

_____, and W. Hitschfeld, 1954: The development of the size distribution of raindrops during their fall. J. Meteor., 11, 363-372.

Ryde, J.W., 1946: The attenuation and radar echoes produced at centimetre wavelengths by various meteorological phenomena. Meteorological factors in radio wave propagation, Phys. and R. meteor. Soc., London, 169-189.

Schmidt, W., 1908: Zur Erklärung der gesetzmässigen Verteilung der Tropfengrössen bei Regenfällen. Meteor. Z., 25, 496-500.

Sivaramakrishnan, M.V., 1960: The relation between raindrop-size distribution, rate of rainfall and the electrical charge carried down by rain in the tropics. Ind. J. Meteor. and Geophy., 11, 258-268.

_____, 1961: Studies of raindrop-size characteristics in different types of tropical rain using a simple raindrop recorder. Ind. J. Meteor. and Geophy., 12, 189-216.

Spilhaus, A.F., 1948: Raindrop size, shape, and falling speed. J. Meteor., 5, 541-546.

Srivastava, R.C., and R.K. Kapoor, 1961: Thunderstorm rain vs. steady precipitation from layer type clouds, as judged by study of raindrop sizes. Ind. J. of Meteor. and Geophy., 12, 93-102.

Todd, C.J., 1960: Physics of precipitation in winter storms at Santa Barbara, California. In Physics of Precipitation, Geophysical Monograph No. 5, ed. H. Weickmann, Amer. Geophy. Un., Washington, D.C., 435 pp.

Twomey, S., 1953: On the measurement of precipitation intensity by radar. J. Meteor., 10, 66-67.

Warner, J., and T.D. Newnham, 1952: A new method of measurement of cloud-water content. Quart. J. R. meteor. Soc., 78, 46-52.

Wexler, R., 1948: Rain intensities by radar. J. Meteor., 5, 171-173.

Wexler, R., 1951: Theory and observation of radar storm detection. In Comp. of Meteor., ed. T.F. Malone (Boston: Amer. Meteor. Soc.), 1283-1289.

————, and D. Atlas, 1958: Moisture supply and growth of stratiform precipitation. J. Meteor., 15, 531-538.

Wiesner, J., 1895: Beiträge zur Kenntniss des tropischen Regens. Akademie d. Wissenschaften, Vienna, Math-Naturw. Klasse, Sitzungsberichte, 104, 1397-1434.

Willett, H.C., 1944: Descriptive meteorology, New York, Academic Press, Inc., 310 pp.

Woodcock, A.H., 1952: Atmospheric salt particles and raindrops. J. Meteor., 9, 200-212.

AD

UNCLASSIFIED

The University of Michigan, Office of Research Administration, Ann Arbor. A STUDY OF RAINDROP-SIZE DISTRIBUTIONS AND THEIR VARIATION WITH HEIGHT, by Kenneth R. Hardy. December 1962. 174 p. incl. illus. tables. (Proj. 8620; Task 862002) (Scientific Report No. 1; ORA Report 05016-1-S; AFCRL-62-1091) (Contract AF 19(628)-281)Unclassified report

Computations of the changes of the raindrop-size distributions with distance fallen are made using an electronic digital computer. Coalescence, accretion and evaporation processes are considered. It is found that an initial exponential distribution having a relatively large negative slope is considerably modified as the rain falls and a distribution with a relatively small negative

UNCLASSIFIED

AD

UNCLASSIFIED

The University of Michigan, Office of Research Administration, Ann Arbor. A STUDY OF RAINDROP-SIZE DISTRIBUTIONS AND THEIR VARIATION WITH HEIGHT, by Kenneth R. Hardy. December 1962. 174 p. incl. illus. tables. (Proj. 8620; Task 862002) (Scientific Report No. 1; ORA Report 05016-1-S; AFCRL-62-1091) (Contract AF 19(628)-281)Unclassified report

Computations of the changes of the raindrop-size distributions with distance fallen are made using an electronic digital computer. Coalescence, accretion and evaporation processes are considered. It is found that an initial exponential distribution having a relatively large negative slope is considerably modified as the rain falls and a distribution with a relatively small negative

UNCLASSIFIED

UNCLASSIFIED

slope is only slightly modified by the above three processes.

A procedure is presented whereby the raindrop-size distribution at the melting level can be deduced. One study of this type shows that at the melting level (1) more large drops must be present than is indicated by the M-P distribution, and (2) the concentration of the larger drops must not be substantially different from their concentration observed at the ground.

UNCLASSIFIED

UNCLASSIFIED

slope is only slightly modified by the above three processes.

A procedure is presented whereby the raindrop-size distribution at the melting level can be deduced. One study of this type shows that at the melting level (1) more large drops must be present than is indicated by the M-P distribution, and (2) the concentration of the larger drops must not be substantially different from their concentration observed at the ground.

UNCLASSIFIED